

CAPITAL UNIVERSITY OF SCIENCE AND
TECHNOLOGY, ISLAMABAD



Finite Element Analysis of Heat Transfer through a Higher Grade Darcy-Forchheimer Porous Medium

by

Ambreen Zahra

A thesis submitted in partial fulfillment for the
degree of Master of Philosophy

in the

Faculty of Computing

Department of Mathematics

2024

Copyright © 2024 by Ambreen Zahra

All rights reserved. No part of this thesis may be reproduced, distributed, or transmitted in any form or by any means, including photocopying, recording, or other electronic or mechanical methods, by any information storage and retrieval system without the prior written permission of the author.

*I dedicate my thesis to
my beloved family, friends specially*

My Mother(Umm.e.Salma),

*A determined and aristocratic embodiment who educate me to belief in ALLAH,
believe in hard work and that so much could be done with little,*

My Father(Syed Shabbir Hussain Shah)

I quote the remarkable words of Hadith,

“A father gives his child nothing better than an education.”



CERTIFICATE OF APPROVAL

Finite Element Analysis of Heat Transfer through a Higher Grade Darcy-Forchheimer Porous Medium

by

Ambreen Zahra

(Registration No: MMT213009)

THESIS EXAMINING COMMITTEE

S. No.	Examiner	Name	Organization
(a)	External Examiner	Dr. Saqib Zia	CUI, Islamabad
(b)	Internal Examiner	Dr. Rashid Ali	CUST, Islamabad
(c)	Supervisor	Dr. Muhammad Sabeel Khan	CUST, Islamabad

(Signatures)

Dr. Muhammad Sabeel Khan

Dr. Muhammad Sabeel Khan

Thesis Supervisor

September, 2024


Dr. Muhammad Sagheer
Head
Dept. of Mathematics
September, 2024

Dr. M. Abdul Qadir
Dean
Faculty of Computing
September, 2024

Author's Declaration

I, **Ambreen Zahra** hereby state that my MPhil thesis titled “**Finite Element Analysis of Heat Transfer through a Higher Grade Darcy-Forchheimer Porous Medium**” is my own work and has not been submitted previously by me for taking any degree from Capital University of Science and Technology, Islamabad or anywhere else in the country/abroad.

At any time if my statement is found to be incorrect even after my graduation, the University has the right to withdraw my MPhil Degree.



(**Ambreen Zahra**)

Registration No: MMT213009

Plagiarism Undertaking

I solemnly declare that research work presented in this thesis titled “**Finite Element Analysis of Heat Transfer through a Higher Grade Darcy-Forchheimer Porous Medium**” is solely my research work with no significant contribution from any other person. Small contribution/help wherever taken has been duly acknowledged and that complete thesis has been written by me.

I understand the zero tolerance policy of the HEC and Capital University of Science and Technology towards plagiarism. Therefore, I as an author of the above titled thesis declare that no portion of my thesis has been plagiarized and any material used as reference is properly referred/cited.

I undertake that if I am found guilty of any formal plagiarism in the above titled thesis even after award of MPhil Degree, the University reserves the right to withdraw/revoke my MPhil degree and that HEC and the University have the right to publish my name on the HEC/University website on which names of students are placed who submitted plagiarized work.



(Ambreen Zahra)

Registration No: MMT213009

Acknowledgement

In the name of **ALLAH**, who is the most merciful and beneficent, created the universe and blessed the mankind with intelligence and wisdom to explore its secret. I would like to express my heart felt gratitude and immeasurable respect to my supervisor **Dr. Muhammad Sabeel Khan** for his passionate interest, willingness help, superb guidance and inspiration throughout this investigation. His textural and verbal criticism enabled me in formatting this thesis.

I am extremely grateful to my all teachers for their encouragement and emphasis on striving for excellence when teaching mathematics. I would like to acknowledge the CUST for providing me such a favourable environment to this research.

I must express my very profound gratitude to my dear parents and whole members of my family including my Husband **Syed Zain ul Abideen Ali Kazmi** and my beloved Daughter **Abrish Fatima** for providing me with unfailing support and continuous encouragement throughout my years of study and through the process of researching and writing this thesis.

Finally, I want to express my gratitude to my Friends who encouraged me throughout my MPhil research. I am grateful to my fellow researchers at CUST for valuable discussions on this research. I have enjoyed working alongside them in a pleasant working environment.



(**Ambreen Zahra**)

Registration No: MMT213009

Abstract

In this thesis, a higher grade Darcy Forchheimer porous model is presented and Solved by using finite element method. The Darcy–Forchheimer law of porosity is a modification of Darcy’s law, which describes fluid flow through porous media. It is an extension of Darcy’s law to account for non-linear flow behavior at high velocities or in highly permeable media. To this end, the governing flow dynamics of Higher grade Darcy-Forchheimer model is described by a set of partial differential equations (PDEs) in vector tensor notations. The component forms of the model is calculated by the concepts of tensor calculus. The governing set of PDEs are obtained which are then non-dimensionalized by suitable transformation of the associated variables. The domain of computation along with prescribed boundary conditions are discussed. To solve the developed higher grade Darcy Forchheimer model problem finite element procedure is adopted. Finite element method is briefly discussed and weak formulation of the model problem is derived. The finite element model problem is implemented in open source code FreeFEM++. Results are computed and discussed for varying values of the physical parameters of the problems. Mesh independence of the solution is shown through mesh independence analysis. Moreover, streamline plots of velocities and isotherms are plotted and discussed.

Contents

Author's Declaration	iv
Plagiarism Undertaking	v
Acknowledgement	vi
Abstract	vii
List of Figures	x
List of Tables	xi
Abbreviations	xii
Symbols	xiii
1 Introduction and Literature Survey	1
1.1 Thesis Contribution	5
1.2 Objectives	5
1.3 Thesis Layout	6
2 Basic Terminologies	8
2.1 Basic Definitions	8
2.1.1 Physical Properties of the Fluid	8
2.2 Dimensionless Parameters	9
2.3 Types of Fluid Flow	12
2.3.1 Steady and Unsteady Flows	12
2.3.2 One, Two and Three Dimensional Flows	13
2.3.3 Laminar and Turbulent Flows	14
2.3.4 Compressible and Incompressible Flows	14
2.4 Fundamental Laws	15
2.4.1 Conservation of Mass; the Continuity Equation	15
2.4.2 Conservation of Momentum	16
2.4.3 Conservation of Energy	17
2.5 Porous Medium	18
2.6 Darcy Forchheimer Porous Flow	18

2.6.1	Darcy's Law:	18
2.6.2	Forchheimer's Law:	19
2.7	Darcy Forchheimer Medium	19
2.8	Higher Grade Darcy Forchheimer Flow Model and its Applications	20
2.8.1	Extended Forchheimer Terms:	21
2.8.2	Non-Newtonian Fluid Models:	21
2.8.3	Anisotropic and Heterogeneous Porous Media:	21
2.8.4	Multi-Phase Flow:	21
2.8.5	Thermal and Chemical Effects:	22
2.9	Heat and Mass Transfer Phenomenon and Related Properties	23
2.10	Magnetohydrodynamics	25
3	Basics of Finite Element Method	26
3.1	Formulation of FEM Model	26
3.1.1	Weighted Residual Method	27
3.1.1.1	Galerkin Finite Element Method	30
4	Mathematical Model of Two Dimensional higher grade Darcy Forchheimer porous model	34
4.1	Problem Description	43
4.1.1	Dimensional Form of the Governing Equations	44
4.1.2	Dimensionless Parameters	46
4.2	Conversion of Dimensional equations into Dimensionless equations	46
4.3	Dimensionless Governing Equations	55
5	Finite Element Formulation and Numerical Procedure	57
5.1	Numerical Solution	57
5.1.1	Strong Form of Governing Equations	57
5.1.2	Weak/Variational Formulation	58
6	Numerical Results and Discussion	76
6.1	Validation	76
6.2	Results and Discussion	77
7	Conclusions and Future Work	88
	Bibliography	90

List of Figures

4.1	Computational Domain with two semi-circular heaters.	44
5.1	Systematic Computational Domain	72
5.2	Linear Triangular Element	72
6.1	Streamline plots for varying values of Forchheimer number Fr	81
6.2	Streamline plots for varying values of Grashof number Gr in the non-Forchheimer medium.	82
6.3	Streamline plots for varying values of Grashof number Gr in the Forchheimer medium.	83
6.4	Time evolution of the Streamline function Ψ	84
6.5	Isotherm plots for varying values of Prandtl number Pr in the Forchheimer medium.	85
6.6	Isotherm plots for varying values of Hartmann number Ha in the Forchheimer medium.	86
6.7	Isotherm plots for varying values of porosity parameter λ	87

List of Tables

6.1	L_2 – <i>error</i> norms of pressure and velocity values for $Re = 20$ at different mesh refinement levels.	77
6.2	Streamline values at different mesh levels	78
6.3	Velocity values at different mesh levels	79

Abbreviations

BDM	Brinkman extended Darcy Model
BFDM	Brinkman Forchheimer Darcy Model
CFD	Computational Fluid Dynamics
DFPM	Darcy Forchheimer Porous Model
FEM	Finite Element Method
GFEM	Galerkin Finite Element Method
MHD	Magnetohydrodynamics
NEN	Number of Elemental Nodes

Symbols

L	Distance between the two plates
t	Time
V	Flow velocity vector field
A_1	First order Rivlin-Ericksen strain tensor
A_2	Second order Rivlin-Ericksen strain tensor
τ	Cauchy stress tensor
∇	Gradient operator
I	Identity tensor
p	Hydrodynamic pressure field
μ	Viscosity
α_1, α_2	Material constants
K	Permeability
φ	Porosity
g	Gravitational constant
θ	Particles temperature
C_p	Specific heat
k	Thermal conductivity of the nano-medium
u	x -component of velocity
v	y -component of velocity
x, y	Cartesian coordinates
w_h	Approximate function
∂_x	Partial derivative with respect to coordinate x
β_θ	Volumetric thermal expansion coefficient
r	Darcy-Forchheimer resistance

c_F	Dimensionless Forchheimer coefficient
B_o	The magnitude of applied magnetic field
σ	Dimensionless Forchheimer coefficient
β	Viscoelastic parameters
λ	Porosity parameter
h	Length of each finite element subinterval
ϕ_i	Basis functions
Pr	Prandtl number
Re	Reynolds number
Ha	Hartmann number
F_r	Forchheimer constant
Gr	Grashof number
w_i	Weight functions
ψ_i	Known shape function
Ω	Computational domain
ξ_j, η_j	Shape functions
$v_{,x}$	$\frac{\partial v}{\partial x}$
$u_{,y}$	$\frac{\partial u}{\partial y}$

Chapter 1

Introduction and Literature Survey

Heat transfer mechanism has been known for its great importance in many engineering and medical sciences for last many decades. Because of the great utility of heat energy for mankind, thermodynamics is really related to many other areas. Applications of heat transfer process are playing an important role in construction [1], fuel filling system [2], air compressor [3], and food industry [4]. In this context, the working fluids with excellent thermophysical properties have a significant task to carry out in managing thermal energy and for this purpose, fluid dynamics is indeed playing a critical role. Researchers highlight various important factors to improve the thermal process, such as the participation of porous medium, open and closed cavities, application of magnetic effects, nanofluids, micro-sized channel, etc. to improve the thermal convection process. Studies have clearly demonstrated that heat convection in fluids can be enhanced by the physical geometry, boundary conditions, and thermal characteristics of the flow.

Heat transfer through Forchheimer porous media has been examined in literature in a variety of contexts that are relevant to their uses. For example, Dero et al. [5] used to analyze radiative magnetized rotating hybrid nanofluid in order to investigate the radiation's effect in a Darcy-Forchheimer porous medium. They came to understand that the problem's dual solutions are impacted by the medium's porosity. Ganesh et al. [6] employed a Darcy-Forchheimer medium in their analysis of the boundary layer flow of a thermally stratified liquid with slip, viscous, and ohmic dissipation effects. They utilized Runge Kutta method with shooting method to calculate the results numerically.

Elbashbeshy and Bazid [7] examined the creation of heat internally as well as suction or injection across a stretching surface in a porous media. In a porous medium, Abbas et al. [8] investigated the behavior of Magnetohydrodynamics Williamson nanoflow in relation to heat generation and viscous dissipation. Saleem et al. [9, 10] investigated how nanoflow behaved in a porous media and its relevant consequences. The unsteady viscous incompressible flow through a porous medium confined between two constant porous plates is analyzed by Attia et al. [11]. The effect of the medium's porosity was examined using plates with a constant pressure gradient condition. Naganthran and colleagues [12] examined the free convection problem.

They used the RK method with the shooting method to analyze heat transfer within the context of the Cosserat boundary layer flow. Their analysis shows that there is a strong momentum transport as the Darcy number increases. Khan and Kaneez [13] also looked into the hybrid nanofluid flow within the context of the Cosserat continuum. They numerically solved the problem using a finite element method of continuous time discretization. In a non-Newtonian setting, Riaz et al. [14] analyzed the nanofluid flow through a porous rectangular channel using the Nelder Mead method in conjunction with the genetic algorithm and Homotopy perturbation method.

In the Darcy-Forchheimer porous medium, Loganathan et al. [15] presented on the entropy features in a higher-grade continuum flow. Using a Darcy-Forchheimer porous medium, Rasool et al. [16] seek to study the magnetohydrodynamic Jeffery nanofluid flow for the transfer of heat and mass.

They investigated the impact of a fluctuating magnetic field on mass and heat transfer in a porous medium. The reader is referred to Habibishandiz and Saghir [17] for a critical review and comprehensive literature study on the heat transfer enhancement methods within porous considerations. A comprehensive examination of the analysis of microorganisms and nanofluids in relation to porous considerations is carried out in their study. In a porous flow between two parallel plates, Umavathi [18] examined the chemical reactive flow with convective boundary conditions. The common method based on RK and shooting was used to calculate the effect of Darcy and viscous dissipation. They addressed the issue in a non-Fourier thermal setting, Loganathan [19] also investigated the viscoelastic flow over a convectively heated porous surface using the RK method. In the presence of a porous medium, Kataria and Mittal [20] investigated

the thermal and hydrodynamic effects on the oscillating vertical plate. Sheikholeslami et al. [21] have studied the effects of heat generation and thermal diffusion in nanofluid porous flow passing by a plate. Using the homotopy analysis method, Patel et al. [22] examined nanofluid flow over a shrinking/stretching sheet while taking radiation effects into account in a Cosserat continuum. Mittal et al. [23] have studied the Micropolar ferrofluid flow with convective heat treatments using a similar semi-analytical approach. With viscous dissipation taken into account, Kataria et al. [24] also examine the non-linear radiation effect on micropolar Magneto-hydrodynamics flow. Mittal and Patel [25] investigated the effects of heat generation with nonlinear radiation in two-dimensional Casson fluid flow with mixed convective heat transfer. Sheikholeslami et al. [26] have also investigated the effects of radiation on heat transfer in three-dimensional settings with suspension micro-mixing. Boundary conditions for thermal flux were investigated, and the impact of the Darcy number on various physical attributes was demonstrated.

Magneto-hydro-dynamics (MHD), is the study of electrically active flows, such as plasma, liquid metals, and salt water, with the help of external or internal induced magnetic field effects [27]. Numerous studies have already been conducted to examine how MHD effects can enhance heat transport mechanisms.

Grosan et al. [28] have numerically investigated buoyancy force dominated convective flow to investigate the effects of an external magnetic field and internal heat generation within a rectangular enclosure with a porous medium. An analysis has been conducted of the governing parameters, which include the cavity aspect ratio (a), inclination angle (γ), Hartmann number (Ha), Rayleigh number (Ra), and so on. Variations in the external magnetic field caused a reduction in the convective heat distribution.

In a lid-driven enclosure with porous media, Khanefar and Chamka [29] numerically investigated the unsteady mixed convection. Utilizing the Brinkman-extended Darcy model has an impact on the average Nusselt number. He discovered that raising Darcy number increases the rate of heat transfer, and that raising Darcy number while lowering Richardson number also raises Nusselt number. Rahman et al. [30] present a similar observation with unsteady flow and reach the same conclusions when using the Brinkman extended Darcy model with induced semi-circular heaters induced at the bottom wall of a lid-driven cavity. In a two-dimensional experiment, Vishnuvardhanarao and Das [31]

drove a two-sided lid parallel in a square cavity that was filled with a saturated fluid porous medium. According to this observation, heat transfer through the lid enclosure increases when the porosity in the enclosure decreases and the Grashof number effect is more pronounced when Grashof number increases. The Maxwell Brinkman model inside a lid-driven square cavity was used to introduce the porous medium by Hassan and Ismael [32].

The findings unequivocally demonstrate that an increase in heat transfer is observed with a decreasing Darcy number because there are porous layers present at two distinct locations. A review of the literature also revealed that the Brinkman Forchheimer-extended Darcy model, which combines Brinkman extended Darcy Model and Brinkman Forchheimer Darcy Model, is an advanced model for confining porous media. Numerically mixed convection flow in a porous vertical channel with heat sources at the walls was the conclusion reached by Hadim and Chen [33]. Porosity has the effect of making average Nusselt number in the vertical flow increase as Darcy number decreases. In 2016, Sureshkumar and Muthtamilselvan [34] observed Copper nanoparticles in a fluid in a porous enclosed geometry. A similar model was recently considered for this geometry. A longer Brinkman Forchheimer Darcy Model is used to determine the impact of heat transfer rate. While porosity remains constant, average Nusselt number rises with a high Darcy number because a higher Darcy number causes the fluid's permeability and flow conductance to increase.

Additionally, a higher heat transfer rate is observed in the enclosure with a decrease in the Richardson number. The numerical modeling of mixed convection with Copper nanoparticles in a square-filled enclosure that divided the moving plate kept in the middle was investigated by Nagarajan and Akbar [35]. A small adjustment to the parameters has no effect on the average Nusselt number because the heat transfer rate increases with a rise in the Darcy number. Kumar et al. [36] found a significant comparison between Brinkman Forchheimer Darcy Model and Brinkman extended Darcy Model. The outcomes shown in this model are the same as those of [35], but in each case there are distinct changes due to the effects of the Darcy, Grashof, and Richardson numbers. When the inertial term that is displayed in the BFDM is absent, the BDM yields increasing values for Jeng, Tzeng, and average Nusselt number. The investigation incorporating aluminum foams in fluid-saturated porous media was examined in [37]. Thus, higher heat transfer rate results for low Darcy number due to greater porosity effect on momentum and energy equation. In a similar way, Kumar and Gupta

investigated flow and heat transfer in non-darcy porous media in ([38, 39]). The numerical analysis of forced flow in a horizontal open channel with a cavity demonstrating the induction of a porous medium containing Titanium oxide nanoparticles was investigated by Nasrin and Alim [40]. It was observed that the rate of heat transfer is greatly increased by an increase in Titanium oxide nanoparticles. Also, for low Darcy number values, the average Nusselt number increases.

1.1 Thesis Contribution

In this thesis, we present a higher grade Darcy-Forchheimer porous flow in a square cavity with semi-circular heaters at the bottom wall. To this end, the governing dynamics of the flow model are presented in the form of partial differential equations (PDEs) in vector-tensor notation.

The component form of the governing PDEs is calculated using concepts from tensor calculus. The obtained model is non-dimensionalized with chosen Similarity transformations. Weak formulation of the model problem is constructed. Finite element model is derived which is afterwards implemented through FreeFEM++. A brief introduction of FreeFEM++ can be found at <https://freefem.org/>. The implemented code is used to analyze the flow mechanics within a square cavity with two heaters at the bottom wall of the cavity. Mesh independence of the solutions is achieved and presented through Tables. Results are presented and discussed for varying physical parameters of interest.

1.2 Objectives

The objectives of this study are:

- To develop a two dimensional higher grade Darcy Forchheimer model using tensor calculus.
- To develop Finite element weak formulation of the presented two-dimensional higher grade Darcy Forchheimer model.

-
- To implement the presented model in open source code Free Fem++.
 - To compute the developed Finite Element model numerically through Free Fem++.
 - To simulate the presented model on a square domain with semi-circular heaters at the bottom wall of computational domain.
 - To analyze different material parameters effect on the higher grade Darcy Forchheimer flow within cavity under suitable chosen boundary conditions.

1.3 Thesis Layout

This thesis is further composed of the following chapters:

- **Chapter 2** demonstrates the introductory basics of fluid dynamics. A brief discussion about the basic definitions, governing laws for fluid motion and governing equations have been illustrated. Dimensionless physical quantities of interest are also mentioned briefly related to the problems.
- In **Chapter 3**, the finite element method has been explained by taking an example of a simple two-dimensional poisson problem is solved to explain the numerical procedure for the achievement of results.
- In **Chapter 4**, numerical simulations of heat transfer through a higher grade Darcy Forchheimer porous model are presented using the Finite Element Method (FEM) based on the Galerkin weighted residual.
We convert the system of dimensional equations into the dimensionless equations and add the necessary boundary conditions in order to solve the governing equations.

- With appropriate transformations, in **Chapter 5** the dimensional form is transformed into a dimensionless form.

The equations are integrated over the whole domain and are transformed from the strong form to the weak form by multiplying PDEs by test functions of the same space. Ultimately, we obtained an approximated solution by using the set of approximated trial functions that are valid only over a portion of the domain.

- **Chapter 6** Results are presented in the form of graphs, isotherms and streamlines.
- **Chapter 7** contains the conclusion of this work.

The work's references are enumerated in Bibliography.

Chapter 2

Basic Terminologies

In this chapter we are going to discuss basic concepts, definitions and governing laws related to the fluid dynamics. Dimensionless quantities are also discussed which seems to be helpful in the subsequent chapters.

2.1 Basic Definitions

2.1.1 Physical Properties of the Fluid

- **Mass Density or Density**

Density or Mass Density of a fluid is defined as the ratio of the mass of a fluid to its volume. Thus mass per unit volume of a fluid is called density. It is denoted by ρ . The unit of mass density in SI unit is Kg per cubic metre, i.e., Kg/m³.

Mathematically, mass density is written as:

$$\rho = \frac{\text{Mass of fluid}}{\text{Volume of fluid}}.$$

The value of density of water is 1 gm/cm³ or 1000 Kg/m³.

- **Pressure**

When a fluid is contained in a vessel, it exerts force at all points on the sides and bottom and top of the container. The force per unit area is called pressure.

If,

P = The force, and

A = Area on which the force acts; then intensity of pressure,

$$p = \frac{P}{A}.$$

The pressure of a fluid on a surface will always act normal to the surface.

- **Viscosity**

Viscosity is defined as the property of a fluid which determines its resistance to shearing stresses. It is a measure of the internal fluid friction which causes resistance to flow. It is primarily due to cohesion and molecular momentum exchange between fluid layers, and as flow occurs, these effects appear as shearing stresses between the moving layers of fluid.

- **Kinematic Viscosity**

It is defined as the ratio between the dynamic viscosity and density of fluid. It is denoted by symbol ν read as “**nu**”.

Mathematically,

$$\nu = \frac{\mu}{\rho}.$$

- **Thermal Conductivity**

The Fourier heat conduction law states that the heat flow is proportional to the temperature gradient. The coefficient of proportionality is a material parameter known as the thermal conductivity, which may be a function of several variables.

2.2 Dimensionless Parameters

The following dimensionless numbers will appear in the discussion given in the next chapters.

Prandtl Number

This number expresses the ratio of the momentum diffusivity (viscosity) to the thermal

diffusivity. It characterizes the physical properties of a fluid with convective and diffusive heat transfers. It describes, for example, the phenomena connected with the energy transfer in a boundary layer. It expresses the degree of similarity between velocity and diffusive thermal fields or, alternatively, between hydrodynamic and thermal boundary layers. With $Pr = 1$ and $\text{grad } p = 0$, the thermal and hydrodynamic fields are similar. For example, if diverse molten materials have equal Prandtl numbers, they have similar velocity and temperature fields in crystallization.

$$Pr = \frac{\eta c_p}{\lambda},$$

where, η represents the dynamic viscosity, c_p denotes the specific heat capacity and λ stands for thermal conductivity.

Reynolds Number

$$Re = \frac{wL}{\nu},$$

This number expresses the ratio of the fluid inertia force to that of molecular friction (viscosity). It characterizes the hydrodynamic conditions for viscous fluid flow. It determines the character of the flow (laminar, turbulent and transient flows). For a laminar flow $Re < 2000$ is valid, for a transient flow $2000 < Re < 4000$, and for a turbulent flow it is $Re > 4000$. With low values of the Re number, the viscous friction muffles the originating dynamic influence of the flow relatively quickly and intensively, due to which the streamlines and elementary fluid volumes cannot be deformed substantially and the flow remains laminar. With large Re numbers, the dynamic flow effect cannot be equalized by viscous friction and the flow stability is lost, which is manifested by swirls and turbulence in the fluid.

Grashof Number

$$Gr = \frac{L^3 g \beta \Delta T}{\nu^2},$$

It expresses the buoyancy-to-viscous forces ratio and its action on a fluid. It characterizes the free non-isothermal convection of the fluid due to the density difference caused by the temperature gradient in the fluid.

Hartmann Number

The Hartmann number (Ha) is a dimensionless number used in fluid mechanics and magnetohydrodynamics (MHD) to characterize the relative importance of electromagnetic forces to viscous forces within a flow. It's particularly relevant in situations where a conducting fluid is influenced by a magnetic field.

The formula for the Hartmann number is:

$$Ha = B_o \sqrt{\frac{\mu\sigma}{\rho}},$$

The Hartmann number indicates the relative dominance of magnetic forces over viscous forces. A high Hartmann number implies that the magnetic forces are strong compared to viscous forces, leading to significant suppression of flow instabilities and turbulence due to the magnetic field. On the other hand, a low Hartmann number indicates that viscous forces are dominant, and the magnetic effects may be negligible in influencing the flow behavior.

Forchheimer Number

The Forchheimer number (Fr) is indeed a dimensionless parameter used in fluid mechanics, but it's not directly related to the resistance in porous media as previously mentioned. Instead, the Forchheimer number pertains to the inertial forces relative to gravitational forces in a flow.

The Forchheimer number is defined as:

$$Fr = \frac{u^2}{gL}.$$

The Forchheimer number indicates the importance of inertial forces compared to gravitational forces in the flow. It is particularly relevant in situations where gravitational effects are significant, such as in free-surface flows or flows involving sloping surfaces.

Porosity Number

The term porosity number λ typically refers to a dimensionless parameter used in the study of flow through porous media, particularly in the context of permeability and effective porosity. This parameter is also known as the Carman-Kozeny constant or the

Kozeny-Carman constant. The porosity number is important in understanding and predicting the flow behavior through porous materials, such as packed beds, porous membranes, or soil. It quantifies how the porosity affects the resistance to fluid flow, taking into account the structure and geometry of the porous medium.

2.3 Types of Fluid Flow

2.3.1 Steady and Unsteady Flows

- **Steady Flow**

The type of flow in which the fluid characteristics like velocity, pressure, density, etc. at a point do not change with time is called steady flow. Mathematically, we have:

$$\left(\frac{\partial u}{\partial t}\right)_{x_0, y_0, z_0} = 0; \left(\frac{\partial v}{\partial t}\right)_{x_0, y_0, z_0} = 0; \left(\frac{\partial w}{\partial t}\right)_{x_0, y_0, z_0} = 0;$$

$$\left(\frac{\partial p}{\partial t}\right)_{x_0, y_0, z_0} = 0; \left(\frac{\partial \rho}{\partial t}\right)_{x_0, y_0, z_0} = 0; \text{ and so on}$$

where (x_0, y_0, z_0) is a fixed point in a fluid field where these variables are being measured w.r.t. time.

Example: Flow through a prismatic or non-prismatic conduit at a constant flow rate Qm^3/s is steady. (A prismatic conduit has a constant size shape and has a velocity equation in the form $u = ax^2 + bx + c$, which is independent of time t).

- **Unsteady Flow**

It is that type of flow in which the velocity, pressure or density at a point change w.r.t. time. Mathematically, we have:

$$\left(\frac{\partial u}{\partial t}\right)_{x_0, y_0, z_0} \neq 0; \left(\frac{\partial v}{\partial t}\right)_{x_0, y_0, z_0} \neq 0; \left(\frac{\partial w}{\partial t}\right)_{x_0, y_0, z_0} \neq 0;$$

$$\left(\frac{\partial p}{\partial t}\right)_{x_0, y_0, z_0} \neq 0; \left(\frac{\partial \rho}{\partial t}\right)_{x_0, y_0, z_0} \neq 0 \text{ and so on}$$

Example: The flow in a pipe whose valve is being opened or closed gradually (velocity equation is in the form $u = ax^2 + bx(t)$).

2.3.2 One, Two and Three Dimensional Flows

- **One Dimensional Flow**

It is that type of flow in which the flow parameter such as velocity is a function of time and one space co-ordinate only. Mathematically:

$$u = f(x),$$

$$v = 0, \quad w = 0.$$

where u , v and w are velocity components in x , y and z directions respectively.

Example:

Flow in a pipe where average flow parameters are considered for analysis.

- **Two Dimensional Flow**

The flow in which the velocity is a function of time and two rectangular space coordinates is called two dimensional flow. Mathematically:

$$u = f_1(t, x, y),$$

$$v = f_2(t, x, y),$$

$$w = 0.$$

Examples:

- (i) Flow between parallel plates of infinite extent.
- (ii) Flow in the main stream of a wide river.

- **Three Dimensional Flow**

It is that type of flow in which the velocity is a function of time and three mutually perpendicular directions. Mathematically:

$$u = f_1(t, x, y, z),$$

$$v = f_2(t, x, y, z),$$

$$w = f_3(t, x, y, z).$$

Examples:

- (i) Flow in a converging or diverging pipe or channel.
- (ii) Flow in a prismatic open channel in which the width and the water depth are of the same order of magnitude.

2.3.3 Laminar and Turbulent Flows

- **Laminar Flow**

A laminar flow is one in which paths taken by the individual particles do not cross one another and move along well defined paths.

Examples:

- (i) Flow through a capillary tube.
- (ii) Flow of blood in veins and arteries.
- (iii) Ground water flow.

- **Turbulent Flow**

A turbulent flow is that flow in which fluid particles move in a zig zag way.

Example: High velocity flow in a conduit of large size. The majority of fluid flow issues that arise in engineering practice are turbulent in nature.

2.3.4 Compressible and Incompressible Flows

- **Compressible Flow**

It is that type of flow in which the density ρ of the fluid changes from point to point (or in other words density is not constant for this flow). Mathematically:

$$\rho \neq \text{constant.}$$

Example: Flow of gases through orifices, nozzles, gas turbines, etc.

- **Incompressible Flow**

It is that type of flow in which density is constant for the fluid flow. Liquids are generally considered flowing incompressibly. Mathematically, $\rho = \text{constant}$.

Example: Subsonic aerodynamics.

2.4 Fundamental Laws

2.4.1 Conservation of Mass; the Continuity Equation

The principle of conservation of mass can be stated as the time rate of change of mass in a fixed volume is equal to the net rate of flow of mass across the surface. The mathematical statement of the principle results in the following equation, known as the continuity (of mass) equation

$$\frac{\partial \rho}{\partial t} + \nabla \cdot (\rho \mathbf{v}) = 0, \quad (2.1)$$

where ρ is the density of the medium, \mathbf{v} the velocity vector, and ∇ is the nabla or del operator. The continuity equation in (2.1) is in conservation (or divergence) form since it can be derived directly from an integral statement of mass conservation. By introducing the material derivative or Eulerian derivative operator $\frac{D}{Dt}$

$$\frac{D}{Dt} = \frac{\partial}{\partial t} + \mathbf{v} \cdot \nabla, \quad (2.2)$$

the continuity equation (2.1) can be expressed in the alternate, non-conservation (or advective) form

$$\frac{\partial \rho}{\partial t} + \mathbf{v} \cdot \nabla \rho + \rho \nabla \cdot \mathbf{v} = \frac{D\rho}{Dt} + \rho \nabla \cdot \mathbf{v} = 0. \quad (2.3)$$

For steady-state conditions, the continuity equation becomes

$$\nabla \cdot (\rho \mathbf{v}) = 0. \quad (2.4)$$

When the density changes following a fluid particle are negligible, the continuum is termed incompressible and we have $\frac{D\rho}{Dt} = 0$. The continuity equation (2.3) then becomes

$$\nabla \cdot \mathbf{v} = 0, \quad (2.5)$$

which is often referred to as the incompressibility condition or incompressibility constraint.

2.4.2 Conservation of Momentum

The principle of conservation of linear momentum (or Newton's Second Law of motion) states that the time rate of change of linear momentum of a given set of particles is equal to the vector sum of all the external forces acting on the particles of the set, provided Newton's Third Law of action and reaction governs the internal forces. Newton's Second Law can be written as

$$\frac{\partial \rho \mathbf{v}}{\partial t} + \nabla \cdot (\rho \mathbf{v} \otimes \mathbf{v}) = \nabla \cdot \boldsymbol{\sigma} + \rho \mathbf{f}, \quad (2.6)$$

where \otimes is the tensor (or dyadic) product of two vectors, $\boldsymbol{\sigma}$ is the Cauchy stress tensor (N/m^2) and \mathbf{f} is the body force vector, measured per unit mass and normally taken to be the gravity vector. Equation (2.6) describes the motion of a continuous medium, and in fluid mechanics they are also known as the Navier equations. The form of the momentum equation shown in (2.6) is the conservation (divergence) form that is most often utilized for compressible flows. This equation may be simplified to a form more commonly used with incompressible flows. Expanding the first two derivatives and collecting terms

$$\rho \left(\frac{\partial \mathbf{v}}{\partial t} + \mathbf{v} \nabla \cdot \mathbf{v} \right) + \mathbf{v} \left(\frac{\partial \rho}{\partial t} + \nabla \cdot \rho \mathbf{v} \right) = \nabla \cdot \boldsymbol{\sigma} + \rho \mathbf{f}. \quad (2.7)$$

The second term in parentheses is the continuity equation (2.1) and neglecting this term allows (2.7) to reduce to the non-conservation (advective) form

$$\rho \frac{D\mathbf{v}}{Dt} = \nabla \cdot \boldsymbol{\sigma} + \rho \mathbf{f}, \quad (2.8)$$

where the material derivative (2.2) has been employed.

The principle of conservation of angular momentum can be stated as the time rate of change of the total moment of momentum of a given set of particles is equal to the vector sum of the moments of the external forces acting on the system. In the absence of distributed couples, the principle leads to the symmetry of the stress tensor:

$$\boldsymbol{\sigma} = (\boldsymbol{\sigma})^T, \quad (2.9)$$

where the superscript T denotes the transpose of the enclosed quantity.

2.4.3 Conservation of Energy

The law of conservation of energy (or the First Law of Thermodynamics) states that the time rate of change of the total energy is equal to the sum of the rate of work done by applied forces and the change of heat content per unit time. In the general case, the First Law of Thermodynamics can be expressed in conservation form as

$$\frac{\partial \rho e^t}{\partial t} + \nabla \cdot \rho \mathbf{v} e^t = -\nabla \cdot \mathbf{q} + \nabla \cdot (\boldsymbol{\sigma} \cdot \mathbf{v}) + Q + \rho \mathbf{f} \cdot \mathbf{v}, \quad (2.10)$$

where $e^t = e + 1/2 \mathbf{v} \cdot \mathbf{v}$ is the total energy (J/m^3), e is the internal energy, \mathbf{q} is the heat flux vector (W/m^2) and Q is the internal heat generation (W/m^3). The total energy equation (2.10) is useful for high speed compressible flows where the kinetic energy is significant. For incompressible flows, an internal energy equation is more appropriate and can be derived from (2.10) with use of the momentum equation (2.6). Taking the dot product of the velocity vector with the momentum equation produces an equation for the kinetic energy; this equation is subtracted from the total energy equation (2.10) to produce the conservation (divergence) form of the internal energy equation

$$\frac{\partial \rho e}{\partial t} + \nabla \cdot \rho \mathbf{v} e = -\nabla \cdot \mathbf{q} + Q + \Phi, \quad (2.11)$$

where Φ is a dissipation function that is defined by

$$\Phi = \boldsymbol{\sigma} : \nabla \mathbf{v}. \quad (2.12)$$

In Eq. (2.12) $\nabla \mathbf{v}$ is the velocity gradient tensor which will be defined more completely in the following sections. The thermal energy equation in (2.11) can be simplified further by expanding the derivatives on the left-hand side of the equation and using the continuity equation. The resulting equation is the non-conservative (advective) form of the energy equation

$$\rho \frac{De}{Dt} = -\nabla \cdot \mathbf{q} + Q + \Phi, \quad (2.13)$$

which is the standard form used for incompressible flows. Constitutive relations for e and \mathbf{q} will be defined in the next sections and allow (2.13) to be expressed in terms of the temperature T .

2.5 Porous Medium

A porous medium refers to a material containing voids or pores that allow fluid (such as liquids or gases) to pass through. These voids can vary in size and shape, and the material itself can range from natural substances like soil and rock to engineered materials such as ceramics and foams.

Key characteristics of porous media include:

Permeability: This describes how easily fluids can flow through the material. It depends on factors like pore size, shape, and connectivity.

Porosity: This is the fraction of the total volume of the material that is occupied by voids or pores. It indicates the potential storage capacity for fluids within the medium. Porous media are important in various fields such as geology, hydrology, civil engineering, chemical engineering, and biology. They play a crucial role in processes like groundwater flow, oil extraction, filtration, and catalysis. The behavior of fluids in porous media is often complex and can be described by various mathematical models, including Darcy's law for fluid flow and models for solute transport.

2.6 Darcy Forchheimer Porous Flow

A fluid flow regime through porous media in which Forchheimer's quadratic resistance law and Darcy's law are both simultaneously applicable is known as a Darcy-Forchheimer flow.

An explanation of each part is provided below:

2.6.1 Darcy's Law:

This law states that the velocity of flow (μ) is directly proportional to the pressure gradient and describes the flow of a fluid through a porous medium (such as soil or a filter).

$$v = -\frac{k}{\mu} \nabla p$$

where:

- v is the velocity vector,
- k is the permeability of the porous medium,
- μ is the dynamic viscosity of the fluid,
- ∇p is the pressure gradient.

2.6.2 Forchheimer's Law:

This law extends Darcy's law by incorporating a quadratic resistance term to account for inertial effects at higher flow velocities:

$$v = -\frac{k}{\mu}\nabla p - \frac{B}{\mu}v|v|.$$

Here,

- B is the Forchheimer coefficient,
- $v|v|$ represents the magnitude of the velocity vector squared.

When both Forchheimer's law and Darcy's law hold true, it means that viscous forces (which are governed by Darcy's law) and inertial forces (which are accounted for by Forchheimer's law) combine to characterize the flow through the porous medium. Applications of Darcy-Forchheimer flow can be found in many natural and engineering systems, including groundwater flow, oil reservoir engineering, filtration processes, and more, where fluid flow through porous media needs to be accurately modeled.

2.7 Darcy Forchheimer Medium

This is known as the Darcy-Forchheimer equation, which represents fluid flow through porous media. It extends the application of Darcy's law to laminar flow by including additional terms to account for inertial and non-linear effects that become significant

at higher flow velocities or in more complex porous structures. The equation typically appears like this:

$$\Delta P = -\frac{\mu}{k}Q - \frac{\rho}{k}\alpha Q^2,$$

where

- ΔP is the pressure drop across the porous medium,
- μ is the dynamic viscosity of the fluid,
- k is the permeability of the porous medium,
- ρ is the fluid density,
- α is the Forchheimer coefficient,
- Q is the volumetric flow rate.

The Darcy term in this equation is represented by the first term on the right-hand side. It is inversely proportional to the permeability k and proportional to the flow rate Q . The Forchheimer effect is taken into account by the second term, which is proportional to Q^2 . This effect becomes significant in more complex geometries or at higher flow rates. When flow through porous media changes from laminar to turbulent or when the porosity and geometry of the medium have a substantial impact on the flow characteristics, the Darcy-Forchheimer equation comes in handy.

2.8 Higher Grade Darcy Forchheimer Flow Model and its Applications

The term higher grade Darcy-Forchheimer flow model generally describes additions to or changes made to the fundamental Darcy-Forchheimer model in order to add more complexity or enhance accuracy in particular situations. An outline of these improvements and their uses is provided below:

2.8.1 Extended Forchheimer Terms

In order to more accurately represent non-linear effects at high flow velocities, higher-order terms in Forchheimer's law beyond the quadratic term may occasionally be taken into consideration. This may entail adding higher-order or cubic terms to the velocity dependency, like:

$$v = -\frac{k}{\mu}\nabla p - \frac{B_1}{\mu}v|v| - \frac{B_2}{\mu}v|v|^2 - \dots$$

These higher-order terms account for more complex fluid-solid interactions in porous media.

2.8.2 Non-Newtonian Fluid Models

The Darcy-Forchheimer model must be modified for fluids that behave non-Newtonianly, such as viscoelastic fluids, power-law fluids, or Herschel-Bulkley fluids. This entails describing how viscosity changes with shear rate using rheological parameters incorporated into the flow equations.

2.8.3 Anisotropic and Heterogeneous Porous Media

A common feature of porous media in the real world is heterogeneity, or the spatial variation in permeability, or anisotropic permeability, which is direction-dependent. In order to handle spatial variability, advanced Darcy-Forchheimer models incorporate stochastic techniques or introduce tensors to describe permeability.

2.8.4 Multi-Phase Flow

The Darcy-Forchheimer model can be expanded to include extra terms that take into account interfacial forces, capillary pressure effects, and the relative permeabilities of various phases in applications involving multiphase flow (such as oil-water or gas-liquid flows).

2.8.5 Thermal and Chemical Effects

The Darcy-Forchheimer model can be combined with mass and energy conservation equations for applications involving chemical transport (solute transport and reactions) or heat transfer (thermal convection in porous media). This enables precise simulation of transport processes in porous media and includes terms for heat conduction, advection, and dispersion.

Applications:

- **Petroleum Engineering:**

Modeling fluid flow in oil reservoirs considering non-linear flow behavior due to high velocities or complex fluid rheology.

- **Environmental Engineering:**

Studying ground water flow and contaminant transport in heterogeneous aquifers.

- **Geotechnical Engineering:**

Assessing seepage through soil structures considering anisotropic permeability and non-Newtonian behavior of pore fluids.

- **Biomedical Engineering:**

Simulating blood flow in porous tissues or artificial implants where non-Newtonian effects or porous structure influence flow characteristics.

For the purpose of representing more realistic flow behaviors in intricate porous media systems, higher grade Darcy-Forchheimer flow models are necessary. They have applications in many different fields, including engineering design, environmental remediation, and biomedical applications, where precise prediction of fluid flow and transport phenomena is essential. As computational and experimental techniques progress, these models also do, providing a greater understanding and means of simulating interactions between fluid-porous media in a variety of real-world scenarios.

2.9 Heat and Mass Transfer Phenomenon and Related Properties

Heat transfer is the phenomenon of transferring energy and entropy from one place to another. The formal definition of heat transfer and its different types are given below.

- **Heat Transfer**

Heat transfer is a branch of engineering that deals with the transfer of thermal energy from one point to another within a medium or from one medium to another due to the occurrence of a temperature difference. Heat transfer may take place in one or more of its three basic forms: conduction, convection, and radiation.

- **Mass Transfer**

Mass transfer is the flow of molecules from one body to another when these bodies are in contact or within a system consisting of two components when the distribution of materials is not uniform. When a copper plate is placed on a steel plate, some molecules from either side will diffuse into the otherside. When salt is placed in a glass and water poured over it, after sufficient time the salt molecules will diffuse into the water body. A more common example is drying of clothes or the evaporation of water spilled on the floor when water molecules diffuse into the air surrounding it. Usually, mass transfer takes place from a location where the particular component is proportionately high to a location where the component is proportionately low. Mass transfer may also take place due to potentials other than concentration difference.

- **Conduction**

Conduction is the transfer of heat from one part of a body at a higher temperature to another part of the same body at a lower temperature, or from one body at a higher temperature to another body in physical contact with it at a lower temperature. The conduction process takes place at the molecular level and involves the transfer of energy from the more energetic molecules to those with a lower energy level. This can be easily visualized within gases, where we note that the average kinetic energy of molecules in the higher-temperature regions is greater than that of those

in the lower-temperature regions. The more energetic molecules, being in constant and random motion, periodically collide with molecules of a lower energy level and exchange energy and momentum. In this manner, there is a continuous transport of energy from the high-temperature regions to those of lower temperature. In liquids, the molecules are more closely spaced than in gases, but the molecular energy exchange process is qualitatively similar to that in gases. In the solids that are nonconductors of electricity (dielectrics), heat is conducted by lattice waves caused by atomic motion. In the solids that are good conductors of electricity, this lattice vibration mechanism is only a small contribution to the energy transfer process, the principal contribution being that due to the motion of free electrons, which move in a similar way to molecules in a gas.

- **Convection**

The process of heat transfer between a surface and a fluid flowing in contact with it is called convection.

Types of Convection:

- **Natural Convection or Free Convection**

If the flow is caused by the buoyant forces generated by heating or cooling of the fluid the process is called as natural or free convection.

- **Forced Convection**

If the flow is caused by an external device like a pump or blower, it is termed as forced convection.

- **Radiation**

Radiation, or more correctly thermal radiation, is electromagnetic radiation emitted by a body by virtue of its temperature and at the expense of its internal energy. Thus thermal radiation is of the same nature as visible light, *X*-rays, and radio waves, the difference between them being in their wavelengths and the source of generation. The eye is sensitive to electromagnetic radiation in the region from 0.39 to 0.78 μm ; this is identified as the visible region of the spectrum. Radio waves have a wavelength of 1×10^3 to 2×10^{10} μm , and *X*-rays have wavelengths

of 1×10^{-5} to $2 \times 10^{-2} \mu m$, while the bulk of thermal radiation occurs in rays from approximately 0.1 to 100 μm . All heated solids and liquids, as well as some gases, emit thermal radiation. The transfer of energy by conduction requires the presence of a material medium, while radiation does not. In fact, radiation transfer occurs most efficiently in a vacuum. On the macroscopic level, the calculation of thermal radiation is based on the Stefan-Boltzmann law, which relates the energy flux emitted by an ideal radiator (or blackbody) to the fourth power of the absolute temperature.

2.10 Magnetohydrodynamics

The study of electrically conducting fluid motion in the presence of a magnetic field, such as that of liquid metals and plasmas, is known as magnetohydrodynamics. Magnetohydrodynamics' central premise is that current may be produced by magnetic fields in conductive fluids in motion, which in turn exerts force on the fluid and modifies the magnetic field itself. Hannes Alfvén, who understood the significance of the electric currents carried by a plasma and the magnetic field they create, established the fundamental equations of magnetohydrodynamics. Alfvén combined the fluid dynamics equations with Ampère and Faraday's electrodynamics rules to create a revolutionary mathematical theory. The physics of the sun, solar wind, and stellar atmospheres, as well as space plasmas in earth and planetary magnetospheres, were all explained by this theory.

Chapter 3

Basics of Finite Element Method

There are numerous similarities between the finite volume method and the finite element method. In **2D**, the domain is composed of a set of discrete finite elements, which are typically triangles or quadrilaterals; in **3D**, however, tetrahedra or hexahedra are more frequently utilized. Before the equations are integrated over the whole domain, they are multiplied by a weight function. To ensure continuity of the solution across element boundaries, the simplest finite element methods approximate the solution within each element using a linear shape function. From its values at the corners of the elements, such a function can be built. Typically, the weight function takes the same shape. After substituting this approximation into the weighted integral of the conservation law, the equations that need to be solved are derived by requiring that the integral's derivative with respect to each nodal value be zero. This means that the best solution within the set of permitted functions should be chosen (the one with the least residual). A collection of non-linear algebraic equations is the end product. Moreover, a brief discussion has been done for the numerical methodology adopted for the solution of governing equations. A simple two-dimensional poisson problem is also solved here to explain the numerical procedure for the achievement of results.

3.1 Formulation of FEM Model

The Formulation of FEM Model is based on the following methods:

- **Direct Method**
- **Variational Method**
- **Weighted Residuals**

If the physical formulation of the problem is described as a differential equation, then the most popular solution method is the **Method of Weighted Residuals**.

3.1.1 Weighted Residual Method

Method of weighted residual is useful method to find approximate solutions if the physical problem is described as a differential equation of the form

$$\mathcal{L}u = f, \quad (3.1)$$

where f is known function, u represent dependent variable and it is considered as unknown function, \mathcal{L} shows differential operator for spatial derivative of u . Using weighted residual method, approximate solution or trial solution $\tilde{u}(x)$ which satisfy boundary conditions is assumed. Since \tilde{u} is an approximate solution, so it will not satisfies the differential equation (3.1).

$$R(\tilde{u}(x)) = \mathcal{L}\tilde{u} - f \neq 0, \quad (3.2)$$

where

$$\tilde{u}(x) = \sum_{i=1}^N u_i \phi_i(x), \quad (3.3)$$

and

$$\tilde{u}(x) = u_1 \phi_1(x) + u_2 \phi_2(x) + u_3 \phi_3(x) + \dots + u_N \phi_N(x).$$

The functions ϕ_i are used as basis functions. As the function space ϕ has finite dimensions, in general the expression (3.3) cannot satisfy the differential equation (3.1) in the domain for each point. This implies that the approximate solution or trial solution \tilde{u} cannot be same like u (exact solution). By letting N grow, the approximate solution becomes very close to the exact solution. From residual (3.2), by finding a way to make this residual small or approximately zero, the approximated solution of BVP can be evaluated. In finite

element method (FEM), the approximate solution can be obtained by making suitable number of weighted integrals of residual over the domain Ω , be zero.

$$\int_{\Omega} wRd\Omega = 0, \quad (3.4)$$

where $w = \{w_i; i = 1, 2, \dots, N\}$ is the suitable collection of weighting functions, which shows that obtained approximated solution is for N being finite.

$$w(x) = \sum_{i=1}^N w_i \psi_i(x) = w_1 \psi_1(x) + w_2 \psi_2(x) + \dots + w_N \psi_N(x), \quad (3.5)$$

where $\psi_i(x)$ are “known functions” and w_i are “constant parameters”.

By using (3.5) in (3.4), we get

$$[A]\mathbf{u} = \mathbf{F},$$

as a system of algebraic equations. By solving above system for N –unknowns, u_i is provided that a suitable weight function w is selected.

Example To obtain approximate solutions to a differential governing equation.

$$\frac{d^2u}{dx^2} - u = -x, \quad 0 < x < 1, \quad (3.6)$$

$$u(0) = 0, \quad \text{and} \quad u(1) = 0.$$

- The first step in the methods of weighted residual is to assume a trial function which contains unknown coefficients to be determined later. For example, a trial function,

$$\tilde{u}(x) = ax(1 - x) = ax - ax^2, \quad (3.7)$$

is selected as an approximate solution to Eq. (3.6). Here, “ \sim ” denotes an approximate solution which is usually different from the exact solution.

- The trial function is chosen here such that it satisfies the boundary conditions i.e.,

$$\tilde{\mathbf{u}}(0) = 0 \quad \text{and} \quad \tilde{\mathbf{u}}(1) = 0,$$

and it has one unknown coefficient “ \mathbf{a} ” to be determined.

- In general, accuracy of an approximated solution is dependent upon proper selection of the trial function. However, a simple form of trial function is selected for the present example to show the basic procedure of the methods of weighted residual.
- Once a trial function is selected, residual is computed by substituting the trial function into the differential equation. That is, the residual $R(x)$ becomes

$$\begin{aligned} R(x) &= \frac{d^2\tilde{u}}{dx^2} - \tilde{u} + x \\ &= -2a - ax(1-x) + x. \\ R(x) &= -2a - ax + ax^2 + x. \end{aligned} \tag{3.8}$$

- Because \tilde{u} is different from the exact solution, the residual does not vanish for all values of “ x ” within the domain. Some of the methods of weighted residual are explained below.

In the Galerkin Method, the weight function w is the derivative of the approximating function $\tilde{u}(x)$ with respect to the unknown coefficient (a):

$$\begin{aligned} w &= \frac{d\tilde{u}(x)}{da} = \frac{d}{da} (ax - ax^2). \\ &= x - x^2. \end{aligned}$$

So the weighted residual statement becomes

$$\begin{aligned} \int_0^1 wR(x)dx &= 0. \\ \int_0^1 (x - x^2)\{-2a - ax + ax^2 + x\}dx &= 0. \end{aligned}$$

Again, the math is straightforward but tedious. Direct evaluation leads to the algebraic equation:

$$a = \frac{0.083}{0.366} = 0.2267.$$

Now putting $a = 0.2267$ in (3.7), we get

$$\tilde{u}(x) = ax - ax^2 = (0.2267)x - (0.2267)x^2 = 0.2267x(1-x).$$

3.1.1.1 Galerkin Finite Element Method

This is a Finite Element Analysis technique which uses “Galerkin weighted residual method” to get variational formulation of continuous problem for each individual element. These elements are the subdomains of the whole physical domain Ω . Main steps of GFEM for one-dimensional problem are given below:

- Discretize the whole computational domain say $\Omega = [c, d]$ of physical problem into different number of small subdomains, i.e., $y_0 = c, y_1, \dots, y_L = d$. Define the size for each subdomain say h_i such that $h_i = (y_{i+1} - y_i)$, for $i = 1, 2, \dots, (L - 1)$. Each subdomain is known as element ‘ e ’. Here y_i 's are nodal points or node values and h_i is called mesh size or element size. All the elements should be non-overlapping, i.e., $e_i \cap e_j = 0$, for $i \neq j$.
- The strong form of PDEs of the given problem is converted to weak form. To get weak formulation, multiply the differential equation by the weight functions (test functions) say w . These test functions must satisfy the homogeneous Dirichlet boundary conditions for the Dirichlet boundary data. Apply integration by parts using Neumann and Robin type boundary conditions to set boundary integrals if required.
- Approximate the infinite dimensional solution and test spaces say \mathbf{v} and \mathbf{W} respectively by constructing or defining finite dimensional spaces say \mathbf{v}_h and \mathbf{W}_h for the achievement of discrete solution. Let $\mathbf{v}_h \approx \mathbf{v}$ and $\mathbf{W}_h \approx \mathbf{W}$, where \mathbf{v}_h and \mathbf{W}_h are known as finite dimensional trial solution and test spaces respectively.
- Apply Galerkin discretization to approximate finite dimensional trial solution and trial test spaces. Choose the approximate solution function v_h as find $v_h \in (\mathbf{v}_h \subset \mathbf{v})$ such that $a(v_h, w_h) = b(w_h)$, for all $w_h \in (\mathbf{W}_h \subset \mathbf{W})$. Here $a(v_h, w_h)$ represents bilinear formulation while $b(w_h)$ notifies linear formulation of the respective differential equation.
- Represent the approximate solution over an element with finite dimensional trial solution space \mathbf{v}_h by setting the linear combination of basis function φ_j 's with the

nodal unknowns v'_j s such that

$$v_h^e = \sum_{j=1}^{NEN} v_j^e \varphi_j^e. \quad j = 1, 2, \dots, NEN. \quad (3.9)$$

These basis functions φ'_i s and interpolation polynomial are of same type (geometry). Similarly choose a set of linearly independent basis function φ'_i s for finite dimensional trial test space W_h such that

$$w_h^e = \sum_{j=1}^{NEN} w_j^e \varphi_j^e. \quad i = 1, 2, \dots, NEN. \quad (3.10)$$

- Substitute these approximate solution functions v_h^e and approximate test functions w_h^e from Eqs. (3.9) and (3.10) into variational formulation of problem which yields a linear elemental system of algebraic equations as given below

$$c \left(\sum_{j=1}^{NEN} v_j^e \varphi_j^e, \varphi_i^e \right) = d(\varphi_i^e), \quad (i, j) = 1, 2, \dots, NEN. \quad (3.11)$$

$$\sum_{j=1}^{NEN} c(\varphi_j^e, \varphi_i^e) v_j^e = d(\varphi_i^e), \quad (i, j) = 1, 2, \dots, NEN. \quad (3.12)$$

where v_j^e are the solution values at respective nodal points of element e .

- The above formulations will generate an algebraic linear system of equations, which contains equal number of equations as the number of elemental nodes and will be written in compact form as

$$[A^e] \{\mathbf{v}^e\} = \{B^e\}. \quad (3.13)$$

- Combine all local elemental systems like in Eq. (3.13) to get a global system of equations which will give the approximate solution over the whole computational domain $\Omega = [c, d]$.

$$[A^e] \{\mathbf{v}\} = \{B\}. \quad (3.14)$$

- The global system of equations in Eq. (3.14) comprises of algebraic equations is then solved by using any linear solver to get the final approximate solution.

Consider a following 2D poisson problem for the illustration of solution methodology by GFEM.

Example Given below is a steady 2D poisson equation over the domain.

$$-\nabla \cdot (\nabla S) = f. \quad \text{or} \quad (3.15)$$

$$-\left(\frac{\partial^2 S}{\partial x^2} + \frac{\partial^2 S}{\partial y^2}\right) = f \quad \text{in } \Omega \quad (3.16)$$

$$S = 0 \quad \text{on } d\Omega \quad (3.17)$$

S is to be found, f is known, Ω is domain which is bounded, open and connected and $\partial\Omega$ is the boundary.

- To make weak formulation, select test function $w(x, y)$ satisfying the homogenous Dirichlet boundary condition, i.e., $w(x, y) = 0$ on $\partial\Omega$. By multiplying Eq. (3.15) with test function and integrate over the elemental domain gives the following variational form

$$-\int_{\Omega^e} w \Delta S d\Omega = \int_{\Omega^e} w f d\Omega, \quad \text{or} \quad (3.18)$$

$$-\int_{\Omega^e} w \frac{\partial}{\partial x} \left(\frac{\partial S}{\partial x} d\Omega \right) - \int_{\Omega^e} w \frac{\partial}{\partial y} \left(\frac{\partial S}{\partial y} d\Omega \right) = \int_{\Omega^e} w f d\Omega. \quad (3.19)$$

- Reduce second order derivatives of S in Eq. (3.19) to get first order derivatives by applying following Green's identity

$$\int_{\Omega} w \frac{\partial G}{\partial n} d\Omega = - \int_{\Omega} G \frac{\partial w}{\partial n} d\Omega + \oint_{\Gamma} w G \rightarrow n d\Gamma, \quad (3.20)$$

we get the following elemental weak formulation

$$\int_{\Omega^e} \left(\frac{\partial w}{\partial x} \frac{\partial S}{\partial x} + \frac{\partial w}{\partial y} \frac{\partial S}{\partial y} \right) d\Omega = \int_{\Omega^e} w f d\Omega. \quad (3.21)$$

- Approximate the solution over the element e by using

$$S^e(x, y) = \sum_{j=1}^{NEN} S_j^e \varphi_j^e(x, y), \quad (3.22)$$

where S_j 's are approximate solution values at the elemental nodal points and φ_j 's are preselected basis functions.

- Substitute the approximate solution Eq. (3.22) into variational formulation Eq. (3.21) we get

$$\int_{\Omega^e} \left[\left(\sum_{j=1}^{NEN} S_j^e \frac{\partial \varphi_j^e}{\partial x} \right) \frac{\partial w}{\partial x} + \left(\sum_{j=1}^{NEN} S_j^e \frac{\partial \varphi_j^e}{\partial y} \right) \frac{\partial w}{\partial y} \right] d\Omega = \int_{\Omega^e} w f d\Omega. \quad (3.23)$$

- For Galerkin FEM approximation to choose weight function of type $w(x, y) = \phi_i^e(x, y)$ to get the following elemental system

$$\int_{\Omega^e} \left[\left(\sum_{j=1}^{NEN} S_j^e \frac{\partial \varphi_j^e}{\partial x} \right) \frac{\partial \phi_i^e}{\partial x} + \left(\sum_{j=1}^{NEN} S_j^e \frac{\partial \varphi_j^e}{\partial y} \right) \frac{\partial \phi_i^e}{\partial y} \right] d\Omega = \int_{\Omega^e} \phi_i^e f d\Omega. \quad (3.24)$$

Equation (3.22) gives

$$\sum_{j=1}^{NEN} \left[\int_{\Omega^e} \left(\frac{\partial \varphi_j^e}{\partial x} \frac{\partial \phi_i^e}{\partial x} + \frac{\partial \varphi_j^e}{\partial y} \frac{\partial \phi_i^e}{\partial y} \right) d\Omega \right] \{S_j^e\} = \int_{\Omega^e} \phi_i^e f d\Omega. \quad (3.25)$$

- The i^{th} elemental system in Eq. (3.25) will generate a discrete system of algebraic i_{th} number of equations which is expressed as

$$AS = F, \quad (3.26)$$

where A^e , S^e , F^e are elemental stiffness matrix, elemental solution and elemental force vector matrix respectively.

- All such local elemental systems combine to give global system as below, which will finally provide the approximate solution of problem in Eq. (3.15).

$$\mathbb{A}\mathbf{S} = \mathbf{F}, \quad (3.27)$$

Chapter 4

Mathematical Model of Two Dimensional higher grade Darcy Forchheimer porous model

To derive the mathematical problem we consider an unsteady mixed convective higher order flow through a porous-medium. The time $t > 0$, and the particles of fluid are assumed to attain the flow velocity generally represented by the vector field

$$V = (u, v, w)^T. \quad (4.1)$$

In this consideration, we consider square cavity as shown in Figure 4.1. The velocity therefore reduces to $V = (u, v)^T$. The strain in the motion of the particles is calculated from the first and second order Rivlin-Ericksen tensors defined respectively by

$$A_1 = \nabla \mathbf{V} + (\nabla \mathbf{V})^T, \quad (4.2)$$

and

$$A_2 = \partial_t A_1 + (\mathbf{V} \cdot \nabla) A_1 + (\nabla \mathbf{V}) \cdot A_1 + A_1 \cdot (\nabla \mathbf{V})^T, \quad (4.3)$$

The strain leads to Cauchy stress which is assumed here in the framework of higher grade continuum as follows

$$\tau = -pI + \mu A_1 + \alpha_1 A_2 + \alpha_2 A_1 \cdot A_1, \quad (4.4)$$

where p presents the hydrostatic pressure, I denotes the identity tensor, $\mu > 0$, characterize nanofluid dynamic viscosity. The parameters α_1 and α_2 are material constants.

$$\alpha_1 \geq 0, \quad \mu \geq 0 \quad \text{and} \quad \alpha_1 + \alpha_2 = 0.$$

Following the Darcy law in case of viscoelastic porous medium is taken to be

$$\nabla p = -\frac{\varphi}{K} \left(\mu + \alpha_1 \frac{\partial}{\partial t} \right) \mathbf{V}. \quad (4.5)$$

Where K represents permeable parameter and φ denotes the porosity parameter in the porous nano-medium.

The Darcy-Forchheimer resistance 'r' is defined as

$$r = \nabla p - \frac{c_F \rho \varphi}{\sqrt{K}} \mathbf{V}^2. \quad (4.6)$$

putting Eq. (4.5) in eq. (4.6), we get

$$r = -\frac{\varphi}{K} \left(\mu \mathbf{V} + \alpha_1 \frac{\partial \mathbf{V}}{\partial t} \right) - \frac{c_F \rho \varphi}{\sqrt{K}} \mathbf{V}^2.$$

Consider Eq. (4.4),

$$\tau = -p\mathbf{I} + \mu A_1 + \alpha_1 A_2 + \alpha_2 A_1^2,$$

where

$$A_1 = \nabla \mathbf{V} + (\nabla \mathbf{V})^T, \quad \text{and} \quad A_2 = \frac{dA_1}{dt} + A_1(\nabla \mathbf{V}) + (\nabla \mathbf{V})^T A_1.$$

let $\alpha_2 = -\alpha_1$, then Eq. (4.4) becomes:

$$\tau = -p\mathbf{I} + \mu[\nabla \mathbf{V} + (\nabla \mathbf{V})^T] + \alpha_1 \left[\frac{dA_1}{dt} + A_1(\nabla \mathbf{V}) + (\nabla \mathbf{V})^T A_1 \right] + (-\alpha_1)A_1^2,$$

$$\tau = -p\mathbf{I} + \mu[\nabla \mathbf{V} + (\nabla \mathbf{V})^T] + \alpha_1 \left[\frac{dA_1}{dt} + A_1(\nabla \mathbf{V}) + (\nabla \mathbf{V})^T A_1 - A_1^2 \right],$$

$$\Rightarrow \tau = -p\mathbf{I} + \mu[\nabla \mathbf{V} + (\nabla \mathbf{V})^T] + \alpha_1 \left[\frac{\partial A_1}{\partial t} + (\mathbf{V} \cdot \nabla) A_1 + A_1(\nabla \mathbf{V}) + (\nabla \mathbf{V})^T A_1 - A_1^2 \right],$$

$$\Rightarrow \tau = -p\mathbf{I} + \mu[\nabla \mathbf{V} + (\nabla \mathbf{V})^T] + \alpha_1 \left[\frac{\partial A_1}{\partial t} \right] + \alpha_1 \left[(\mathbf{V} \cdot \nabla) A_1 + A_1(\nabla \mathbf{V}) + (\nabla \mathbf{V})^T A_1 - A_1^2 \right],$$

$$\begin{aligned} \Rightarrow \tau &= -p\mathbf{I} + \mu[\nabla\mathbf{V} + (\nabla\mathbf{V})^T] \\ &\quad + \alpha_1 \frac{\partial}{\partial t} \left(\nabla\mathbf{V} + (\nabla\mathbf{V})^T \right) + \alpha_1 \left[(\mathbf{V} \cdot \nabla)A_1 + A_1(\nabla\mathbf{V}) + (\nabla\mathbf{V})^T A_1 - A_1^2 \right]. \end{aligned} \quad (4.7)$$

Since

$$A_1 = \nabla\mathbf{V} + (\nabla\mathbf{V})^T,$$

In matrix form

$$A_1 = \begin{pmatrix} \frac{\partial u}{\partial x} & \frac{\partial u}{\partial y} \\ \frac{\partial v}{\partial x} & \frac{\partial v}{\partial y} \end{pmatrix} + \begin{pmatrix} \frac{\partial u}{\partial x} & \frac{\partial v}{\partial x} \\ \frac{\partial u}{\partial y} & \frac{\partial v}{\partial y} \end{pmatrix} = \begin{pmatrix} 2\frac{\partial u}{\partial x} & \frac{\partial u}{\partial y} + v_{,x} \\ v_{,x} + u_{,y} & 2v_{,y} \end{pmatrix}. \quad (4.8)$$

Consider

$$\begin{aligned} A_1 \cdot A_1 &= \begin{pmatrix} 2\frac{\partial u}{\partial x} & \frac{\partial u}{\partial y} + v_{,x} \\ v_{,x} + u_{,y} & 2v_{,y} \end{pmatrix} \begin{pmatrix} 2\frac{\partial u}{\partial x} & \frac{\partial u}{\partial y} + v_{,x} \\ v_{,x} + u_{,y} & 2v_{,y} \end{pmatrix}, \\ \Rightarrow A_1^2 &= \begin{pmatrix} 4u^2_{,x} + (u_{,y} + v_{,x})(v_{,x} + u_{,y}) & 2u_{,x}(u_{,y} + v_{,x}) + (u_{,y} + v_{,x})(2v_{,y}) \\ 2u_{,x}(v_{,x} + u_{,y}) + 2v_{,y}(v_{,x} + u_{,y}) & (v_{,x} + u_{,y})(v_{,x} + u_{,y}) + 4v^2_{,y} \end{pmatrix}. \end{aligned}$$

As,

$$(\mathbf{V} \cdot \nabla) = \mathbf{V}_m e_m \cdot \partial_k e_k = \mathbf{V}_k \partial_k = (u\partial_x + v\partial_y).$$

$$\Rightarrow (\mathbf{V} \cdot \nabla)A_1 = (u\partial_x + v\partial_y) \begin{pmatrix} A_1^{11} & A_1^{12} \\ A_1^{21} & A_1^{22} \end{pmatrix}.$$

Also,

$$(A_1)(\nabla\mathbf{V}) = \begin{pmatrix} A_{11} & A_{12} \\ A_{21} & A_{22} \end{pmatrix} \begin{pmatrix} u_{,x} & u_{,y} \\ v_{,x} & v_{,y} \end{pmatrix} = \begin{pmatrix} A_{11}u_{,x} + A_{12}v_{,x} & A_{11}u_{,y} + A_{12}v_{,y} \\ A_{21}u_{,x} + A_{22}v_{,x} & A_{21}u_{,y} + A_{22}v_{,y} \end{pmatrix},$$

and

$$(\nabla\mathbf{V})^T A_1 = \begin{pmatrix} u_{,x} & v_{,x} \\ u_{,y} & v_{,y} \end{pmatrix} \begin{pmatrix} A_{11} & A_{12} \\ A_{21} & A_{22} \end{pmatrix} = \begin{pmatrix} A_{11}u_{,x} + A_{12}v_{,x} & A_{21}u_{,x} + A_{22}v_{,x} \\ A_{11}u_{,y} + A_{12}v_{,y} & A_{21}u_{,y} + A_{22}v_{,y} \end{pmatrix}.$$

Thus τ in Eq. (4.7) becomes:

$$\begin{aligned} \tau = & -p + \mu[A_1] + \alpha_1 \frac{\partial}{\partial t} (A_1) + \alpha_1 \left[(u\partial_x + v\partial_y) \begin{pmatrix} A_1^{11} & A_1^{12} \\ A_1^{21} & A_1^{22} \end{pmatrix} \right] \\ & + \alpha_1 \left[\begin{pmatrix} A_{11} & A_{12} \\ A_{21} & A_{22} \end{pmatrix} \begin{pmatrix} u,x & u,y \\ v,x & v,y \end{pmatrix} = \begin{pmatrix} A_{11}u,x + A_{12}v,x & A_{11}u,y + A_{12}v,y \\ A_{21}u,x + A_{22}v,x & A_{21}u,y + A_{22}v,y \end{pmatrix} \right] \\ & + \alpha_1 \left[\begin{pmatrix} u,x & v,x \\ u,y & v,y \end{pmatrix} \begin{pmatrix} A_{11} & A_{12} \\ A_{21} & A_{22} \end{pmatrix} = \begin{pmatrix} A_{11}u,x + A_{12}v,x & A_{21}u,x + A_{22}v,x \\ A_{11}u,y + A_{12}v,y & A_{21}u,y + A_{22}v,y \end{pmatrix} \right] \\ & - \alpha_1 \left[\begin{pmatrix} 4u^2_{,x} + (u,y + v,x)(v,x + u,y) & 2u,x(u,y + v,x) + (u,y + v,x)(2v,y) \\ 2u,x(v,x + u,y) + 2v,y(v,x + u,y) & (v,x + u,y)(v,x + u,y) + 4v^2_{,y} \end{pmatrix} \right]. \end{aligned}$$

or,

$$\begin{aligned} \tau = & -p + \mu \left[\begin{pmatrix} 2\frac{\partial u}{\partial x} & \frac{\partial u}{\partial y} + v,x \\ v,x + u,y & 2v,y \end{pmatrix} \right] \\ & + \alpha_1 \frac{\partial}{\partial t} \left[\begin{pmatrix} 2\frac{\partial u}{\partial x} & \frac{\partial u}{\partial y} + v,x \\ v,x + u,y & 2v,y \end{pmatrix} \right] + \alpha_1 \left[(u\partial_x + v\partial_y) \begin{pmatrix} A_1^{11} & A_1^{12} \\ A_1^{21} & A_1^{22} \end{pmatrix} \right] \\ & + \alpha_1 \left[\begin{pmatrix} A_{11} & A_{12} \\ A_{21} & A_{22} \end{pmatrix} \begin{pmatrix} u,x & u,y \\ v,x & v,y \end{pmatrix} = \begin{pmatrix} A_{11}u,x + A_{12}v,x & A_{11}u,y + A_{12}v,y \\ A_{21}u,x + A_{22}v,x & A_{21}u,y + A_{22}v,y \end{pmatrix} \right] \\ & + \alpha_1 \left[\begin{pmatrix} u,x & v,x \\ u,y & v,y \end{pmatrix} \begin{pmatrix} A_{11} & A_{12} \\ A_{21} & A_{22} \end{pmatrix} = \begin{pmatrix} A_{11}u,x + A_{12}v,x & A_{21}u,x + A_{22}v,x \\ A_{11}u,y + A_{12}v,y & A_{21}u,y + A_{22}v,y \end{pmatrix} \right] \\ & - \alpha_1 \left[\begin{pmatrix} 4u^2_{,x} + (u,y + v,x)(v,x + u,y) & 2u,x(u,y + v,x) + (u,y + v,x)(2v,y) \\ 2u,x(v,x + u,y) + 2v,y(v,x + u,y) & (v,x + u,y)(v,x + u,y) + 4v^2_{,y} \end{pmatrix} \right]. \end{aligned}$$

The components of the stress tensor τ are thus

$$\begin{aligned} \tau_{11} = & -p + \mu \left(2\frac{\partial u}{\partial x} \right) + \alpha_1 \frac{\partial}{\partial t} \left(2\frac{\partial u}{\partial x} \right) + \alpha_1 \left[(u\partial_x + v\partial_y)A_{11} \right. \\ & \left. + (A_{11}u,x + A_{12}v,x) + (A_{11}u,x + A_{12}v,x) - 4u^2_{,x} - (u,y + v,x)(v,x + u,y) \right], \end{aligned}$$

or,

$$\tau_{11} = -p + 2\mu u_{,x} + 2\alpha_1 \frac{\partial}{\partial t}(u_{,x}) + \alpha_1 \left[(u\partial_x + v\partial_y)A_{11} + 2(A_{11}u_{,x} + A_{12}v_{,x}) - 4u^2_{,x} - (u_{,y} + v_{,x})(v_{,x} + u_{,y}) \right],$$

$$\tau_{22} = -p + \mu(2v_{,y}) + \alpha_1 \frac{\partial}{\partial t}(2v_{,y}) + \alpha_1 \left[(u\partial_x + v\partial_y)A_{22} + (A_{21}u_{,y} + A_{22}v_{,y}) + (A_{21}u_{,y} + A_{22}v_{,y}) - 4v^2_{,y} - (v_{,x} + u_{,y})(v_{,x} + u_{,y}) \right],$$

or,

$$\tau_{22} = -p + 2\mu v_{,y} + 2\alpha_1 \frac{\partial}{\partial t}(v_{,y}) + \alpha_1 \left[(u\partial_x + v\partial_y)A_{22} + 2(A_{21}u_{,y} + A_{22}v_{,y}) - 4v^2_{,y} - (v_{,x} + u_{,y})(v_{,x} + u_{,y}) \right],$$

$$\tau_{21} = \left(\mu + \alpha_1 \frac{\partial}{\partial t} \right) [v_{,x} + u_{,y}] + \alpha_1 \left[(u\partial_x + v\partial_y)A_{21} + A_{21}u_{,x} + A_{22}v_{,x} + A_{11}u_{,y} + A_{12}v_{,y} - 2[u_{,x}(v_{,x} + u_{,y}) + v_{,y}(v_{,x} + u_{,y})] \right],$$

Now, since

$$\nabla \cdot \tau = \partial_m e_m \cdot \tau_{ij} e_i \otimes e_j = \partial_i \tau_{ij} e_j = (\partial_1 \tau_{11} + \partial_2 \tau_{21}, \partial_1 \tau_{12} + \partial_2 \tau_{22}),$$

$$\therefore \tau_{12} = \left(\mu + \alpha_1 \frac{\partial}{\partial t} \right) [u_{,y} + v_{,x}] + \alpha_1 \left[(u\partial_x + v\partial_y)A_{12} + A_{11}u_{,y} + A_{12}v_{,y} + A_{21}u_{,x} + A_{22}v_{,x} - 2[u_{,x}(u_{,y} + v_{,x}) + v_{,y}(u_{,y} + v_{,x})] \right].$$

Now, the conservation law of momentum is considered in porous medium is given by

$$\rho \left(\frac{\partial V}{\partial t} + V \cdot \nabla \right) V = (\nabla \cdot \tau + r) + b + g(\theta - \theta_o)$$

where θ is the temperature field.

The x -component of equation is given by

$$\begin{aligned} \frac{\partial u}{\partial t} + u \frac{\partial u}{\partial x} + v \frac{\partial u}{\partial y} &= \frac{1}{\rho} \left[\partial_x \tau_{11} + \partial_y \tau_{21} - \frac{\varphi}{K} \left(\mu + \alpha_1 \frac{\partial}{\partial t} \right) u - \left(\frac{c_F \rho \varphi}{\sqrt{K}} \right) u^2 \right] \\ &\quad + b_x + g_x(\beta_\theta)(\theta - \theta_o), \end{aligned} \tag{4.9}$$

The y -component of equation is given by

$$\begin{aligned} \frac{\partial v}{\partial t} + u \frac{\partial v}{\partial x} + v \frac{\partial v}{\partial y} = \frac{1}{\rho} \left[\partial_x \tau_{12} + \partial_y \tau_{22} - \frac{\varphi}{K} \left(\mu + \alpha_1 \frac{\partial}{\partial t} \right) v - \left(\frac{c_F \rho \varphi}{\sqrt{K}} \right) v^2 \right] \\ + b_y + g_y(\beta_\theta)(\theta - \theta_o). \end{aligned} \quad (4.10)$$

In Eq. (4.9) and Eq. (4.10), we are left to calculate the terms $(\partial_x \tau_{11} + \partial_y \tau_{21})$ and $(\partial_x \tau_{12} + \partial_y \tau_{22})$, respectively.

Here we show the calculations of the following terms $\partial_x \tau_{11}$, $\partial_y \tau_{21}$, $\partial_x \tau_{12}$, $\partial_y \tau_{22}$. The term $\partial_x \tau_{11}$ is expressed as

$$\begin{aligned} \bullet \partial_x \tau_{11} = \frac{\partial}{\partial x} \left[-p + 2 \left(\mu + \alpha_1 \frac{\partial}{\partial t} \right) \frac{\partial u}{\partial x} + \alpha_1 \left\{ \left(u \frac{\partial}{\partial x} + v \frac{\partial}{\partial y} \right) A_{11} + 2 \left(A_{11} \frac{\partial u}{\partial x} + A_{12} \frac{\partial v}{\partial x} \right) \right. \right. \\ \left. \left. - 4 \left(\frac{\partial u}{\partial x} \right)^2 - \left(\frac{\partial u}{\partial y} + \frac{\partial v}{\partial x} \right)^2 \right\} \right]. \end{aligned} \quad (4.11)$$

Since, A_1 is given as in Eq. (4.8)

$$A_1 = \begin{pmatrix} A_{11} & A_{12} \\ A_{21} & A_{22} \end{pmatrix} = \begin{pmatrix} 2 \frac{\partial u}{\partial x} & \frac{\partial u}{\partial y} + v_{,x} \\ v_{,x} + u_{,y} & 2v_{,y} \end{pmatrix}.$$

using it in Eq. (4.11), we obtain

$$\begin{aligned} \partial_x \tau_{11} &= -\frac{\partial p}{\partial x} + 2 \left(\mu + \alpha_1 \frac{\partial}{\partial t} \right) \frac{\partial}{\partial x} \left(\frac{\partial u}{\partial x} \right) + \alpha_1 \frac{\partial}{\partial x} \left\{ \left(u \frac{\partial}{\partial x} + v \frac{\partial}{\partial y} \right) \left(2 \frac{\partial u}{\partial x} \right) \right. \\ &\quad \left. + 2 \left(\left(2 \frac{\partial u}{\partial x} \right) \frac{\partial u}{\partial x} + \left(\frac{\partial u}{\partial y} + \frac{\partial v}{\partial x} \right) \frac{\partial v}{\partial x} \right) - 4 \left(\frac{\partial u}{\partial x} \right)^2 - \left(\frac{\partial u}{\partial y} + \frac{\partial v}{\partial x} \right)^2 \right\}, \\ \Rightarrow \frac{\partial \tau_{11}}{\partial x} &= -\frac{\partial p}{\partial x} + 2 \left(\mu + \alpha_1 \frac{\partial}{\partial t} \right) \frac{\partial^2 u}{\partial x^2} + \alpha_1 \frac{\partial}{\partial x} \left\{ 2 \left(u \frac{\partial^2 u}{\partial x^2} + v \frac{\partial^2 u}{\partial x \partial y} \right) \right. \\ &\quad \left. + 2 \left(2 \left(\frac{\partial u}{\partial x} \right)^2 + \frac{\partial u}{\partial y} \frac{\partial v}{\partial x} + \left(\frac{\partial v}{\partial x} \right)^2 \right) - 4 \left(\frac{\partial u}{\partial x} \right)^2 - \left(\frac{\partial u}{\partial y} + \frac{\partial v}{\partial x} \right)^2 \right\}, \\ \Rightarrow \frac{\partial \tau_{11}}{\partial x} &= -\frac{\partial p}{\partial x} + 2 \left(\mu + \alpha_1 \frac{\partial}{\partial t} \right) \frac{\partial^2 u}{\partial x^2} + \alpha_1 \frac{\partial}{\partial x} \left\{ 2 \left(u \frac{\partial^2 u}{\partial x^2} + v \frac{\partial^2 u}{\partial x \partial y} \right) \right. \\ &\quad \left. + 4 \left(\frac{\partial u}{\partial x} \right)^2 + 2 \frac{\partial u}{\partial y} \frac{\partial v}{\partial x} + 2 \left(\frac{\partial v}{\partial x} \right)^2 - 4 \left(\frac{\partial u}{\partial x} \right)^2 - \left(\frac{\partial u}{\partial y} \right)^2 - \left(\frac{\partial v}{\partial x} \right)^2 - 2 \frac{\partial u}{\partial y} \frac{\partial v}{\partial x} \right\}, \end{aligned}$$

$$\begin{aligned} \Rightarrow \frac{\partial \tau_{11}}{\partial x} = & -\frac{\partial p}{\partial x} + 2\left(\mu + \alpha_1 \frac{\partial}{\partial t}\right) \frac{\partial^2 u}{\partial x^2} + \alpha_1 \frac{\partial}{\partial x} \left\{ 2\left(u \frac{\partial^2 u}{\partial x^2} + v \frac{\partial^2 u}{\partial x \partial y}\right) \right. \\ & \left. + 2\left(\frac{\partial v}{\partial x}\right)^2 - \left(\frac{\partial u}{\partial y}\right)^2 - \left(\frac{\partial v}{\partial x}\right)^2 \right\}. \end{aligned} \quad (4.12)$$

The term $\partial_y \tau_{21}$ is expressed as:

$$\begin{aligned} \bullet \frac{\partial \tau_{21}}{\partial y} = & \left(\mu + \alpha_1 \frac{\partial}{\partial t}\right) \frac{\partial}{\partial y} \left(\frac{\partial v}{\partial x} + \frac{\partial u}{\partial y}\right) + \alpha_1 \frac{\partial}{\partial y} \left[\left(u \frac{\partial}{\partial x} + v \frac{\partial}{\partial y}\right) A_{21} + A_{21} \frac{\partial u}{\partial x} + A_{22} \frac{\partial v}{\partial x} \right. \\ & \left. + A_{11} \frac{\partial u}{\partial y} + A_{12} \frac{\partial v}{\partial y} - 2\left\{ \frac{\partial u}{\partial x} \left(\frac{\partial v}{\partial x} + \frac{\partial u}{\partial y}\right) + \frac{\partial v}{\partial y} \left(\frac{\partial v}{\partial x} + \frac{\partial u}{\partial y}\right) \right\} \right]. \end{aligned}$$

Using A_{11} , A_{12} , A_{21} , A_{22} from Eq. (4.8) gives

$$\begin{aligned} \frac{\partial \tau_{21}}{\partial y} = & \left(\mu + \alpha_1 \frac{\partial}{\partial t}\right) \left(\frac{\partial^2 v}{\partial x \partial y} + \frac{\partial^2 u}{\partial y^2}\right) + \alpha_1 \frac{\partial}{\partial y} \left[\left(u \frac{\partial}{\partial x} + v \frac{\partial}{\partial y}\right) \left(\frac{\partial v}{\partial x} + \frac{\partial u}{\partial y}\right) \right. \\ & \left. + \left(\frac{\partial v}{\partial x} + \frac{\partial u}{\partial y}\right) \frac{\partial u}{\partial x} + \left(2 \frac{\partial v}{\partial y}\right) \frac{\partial v}{\partial x} + \left(2 \frac{\partial u}{\partial x}\right) \frac{\partial u}{\partial y} + \left(\frac{\partial u}{\partial y} + \frac{\partial v}{\partial x}\right) \frac{\partial v}{\partial y} - 2\left\{ \frac{\partial u}{\partial x} \left(\frac{\partial v}{\partial x} \right. \right. \right. \\ & \left. \left. \left. + \frac{\partial u}{\partial y}\right) + \frac{\partial v}{\partial y} \left(\frac{\partial v}{\partial x} + \frac{\partial u}{\partial y}\right) \right\} \right], \\ \Rightarrow \frac{\partial \tau_{21}}{\partial y} = & \left(\mu + \alpha_1 \frac{\partial}{\partial t}\right) \left(\frac{\partial^2 v}{\partial x \partial y} + \frac{\partial^2 u}{\partial y^2}\right) + \alpha_1 \frac{\partial}{\partial y} \left[u \frac{\partial^2 v}{\partial x^2} + u \frac{\partial^2 u}{\partial x \partial y} + v \frac{\partial^2 v}{\partial x \partial y} + v \frac{\partial^2 u}{\partial y^2} \right. \\ & \left. + \frac{\partial v}{\partial x} \frac{\partial u}{\partial x} + \frac{\partial u}{\partial y} \frac{\partial u}{\partial x} + 2 \frac{\partial v}{\partial y} \frac{\partial v}{\partial x} + 2 \frac{\partial u}{\partial x} \frac{\partial u}{\partial y} + \frac{\partial u}{\partial y} \frac{\partial v}{\partial y} + \frac{\partial v}{\partial x} \frac{\partial v}{\partial y} - 2\left\{ \frac{\partial u}{\partial x} \frac{\partial v}{\partial x} + \frac{\partial u}{\partial x} \frac{\partial u}{\partial y} \right. \right. \\ & \left. \left. \left. + \frac{\partial v}{\partial y} \frac{\partial v}{\partial x} + \frac{\partial v}{\partial y} \frac{\partial u}{\partial y} \right\} \right]. \end{aligned} \quad (4.13)$$

The term $\partial_x \tau_{11}$ and $\partial_y \tau_{21}$ is obtained by adding Eq. (4.12) and Eq. (4.13), as below

$$\begin{aligned} \partial_x \tau_{11} + \partial_y \tau_{21} = & \left[-\frac{\partial p}{\partial x} + 2\left(\mu + \alpha_1 \frac{\partial}{\partial t}\right) \frac{\partial^2 u}{\partial x^2} + \alpha_1 \frac{\partial}{\partial x} \left\{ 2\left(u \frac{\partial^2 u}{\partial x^2} + v \frac{\partial^2 u}{\partial x \partial y}\right) \right. \right. \\ & \left. \left. + 2\left(\frac{\partial v}{\partial x}\right)^2 - \left(\frac{\partial u}{\partial y}\right)^2 - \left(\frac{\partial v}{\partial x}\right)^2 \right\} \right] \\ & + \left[\left(\mu + \alpha_1 \frac{\partial}{\partial t}\right) \left(\frac{\partial^2 v}{\partial x \partial y} + \frac{\partial^2 u}{\partial y^2}\right) + \alpha_1 \frac{\partial}{\partial y} \left[u \frac{\partial^2 v}{\partial x^2} + u \frac{\partial^2 u}{\partial x \partial y} + v \frac{\partial^2 v}{\partial x \partial y} + v \frac{\partial^2 u}{\partial y^2} \right. \right. \\ & \left. \left. + \frac{\partial v}{\partial x} \frac{\partial u}{\partial x} + \frac{\partial u}{\partial y} \frac{\partial u}{\partial x} + 2 \frac{\partial v}{\partial y} \frac{\partial v}{\partial x} + 2 \frac{\partial u}{\partial x} \frac{\partial u}{\partial y} + \frac{\partial u}{\partial y} \frac{\partial v}{\partial y} + \frac{\partial v}{\partial x} \frac{\partial v}{\partial y} - 2\left\{ \frac{\partial u}{\partial x} \frac{\partial v}{\partial x} + \frac{\partial u}{\partial x} \frac{\partial u}{\partial y} \right. \right. \right. \\ & \left. \left. \left. + \frac{\partial v}{\partial y} \frac{\partial v}{\partial x} + \frac{\partial v}{\partial y} \frac{\partial u}{\partial y} \right\} \right] \right], \end{aligned}$$

or,

$$\begin{aligned} \partial_x \tau_{11} + \partial_y \tau_{21} = & \left[-\frac{\partial p}{\partial x} + 2\left(\mu + \alpha_1 \frac{\partial}{\partial t}\right) \frac{\partial^2 u}{\partial x^2} + \alpha_1 \frac{\partial}{\partial x} \left\{ 2\left(u \frac{\partial^2 u}{\partial x^2} + v \frac{\partial^2 u}{\partial x \partial y}\right) \right. \right. \\ & \left. \left. + 2\left(\frac{\partial v}{\partial x}\right)^2 - \left(\frac{\partial u}{\partial y}\right)^2 - \left(\frac{\partial v}{\partial x}\right)^2 \right\} \right] \\ & + \left[\left(\mu + \alpha_1 \frac{\partial}{\partial t}\right) \left(\frac{\partial^2 v}{\partial x \partial y} + \frac{\partial^2 u}{\partial y^2}\right) + \alpha_1 \frac{\partial}{\partial y} \left[u \frac{\partial^2 v}{\partial x^2} + u \frac{\partial^2 u}{\partial x \partial y} + v \frac{\partial^2 v}{\partial x \partial y} + v \frac{\partial^2 u}{\partial y^2} \right. \right. \\ & \left. \left. + \frac{\partial v}{\partial x} \frac{\partial u}{\partial x} + 3 \frac{\partial v}{\partial y} \frac{\partial v}{\partial x} + 3 \frac{\partial u}{\partial x} \frac{\partial u}{\partial y} + \frac{\partial u}{\partial y} \frac{\partial v}{\partial y} - 2 \frac{\partial u}{\partial x} \frac{\partial v}{\partial x} - 2 \frac{\partial u}{\partial x} \frac{\partial u}{\partial y} - 2 \frac{\partial v}{\partial y} \frac{\partial v}{\partial x} \right. \right. \\ & \left. \left. - 2 \frac{\partial v}{\partial y} \frac{\partial u}{\partial y} \right] \right], \end{aligned}$$

or,

$$\begin{aligned} \partial_x \tau_{11} + \partial_y \tau_{21} = & \left[-\frac{\partial p}{\partial x} + 2\left(\mu + \alpha_1 \frac{\partial}{\partial t}\right) \frac{\partial^2 u}{\partial x^2} + \alpha_1 \frac{\partial}{\partial x} \left\{ 2\left(u \frac{\partial^2 u}{\partial x^2} + v \frac{\partial^2 u}{\partial x \partial y}\right) \right. \right. \\ & \left. \left. + 2\left(\frac{\partial v}{\partial x}\right)^2 - \left(\frac{\partial u}{\partial y}\right)^2 - \left(\frac{\partial v}{\partial x}\right)^2 \right\} \right] \\ & + \left[\left(\mu + \alpha_1 \frac{\partial}{\partial t}\right) \left(\frac{\partial^2 v}{\partial x \partial y} + \frac{\partial^2 u}{\partial y^2}\right) + \alpha_1 \frac{\partial}{\partial y} \left[u \frac{\partial^2 v}{\partial x^2} + u \frac{\partial^2 u}{\partial x \partial y} + v \frac{\partial^2 v}{\partial x \partial y} + v \frac{\partial^2 u}{\partial y^2} \right. \right. \\ & \left. \left. - \frac{\partial v}{\partial x} \frac{\partial u}{\partial x} + \frac{\partial v}{\partial y} \frac{\partial v}{\partial x} + \frac{\partial u}{\partial x} \frac{\partial u}{\partial y} - \frac{\partial u}{\partial y} \frac{\partial v}{\partial y} \right] \right]. \end{aligned}$$

The term $\partial_x \tau_{12}$ is given as

$$\begin{aligned} \bullet \frac{\partial \tau_{12}}{\partial x} = & \left(\mu + \alpha_1 \frac{\partial}{\partial t}\right) \frac{\partial}{\partial x} \left(\frac{\partial u}{\partial y} + \frac{\partial v}{\partial x}\right) + \alpha_1 \frac{\partial}{\partial x} \left[\left(u \frac{\partial}{\partial x} + v \frac{\partial}{\partial y}\right) A_{12} + A_{11} \frac{\partial u}{\partial y} + A_{12} \frac{\partial v}{\partial y} \right. \\ & \left. + A_{21} \frac{\partial u}{\partial x} + A_{22} \frac{\partial v}{\partial x} - 2 \left\{ \frac{\partial u}{\partial x} \left(\frac{\partial u}{\partial y} + \frac{\partial v}{\partial x}\right) + \frac{\partial v}{\partial y} \left(\frac{\partial u}{\partial y} + \frac{\partial v}{\partial x}\right) \right\} \right], \end{aligned}$$

which upon substitutions of A_{11} , A_{12} , A_{21} , A_{22} from Eq. (4.8),

$$\begin{aligned} \Rightarrow \frac{\partial \tau_{12}}{\partial x} = & \left(\mu + \alpha_1 \frac{\partial}{\partial t}\right) \left(\frac{\partial^2 u}{\partial x \partial y} + \frac{\partial^2 v}{\partial x^2}\right) + \alpha_1 \frac{\partial}{\partial x} \left[\left(u \frac{\partial}{\partial x} + v \frac{\partial}{\partial y}\right) \left(\frac{\partial u}{\partial y} + \frac{\partial v}{\partial x}\right) \right. \\ & \left. + \left(2 \frac{\partial u}{\partial x}\right) \frac{\partial u}{\partial y} + \left(\frac{\partial u}{\partial y} + \frac{\partial v}{\partial x}\right) \frac{\partial v}{\partial y} + \left(\frac{\partial v}{\partial x} + \frac{\partial u}{\partial y}\right) \frac{\partial u}{\partial x} + \left(2 \frac{\partial v}{\partial y}\right) \frac{\partial v}{\partial x} \right. \\ & \left. - 2 \left\{ \frac{\partial u}{\partial x} \left(\frac{\partial u}{\partial y} + \frac{\partial v}{\partial x}\right) + \frac{\partial v}{\partial y} \left(\frac{\partial u}{\partial y} + \frac{\partial v}{\partial x}\right) \right\} \right], \end{aligned}$$

or,

$$\begin{aligned} \frac{\partial \tau_{12}}{\partial x} = & \left(\mu + \alpha_1 \frac{\partial}{\partial t} \right) \left(\frac{\partial^2 u}{\partial x \partial y} + \frac{\partial^2 v}{\partial x^2} \right) + \alpha_1 \frac{\partial}{\partial x} \left[u \frac{\partial^2 u}{\partial x \partial y} + u \frac{\partial^2 v}{\partial x^2} + v \frac{\partial^2 u}{\partial y^2} + v \frac{\partial^2 v}{\partial x \partial y} \right. \\ & + 2 \frac{\partial u}{\partial x} \frac{\partial u}{\partial y} + \frac{\partial u}{\partial y} \frac{\partial v}{\partial y} + \frac{\partial v}{\partial x} \frac{\partial v}{\partial y} + \frac{\partial v}{\partial x} \frac{\partial u}{\partial x} + \frac{\partial u}{\partial y} \frac{\partial u}{\partial x} + 2 \frac{\partial v}{\partial y} \frac{\partial v}{\partial x} \\ & \left. - 2 \left\{ \frac{\partial u}{\partial x} \frac{\partial u}{\partial y} + \frac{\partial u}{\partial x} \frac{\partial v}{\partial x} + \frac{\partial v}{\partial y} \frac{\partial u}{\partial y} + \frac{\partial v}{\partial y} \frac{\partial v}{\partial x} \right\} \right]. \end{aligned} \quad (4.14)$$

The term $\partial_y \tau_{22}$ is given as

$$\begin{aligned} \bullet \frac{\partial \tau_{22}}{\partial y} = & -\frac{\partial p}{\partial y} + 2 \left(\mu + \alpha_1 \frac{\partial}{\partial t} \right) \frac{\partial^2 v}{\partial y^2} + \alpha_1 \frac{\partial}{\partial y} \left[\left(u \frac{\partial}{\partial x} + v \frac{\partial}{\partial y} \right) A_{22} + 2 \left(A_{21} \frac{\partial u}{\partial y} + A_{22} \frac{\partial v}{\partial y} \right) \right. \\ & \left. - 4 \frac{\partial^2 v}{\partial y^2} - \left(\frac{\partial v}{\partial x} + \frac{\partial u}{\partial y} \right) \left(\frac{\partial v}{\partial x} + \frac{\partial u}{\partial y} \right) \right], \end{aligned}$$

or,

$$\begin{aligned} \Rightarrow \frac{\partial \tau_{22}}{\partial y} = & -\frac{\partial p}{\partial y} + 2 \left(\mu + \alpha_1 \frac{\partial}{\partial t} \right) \frac{\partial^2 v}{\partial y^2} + \alpha_1 \frac{\partial}{\partial y} \left[\left(u \frac{\partial}{\partial x} + v \frac{\partial}{\partial y} \right) \left(2 \frac{\partial v}{\partial y} \right) \right. \\ & \left. + 2 \left(\left(\frac{\partial v}{\partial x} + \frac{\partial u}{\partial y} \right) \frac{\partial u}{\partial y} + \left(2 \frac{\partial v}{\partial y} \right) \frac{\partial v}{\partial y} \right) - 4 \frac{\partial^2 v}{\partial y^2} - \left(\frac{\partial v}{\partial x} + \frac{\partial u}{\partial y} \right) \left(\frac{\partial v}{\partial x} + \frac{\partial u}{\partial y} \right) \right], \end{aligned}$$

or,

$$\begin{aligned} \Rightarrow \frac{\partial \tau_{22}}{\partial y} = & -\frac{\partial p}{\partial y} + 2 \left(\mu + \alpha_1 \frac{\partial}{\partial t} \right) \frac{\partial^2 v}{\partial y^2} + \alpha_1 \frac{\partial}{\partial y} \left[2u \frac{\partial^2 v}{\partial x \partial y} + 2v \frac{\partial^2 v}{\partial y^2} + 2 \left(\frac{\partial v}{\partial x} \frac{\partial u}{\partial y} + \left(\frac{\partial u}{\partial y} \right)^2 \right) \right. \\ & \left. + 2 \left(\frac{\partial v}{\partial y} \right)^2 \right) - 4 \frac{\partial^2 v}{\partial y^2} - \left(\left(\frac{\partial v}{\partial x} \right)^2 + \frac{\partial v}{\partial x} \frac{\partial u}{\partial y} + \frac{\partial u}{\partial y} \frac{\partial v}{\partial x} + \left(\frac{\partial u}{\partial y} \right)^2 \right) \right]. \end{aligned} \quad (4.15)$$

Adding Eq. (4.14) and Eq. (4.15) implies

$$\begin{aligned} \partial_x \tau_{12} + \partial_y \tau_{22} = & \left[\begin{aligned} & \left(\mu + \alpha_1 \frac{\partial}{\partial t} \right) \left(\frac{\partial^2 u}{\partial x \partial y} + \frac{\partial^2 v}{\partial x^2} \right) + \alpha_1 \frac{\partial}{\partial x} \left[u \frac{\partial^2 u}{\partial x \partial y} + u \frac{\partial^2 v}{\partial x^2} + v \frac{\partial^2 u}{\partial y^2} \right. \\ & + v \frac{\partial^2 v}{\partial x \partial y} + 2 \frac{\partial u}{\partial x} \frac{\partial u}{\partial y} + \frac{\partial u}{\partial y} \frac{\partial v}{\partial y} + \frac{\partial v}{\partial x} \frac{\partial v}{\partial y} + \frac{\partial v}{\partial x} \frac{\partial u}{\partial x} + \frac{\partial u}{\partial y} \frac{\partial u}{\partial x} + 2 \frac{\partial v}{\partial y} \frac{\partial v}{\partial x} \\ & \left. - 2 \left\{ \frac{\partial u}{\partial x} \frac{\partial u}{\partial y} + \frac{\partial u}{\partial x} \frac{\partial v}{\partial x} + \frac{\partial v}{\partial y} \frac{\partial u}{\partial y} + \frac{\partial v}{\partial y} \frac{\partial v}{\partial x} \right\} \right] \\ & + \left[\begin{aligned} & -\frac{\partial p}{\partial y} + 2 \left(\mu + \alpha_1 \frac{\partial}{\partial t} \right) \frac{\partial^2 v}{\partial y^2} + \alpha_1 \frac{\partial}{\partial y} \left[2u \frac{\partial^2 v}{\partial x \partial y} + 2v \frac{\partial^2 v}{\partial y^2} + 2 \left(\frac{\partial v}{\partial x} \frac{\partial u}{\partial y} + \left(\frac{\partial u}{\partial y} \right)^2 \right) \right. \\ & \left. + 2 \left(\frac{\partial v}{\partial y} \right)^2 \right) - 4 \frac{\partial^2 v}{\partial y^2} - \left(\left(\frac{\partial v}{\partial x} \right)^2 + \frac{\partial v}{\partial x} \frac{\partial u}{\partial y} + \frac{\partial u}{\partial y} \frac{\partial v}{\partial x} + \left(\frac{\partial u}{\partial y} \right)^2 \right) \right] \end{aligned} \right], \end{aligned}$$

or,

$$\begin{aligned} \partial_x \tau_{12} + \partial_y \tau_{22} = & \left[\begin{aligned} & \left(\mu + \alpha_1 \frac{\partial}{\partial t} \right) \left(\frac{\partial^2 u}{\partial x \partial y} + \frac{\partial^2 v}{\partial x^2} \right) + \alpha_1 \frac{\partial}{\partial x} \left[u \frac{\partial^2 u}{\partial x \partial y} + u \frac{\partial^2 v}{\partial x^2} + v \frac{\partial^2 u}{\partial y^2} \right. \\ & + v \frac{\partial^2 v}{\partial x \partial y} + 3 \frac{\partial u}{\partial x} \frac{\partial u}{\partial y} + \frac{\partial u}{\partial y} \frac{\partial v}{\partial y} + \frac{\partial v}{\partial x} \frac{\partial u}{\partial x} + 3 \frac{\partial v}{\partial y} \frac{\partial v}{\partial x} - 2 \frac{\partial u}{\partial x} \frac{\partial u}{\partial y} - 2 \frac{\partial u}{\partial x} \frac{\partial v}{\partial x} \\ & \left. - 2 \frac{\partial v}{\partial y} \frac{\partial u}{\partial y} - 2 \frac{\partial v}{\partial y} \frac{\partial v}{\partial x} \right] \\ + & \left[\begin{aligned} & -\frac{\partial p}{\partial y} + 2 \left(\mu + \alpha_1 \frac{\partial}{\partial t} \right) \frac{\partial^2 v}{\partial y^2} + \alpha_1 \frac{\partial}{\partial y} \left[2u \frac{\partial^2 v}{\partial x \partial y} + 2v \frac{\partial^2 v}{\partial y^2} + 2 \frac{\partial v}{\partial x} \frac{\partial u}{\partial y} + 2 \left(\frac{\partial u}{\partial y} \right)^2 \right. \\ & \left. + 4 \left(\frac{\partial v}{\partial y} \right)^2 - 4 \frac{\partial^2 v}{\partial y^2} - \left(\frac{\partial v}{\partial x} \right)^2 - 2 \frac{\partial v}{\partial x} \frac{\partial u}{\partial y} - \left(\frac{\partial u}{\partial y} \right)^2 \right] \end{aligned} \right], \end{aligned}$$

or,

$$\begin{aligned} \partial_x \tau_{12} + \partial_y \tau_{22} = & \left[\begin{aligned} & \left(\mu + \alpha_1 \frac{\partial}{\partial t} \right) \left(\frac{\partial^2 u}{\partial x \partial y} + \frac{\partial^2 v}{\partial x^2} \right) + \alpha_1 \frac{\partial}{\partial x} \left[u \frac{\partial^2 u}{\partial x \partial y} + u \frac{\partial^2 v}{\partial x^2} + v \frac{\partial^2 u}{\partial y^2} \right. \\ & \left. + v \frac{\partial^2 v}{\partial x \partial y} + \frac{\partial u}{\partial x} \frac{\partial u}{\partial y} - \frac{\partial u}{\partial y} \frac{\partial v}{\partial y} - \frac{\partial v}{\partial x} \frac{\partial u}{\partial x} + \frac{\partial v}{\partial y} \frac{\partial v}{\partial x} \right] \\ + & \left[\begin{aligned} & -\frac{\partial p}{\partial y} + 2 \left(\mu + \alpha_1 \frac{\partial}{\partial t} \right) \frac{\partial^2 v}{\partial y^2} + \alpha_1 \frac{\partial}{\partial y} \left[2u \frac{\partial^2 v}{\partial x \partial y} + 2v \frac{\partial^2 v}{\partial y^2} + \left(\frac{\partial u}{\partial y} \right)^2 + 4 \left(\frac{\partial v}{\partial y} \right)^2 \right. \\ & \left. - 4 \frac{\partial^2 v}{\partial y^2} - \left(\frac{\partial v}{\partial x} \right)^2 \right] \end{aligned} \right]. \end{aligned}$$

The thermal energy balance is described by

$$\rho C_p \left\{ \frac{\partial}{\partial t} + U \cdot \nabla \right\} \theta = \nabla \cdot (k \nabla \theta),$$

or,

$$\left(\frac{\partial T}{\partial t} + U \cdot \nabla \theta \right) = \frac{k}{\rho C_p} \nabla \cdot (\nabla \theta),$$

or,

$$\left(\frac{\partial T}{\partial t} + U \cdot \nabla \theta \right) = \frac{k}{\rho C_p} (\Delta \theta).$$

4.1 Problem Description

Consider a lid Driven square cavity with two semi-circular heated cylinders at its bottom wall. The computational domain is a square box of fluid, with the configuration and its boundary conditions expressed by the equation for the left-right side wall $u = v = 0$. The

top lid of the square is driven by a velocity of $u = 0$ as shown in the figure below. The physical model consists a square closed cavity with moving top adiabatic ceiling and it has two semi-circular heaters on the bottom wall while vertical walls have lower temperature than that of heaters as presented in Fig. 4.1 with boundary conditions. The length and width of the 2-D cavity is equal to each other and it is filled with porous medium. Diameters of the semicircular heaters are taken as d_1 and d_2 , respectively. Gravity acts in y -direction. In the physical model, the half circular cylinders are heated as isothermally and their temperature is lower than that of vertical walls.

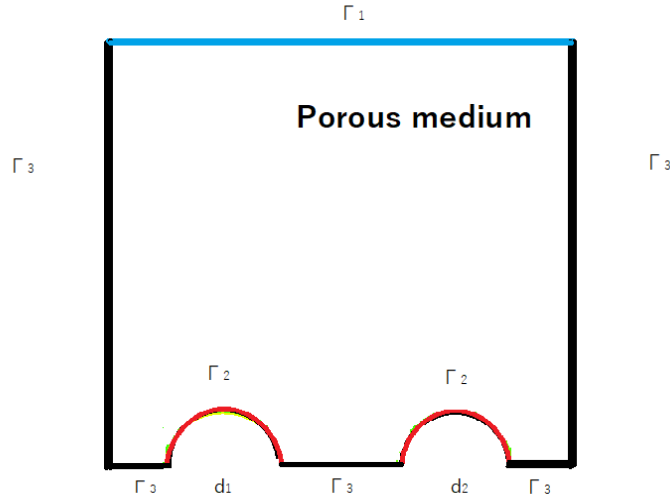


FIGURE 4.1: Computational Domain with two semi-circular heaters.

4.1.1 Dimensional Form of the Governing Equations

On the account of the above discussion, now we are able to describe the dimensional form of the governing equations for the problem.

x -component of momentum equation:

$$\begin{aligned} \frac{\partial u}{\partial t} + u \frac{\partial u}{\partial x} + v \frac{\partial u}{\partial y} &= \frac{1}{\rho} \\ &\left[-\frac{\partial p}{\partial x} + \left(\mu + \alpha_1 \frac{\partial}{\partial t} \right) \left\{ 2 \frac{\partial^2 u}{\partial x^2} + \left(\frac{\partial^2 v}{\partial x \partial y} + \frac{\partial^2 u}{\partial y^2} \right) - \frac{\varphi}{K} u \right\} + \alpha_1 \frac{\partial}{\partial x} \left[2 \left(u \frac{\partial^2 u}{\partial x^2} + v \frac{\partial^2 u}{\partial x \partial y} \right) \right. \right. \\ &\quad \left. \left. + \left(\frac{\partial v}{\partial x} \right)^2 - \left(\frac{\partial u}{\partial y} \right)^2 \right] + \alpha_1 \frac{\partial}{\partial y} \left[u \frac{\partial^2 v}{\partial x^2} + u \frac{\partial^2 u}{\partial x \partial y} + v \frac{\partial^2 v}{\partial x \partial y} + v \frac{\partial^2 u}{\partial y^2} - \frac{\partial v}{\partial x} \frac{\partial u}{\partial x} + \frac{\partial v}{\partial y} \frac{\partial v}{\partial x} \right. \right. \\ &\quad \left. \left. + \frac{\partial u}{\partial x} \frac{\partial u}{\partial y} - \frac{\partial u}{\partial y} \frac{\partial v}{\partial y} \right] - \left(\frac{c_F \rho \varphi}{\sqrt{K}} \right) u^2 \right] \\ &\quad - \sigma B_o^2 u + \rho g_x (\beta_\theta) (\theta - \theta_o). \end{aligned} \tag{4.16}$$

y -component of momentum equation:

$$\begin{aligned} \frac{\partial v}{\partial t} + u \frac{\partial v}{\partial x} + v \frac{\partial v}{\partial y} &= \frac{1}{\rho} \\ &\left[-\frac{\partial p}{\partial y} + \left(\mu + \alpha_1 \frac{\partial}{\partial t} \right) \left\{ 2 \frac{\partial^2 v}{\partial y^2} + \left(\frac{\partial^2 u}{\partial x \partial y} + \frac{\partial^2 v}{\partial x^2} \right) - \frac{\varphi}{K} v \right\} + \alpha_1 \frac{\partial}{\partial x} \left[u \frac{\partial^2 u}{\partial x \partial y} + u \frac{\partial^2 v}{\partial x^2} \right] \right. \\ &+ v \frac{\partial^2 u}{\partial y^2} + v \frac{\partial^2 v}{\partial x \partial y} + \frac{\partial u}{\partial x} \frac{\partial u}{\partial y} - \frac{\partial u}{\partial y} \frac{\partial v}{\partial y} - \frac{\partial v}{\partial x} \frac{\partial u}{\partial x} + \frac{\partial v}{\partial y} \frac{\partial v}{\partial x} \left. \right] + \alpha_1 \frac{\partial}{\partial y} \left[2u \frac{\partial^2 v}{\partial x \partial y} + 2v \frac{\partial^2 v}{\partial y^2} \right. \\ &\quad \left. + \left(\frac{\partial u}{\partial y} \right)^2 + 4 \left(\frac{\partial v}{\partial y} \right)^2 - 4 \frac{\partial^2 v}{\partial y^2} - \left(\frac{\partial v}{\partial x} \right)^2 \right] - \left(\frac{c_F \rho \varphi}{\sqrt{K}} \right) v^2 \\ &\quad - \sigma B_o^2 v + \rho g_y (\beta_\theta) (\theta - \theta_o). \end{aligned} \quad (4.17)$$

Energy equation:

$$\frac{\partial \theta}{\partial t} + u \frac{\partial \theta}{\partial x} + v \frac{\partial \theta}{\partial y} = \frac{k}{\rho C_p} \left(\frac{\partial^2 \theta}{\partial x^2} + \frac{\partial^2 \theta}{\partial y^2} \right). \quad (4.18)$$

The associated conditions for boundaries are given below:

- On the cavity's left wall (Γ_3)

$$u = v = 0, \quad \text{and } T = T_c. \quad (4.19)$$

- On the cavity's right wall (Γ_3)

$$u = v = 0, \quad \text{and } T = T_c. \quad (4.20)$$

- On the cavity's bottom wall (Γ_2, Γ_3)

$$u = v = 0, \quad \text{and } T = T_c \quad \text{on flatted boundary} \\ \text{and} \quad (4.21)$$

$$u = v = 0, \quad \text{and } T = T_h \quad \text{on circular heater.}$$

- On the cavity's top wall (Γ_1)

$$v = 0, \quad T = T_c, \quad \text{and } u = 0. \quad (4.22)$$

4.1.2 Dimensionless Parameters

Let

$$\hat{x} = \frac{x}{L}, \quad \hat{y} = \frac{y}{L}, \quad \hat{u} = \frac{u}{u_o}, \quad \hat{v} = \frac{v}{u_o}, \quad \hat{t} = \frac{u_o t}{L}, \quad \text{and} \quad P = \frac{p}{\rho u_o^2}. \quad (4.23)$$

be the dimensionless parameters.

4.2 Conversion of Dimensional equations into Dimensionless equations

To convert equations (4.16)-(4.18) into the dimensionless form, certain derivatives are required which have been calculated here in this sub-section.

- $\hat{x} = \frac{x}{L} \Rightarrow \frac{\partial \hat{x}}{\partial x} = \frac{1}{L}.$
- $\hat{y} = \frac{y}{L} \Rightarrow \frac{\partial \hat{y}}{\partial y} = \frac{1}{L}.$
- $\hat{u} = \frac{u}{u_o} \Rightarrow u = u_o \hat{u}.$
- $\hat{v} = \frac{v}{u_o} \Rightarrow v = u_o \hat{v}.$
- $\hat{t} = \frac{u_o t}{L} \Rightarrow \frac{\partial \hat{t}}{\partial t} = \frac{u_o}{L}.$
- $\frac{\partial u}{\partial t} = \frac{\partial u}{\partial \hat{t}} \frac{\partial \hat{t}}{\partial t} = \frac{\partial}{\partial \hat{t}}(u) \frac{\partial}{\partial t}(\hat{t}) = \frac{\partial}{\partial \hat{t}}(u_o \hat{u}) \frac{u_o}{L} = u_o \frac{\partial \hat{u}}{\partial \hat{t}} \frac{u_o}{L} = \frac{u_o^2}{L} \frac{\partial \hat{u}}{\partial \hat{t}},$
- $\frac{\partial v}{\partial t} = \frac{\partial v}{\partial \hat{t}} \frac{\partial \hat{t}}{\partial t} = \frac{\partial}{\partial \hat{t}}(v) \frac{\partial}{\partial t}(\hat{t}) = \frac{\partial}{\partial \hat{t}}(u_o \hat{v}) \frac{u_o}{L} = u_o \frac{\partial \hat{v}}{\partial \hat{t}} \frac{u_o}{L} = \frac{u_o^2}{L} \frac{\partial \hat{v}}{\partial \hat{t}},$
- $\frac{\partial u}{\partial x} = \frac{\partial u}{\partial \hat{x}} \frac{\partial \hat{x}}{\partial x} = \frac{\partial}{\partial \hat{x}}(u) \frac{\partial}{\partial x}(\hat{x}) = \frac{\partial}{\partial \hat{x}}(u_o \hat{u}) \frac{1}{L} = \frac{u_o}{L} \frac{\partial \hat{u}}{\partial \hat{x}},$
- $\frac{\partial u}{\partial y} = \frac{\partial u}{\partial \hat{y}} \frac{\partial \hat{y}}{\partial y} = \frac{\partial}{\partial \hat{y}}(u) \frac{\partial}{\partial y}(\hat{y}) = \frac{\partial}{\partial \hat{y}}(u_o \hat{u}) \frac{1}{L} = \frac{u_o}{L} \frac{\partial \hat{u}}{\partial \hat{y}},$
- $\frac{\partial v}{\partial x} = \frac{\partial v}{\partial \hat{x}} \frac{\partial \hat{x}}{\partial x} = \frac{\partial}{\partial \hat{x}}(v) \frac{\partial}{\partial x}(\hat{x}) = \frac{\partial}{\partial \hat{x}}(u_o \hat{v}) \frac{1}{L} = \frac{u_o}{L} \frac{\partial \hat{v}}{\partial \hat{x}},$
- $\frac{\partial v}{\partial y} = \frac{\partial v}{\partial \hat{y}} \frac{\partial \hat{y}}{\partial y} = \frac{\partial}{\partial \hat{y}}(v) \frac{\partial}{\partial y}(\hat{y}) = \frac{\partial}{\partial \hat{y}}(u_o \hat{v}) \frac{1}{L} = \frac{u_o}{L} \frac{\partial \hat{v}}{\partial \hat{y}},$

- $v \frac{\partial^2 v}{\partial x \partial y} = (u_o \hat{v}) \frac{u_o}{L^2} \frac{\partial^2 \hat{v}}{\partial \hat{x} \partial \hat{y}} = \frac{u_o^2}{L^2} \hat{v} \frac{\partial^2 \hat{v}}{\partial \hat{x} \partial \hat{y}},$
- $u \frac{\partial^2 u}{\partial x \partial y} = (u_o \hat{u}) \frac{u_o}{L^2} \frac{\partial^2 \hat{u}}{\partial \hat{x} \partial \hat{y}} = \frac{u_o^2}{L^2} \hat{u} \frac{\partial^2 \hat{u}}{\partial \hat{x} \partial \hat{y}},$
- $u \frac{\partial^2 v}{\partial x \partial y} = (u_o \hat{u}) \frac{u_o}{L^2} \frac{\partial^2 \hat{v}}{\partial \hat{x} \partial \hat{y}} = \frac{u_o^2}{L^2} \hat{u} \frac{\partial^2 \hat{v}}{\partial \hat{x} \partial \hat{y}},$
- $\frac{\partial u}{\partial x} \frac{\partial v}{\partial x} = \frac{u_o}{L} \frac{\partial \hat{u}}{\partial \hat{x}} \frac{u_o}{L} \frac{\partial \hat{v}}{\partial \hat{x}} = \frac{u_o^2}{L^2} \frac{\partial \hat{u}}{\partial \hat{x}} \frac{\partial \hat{v}}{\partial \hat{x}},$
- $\frac{\partial u}{\partial y} \frac{\partial v}{\partial y} = \frac{u_o}{L} \frac{\partial \hat{u}}{\partial \hat{y}} \frac{u_o}{L} \frac{\partial \hat{v}}{\partial \hat{y}} = \frac{u_o^2}{L^2} \frac{\partial \hat{u}}{\partial \hat{y}} \frac{\partial \hat{v}}{\partial \hat{y}},$
- $\frac{\partial u}{\partial x} \frac{\partial u}{\partial y} = \frac{u_o}{L} \frac{\partial \hat{u}}{\partial \hat{x}} \frac{u_o}{L} \frac{\partial \hat{u}}{\partial \hat{y}} = \frac{u_o^2}{L^2} \frac{\partial \hat{u}}{\partial \hat{x}} \frac{\partial \hat{u}}{\partial \hat{y}},$
- $\frac{\partial v}{\partial x} \frac{\partial v}{\partial y} = \frac{u_o}{L} \frac{\partial \hat{v}}{\partial \hat{x}} \frac{u_o}{L} \frac{\partial \hat{v}}{\partial \hat{y}} = \frac{u_o^2}{L^2} \frac{\partial \hat{v}}{\partial \hat{x}} \frac{\partial \hat{v}}{\partial \hat{y}},$
- $\hat{\theta} = \frac{\theta - \theta_o}{\theta_o} \Rightarrow \theta = \theta_o + \theta_o \hat{\theta} = \theta_o (1 + \hat{\theta}),$
- $\frac{\partial \theta}{\partial t} = \frac{\partial}{\partial t}(\theta) = \frac{\partial}{\partial \hat{t}} \frac{\partial \hat{\theta}}{\partial \hat{t}}(\theta) = \frac{\partial}{\partial \hat{t}} \frac{u_o}{L}(\theta) = \frac{u_o}{L} \frac{\partial}{\partial \hat{t}}(\theta_o + \theta_o \hat{\theta}) = \frac{u_o}{L} \theta_o \frac{\partial \hat{\theta}}{\partial \hat{t}},$
- $\rho(C_p) \frac{\partial \theta}{\partial t} = \rho(C_p) \frac{\mu}{\rho L^2} \theta_o \frac{\partial \hat{\theta}}{\partial \hat{t}} = \frac{(C_p) \mu}{L^2} \theta_o \frac{\partial \hat{\theta}}{\partial \hat{t}},$
- $\frac{\partial \theta}{\partial x} = \frac{\partial}{\partial x}(\theta) = \frac{\partial}{\partial \hat{x}} \frac{\partial \hat{\theta}}{\partial \hat{x}}(\theta) = \frac{\partial}{\partial \hat{x}} \frac{1}{L}(\theta) = \frac{1}{L} \frac{\partial}{\partial \hat{x}}(\theta_o + \theta_o \hat{\theta}) = \frac{1}{L} \theta_o \frac{\partial \hat{\theta}}{\partial \hat{x}} = \frac{\theta_o}{L} \frac{\partial \hat{\theta}}{\partial \hat{x}},$
- $\frac{\partial^2 \theta}{\partial x^2} = \frac{\partial}{\partial y} \left(\frac{\partial \theta}{\partial y} \right) = \frac{\partial}{\partial \hat{x}} \frac{\partial \hat{\theta}}{\partial \hat{x}} \left(\frac{\theta_o}{L} \frac{\partial \hat{\theta}}{\partial \hat{x}} \right) = \frac{\partial}{\partial \hat{x}} \frac{1}{L} \left(\frac{\theta_o}{L} \frac{\partial \hat{\theta}}{\partial \hat{x}} \right) = \frac{\theta_o}{L^2} \frac{\partial^2 \hat{\theta}}{\partial \hat{x}^2},$
- $\frac{\partial \theta}{\partial y} = \frac{\partial}{\partial y}(\theta) = \frac{\partial}{\partial \hat{y}} \frac{\partial \hat{\theta}}{\partial \hat{y}}(\theta) = \frac{\partial}{\partial \hat{y}} \frac{1}{L}(\theta) = \frac{1}{L} \frac{\partial}{\partial \hat{y}}(\theta_o + \theta_o \hat{\theta}) = \frac{1}{L} \theta_o \frac{\partial \hat{\theta}}{\partial \hat{y}} = \frac{\theta_o}{L} \frac{\partial \hat{\theta}}{\partial \hat{y}},$
- $\frac{\partial^2 \theta}{\partial y^2} = \frac{\partial}{\partial y} \left(\frac{\partial \theta}{\partial y} \right) = \frac{\partial}{\partial \hat{y}} \frac{\partial \hat{\theta}}{\partial \hat{y}} \left(\frac{\theta_o}{L} \frac{\partial \hat{\theta}}{\partial \hat{y}} \right) = \frac{\partial}{\partial \hat{y}} \frac{1}{L} \left(\frac{\theta_o}{L} \frac{\partial \hat{\theta}}{\partial \hat{y}} \right) = \frac{\theta_o}{L^2} \frac{\partial^2 \hat{\theta}}{\partial \hat{y}^2},$

Equation (4.16) becomes:

$$\begin{aligned} \frac{\partial u}{\partial t} + u \frac{\partial u}{\partial x} + v \frac{\partial u}{\partial y} &= \frac{1}{\rho} \\ \left[-\frac{\partial p}{\partial x} + \left(\mu + \alpha_1 \frac{\partial}{\partial t} \right) \left\{ 2 \frac{\partial^2 u}{\partial x^2} + \left(\frac{\partial^2 v}{\partial x \partial y} + \frac{\partial^2 u}{\partial y^2} \right) - \frac{\varphi}{K} u \right\} + \alpha_1 \frac{\partial}{\partial x} \left[2 \left(u \frac{\partial^2 u}{\partial x^2} + v \frac{\partial^2 u}{\partial x \partial y} \right) \right] \right. \\ &+ \left. \left(\frac{\partial v}{\partial x} \right)^2 - \left(\frac{\partial u}{\partial y} \right)^2 \right] + \alpha_1 \frac{\partial}{\partial y} \left[u \frac{\partial^2 v}{\partial x^2} + u \frac{\partial^2 u}{\partial x \partial y} + v \frac{\partial^2 v}{\partial x \partial y} + v \frac{\partial^2 u}{\partial y^2} - \frac{\partial v}{\partial x} \frac{\partial u}{\partial x} + \frac{\partial v}{\partial y} \frac{\partial v}{\partial x} \right. \\ &\quad \left. + \frac{\partial u}{\partial x} \frac{\partial u}{\partial y} - \frac{\partial u}{\partial y} \frac{\partial v}{\partial y} \right] - \left(\frac{c_{FP} \rho \varphi}{\sqrt{K}} \right) u^2 \\ &\quad - \sigma B_o^2 u + \rho g_x (\beta_\theta) (\theta - \theta_o). \end{aligned}$$

or,

$$\begin{aligned} \frac{u_o^2}{L} \frac{\partial \hat{u}}{\partial \hat{t}} + \frac{u_o^2}{L} \hat{u} \frac{\partial \hat{u}}{\partial \hat{x}} + \frac{u_o^2}{L} \hat{v} \frac{\partial \hat{u}}{\partial \hat{y}} &= \frac{1}{\rho} \\ \left[-\frac{\partial p}{\partial x} + \left(\mu + \alpha_1 \frac{\partial}{\partial \hat{t}} \right) \left\{ 2 \frac{u_o}{L^2} \frac{\partial^2 \hat{u}}{\partial \hat{x}^2} + \left(\frac{u_o}{L^2} \frac{\partial^2 \hat{v}}{\partial \hat{x} \partial \hat{y}} + \frac{u_o}{L^2} \frac{\partial^2 \hat{u}}{\partial \hat{y}^2} \right) - \frac{\varphi}{K} u_o \hat{u} \right\} + \alpha_1 \frac{\partial}{\partial \hat{x}} \frac{\partial \hat{x}}{\partial x} \left[2 \right. \right. \\ &\left. \left(\frac{u_o^2}{L^2} \hat{u} \frac{\partial^2 \hat{u}}{\partial \hat{x}^2} + \frac{u_o^2}{L^2} \hat{v} \frac{\partial^2 \hat{u}}{\partial \hat{x} \partial \hat{y}} \right) + \frac{u_o^2}{L^2} \frac{\partial^2 \hat{v}}{\partial x^2} - \frac{u_o^2}{L^2} \frac{\partial^2 \hat{u}}{\partial \hat{y}^2} \right] + \alpha_1 \frac{\partial}{\partial \hat{y}} \frac{\partial \hat{y}}{\partial y} \left[\frac{u_o^2}{L^2} \hat{u} \frac{\partial^2 \hat{v}}{\partial \hat{x}^2} + \frac{u_o^2}{L^2} \hat{u} \frac{\partial^2 \hat{u}}{\partial \hat{x} \partial \hat{y}} + \frac{u_o^2}{L^2} \hat{v} \right. \\ &\left. \frac{\partial^2 \hat{v}}{\partial \hat{x} \partial \hat{y}} + \frac{u_o^2}{L^2} \hat{v} \frac{\partial^2 \hat{u}}{\partial \hat{y}^2} - \frac{u_o^2}{L^2} \frac{\partial \hat{v}}{\partial \hat{x}} \frac{\partial \hat{u}}{\partial \hat{x}} + \frac{u_o^2}{L^2} \frac{\partial \hat{v}}{\partial \hat{y}} \frac{\partial \hat{v}}{\partial \hat{x}} + \frac{u_o^2}{L^2} \frac{\partial \hat{u}}{\partial \hat{x}} \frac{\partial \hat{u}}{\partial \hat{y}} - \frac{u_o^2}{L^2} \frac{\partial \hat{u}}{\partial \hat{y}} \frac{\partial \hat{v}}{\partial \hat{y}} \right] - \left(\frac{c_{FP} \rho \varphi}{\sqrt{K}} \right) (u_o \hat{u})^2 \right] \\ &\quad - \sigma B_o^2 (u_o \hat{u}). \end{aligned}$$

$$\begin{aligned} \Rightarrow \frac{u_o^2}{L} \left[\frac{\partial \hat{u}}{\partial \hat{t}} + \hat{u} \frac{\partial \hat{u}}{\partial \hat{x}} + \hat{v} \frac{\partial \hat{u}}{\partial \hat{y}} \right] &= \frac{1}{\rho} \\ \left[-\frac{\partial p}{\partial x} + \left(\mu + \alpha_1 \frac{\partial}{\partial \hat{t}} \frac{u_o}{L} \right) \left\{ \frac{u_o}{L^2} \left[2 \frac{\partial^2 \hat{u}}{\partial \hat{x}^2} + \left(\frac{\partial^2 \hat{v}}{\partial \hat{x} \partial \hat{y}} + \frac{\partial^2 \hat{u}}{\partial \hat{y}^2} \right) \right] \right\} - \left(\mu + \alpha_1 \frac{\partial}{\partial \hat{t}} \frac{u_o}{L} \right) \frac{\varphi}{K} u_o \hat{u} \right. \\ &+ \alpha_1 \frac{\partial}{\partial \hat{x}} \frac{1}{L} \left[\frac{u_o^2}{L^2} \left(2 \left(\hat{u} \frac{\partial^2 \hat{u}}{\partial \hat{x}^2} + \hat{v} \frac{\partial^2 \hat{u}}{\partial \hat{x} \partial \hat{y}} \right) + \frac{\partial^2 \hat{v}}{\partial x^2} - \frac{\partial^2 \hat{u}}{\partial \hat{y}^2} \right) \right] + \alpha_1 \frac{\partial}{\partial \hat{y}} \frac{1}{L} \left[\frac{u_o^2}{L^2} \left(\hat{u} \frac{\partial^2 \hat{v}}{\partial \hat{x}^2} \right. \right. \\ &\left. \left. + \hat{u} \frac{\partial^2 \hat{u}}{\partial \hat{x} \partial \hat{y}} + \hat{v} \frac{\partial^2 \hat{v}}{\partial \hat{x} \partial \hat{y}} + \hat{v} \frac{\partial^2 \hat{u}}{\partial \hat{y}^2} - \frac{\partial \hat{v}}{\partial \hat{x}} \frac{\partial \hat{u}}{\partial \hat{x}} + \frac{\partial \hat{v}}{\partial \hat{y}} \frac{\partial \hat{v}}{\partial \hat{x}} + \frac{\partial \hat{u}}{\partial \hat{x}} \frac{\partial \hat{u}}{\partial \hat{y}} - \frac{\partial \hat{u}}{\partial \hat{y}} \frac{\partial \hat{v}}{\partial \hat{y}} \right) \right] - \left(\frac{c_{FP} \rho \varphi}{\sqrt{K}} \right) (u_o \hat{u})^2 \right] \\ &\quad - \sigma B_o^2 (u_o \hat{u}). \end{aligned}$$

$$\begin{aligned} \Rightarrow \frac{u_o^2}{L} \left[\frac{\partial \hat{u}}{\partial \hat{t}} + \hat{u} \frac{\partial \hat{u}}{\partial \hat{x}} + \hat{v} \frac{\partial \hat{u}}{\partial \hat{y}} \right] &= -\frac{1}{\rho} \frac{\partial p}{\partial x} + \\ \frac{1}{\rho} \left(\frac{u_o}{L^2} \mu + \alpha_1 \frac{\partial}{\partial \hat{t}} \frac{u_o^2}{L^3} \right) \left[2 \frac{\partial^2 \hat{u}}{\partial \hat{x}^2} + \left(\frac{\partial^2 \hat{v}}{\partial \hat{x} \partial \hat{y}} + \frac{\partial^2 \hat{u}}{\partial \hat{y}^2} \right) \right] &- \frac{1}{\rho} \left(u_o \mu + \alpha_1 \frac{\partial}{\partial \hat{t}} \frac{u_o^2}{L} \right) \frac{\varphi}{K} \hat{u} \\ + \frac{1}{\rho} \alpha_1 \frac{\partial}{\partial \hat{x}} \left[\frac{u_o^2}{L^3} \left(2 \left(\hat{u} \frac{\partial^2 \hat{u}}{\partial \hat{x}^2} + \hat{v} \frac{\partial^2 \hat{u}}{\partial \hat{x} \partial \hat{y}} \right) + \frac{\partial^2 \hat{v}}{\partial x^2} - \frac{\partial^2 \hat{u}}{\partial \hat{y}^2} \right) \right] &+ \frac{1}{\rho} \alpha_1 \frac{\partial}{\partial \hat{y}} \left[\frac{u_o^2}{L^3} \left(\hat{u} \frac{\partial^2 \hat{v}}{\partial \hat{x}^2} + \hat{u} \frac{\partial^2 \hat{u}}{\partial \hat{x} \partial \hat{y}} \right. \right. \\ + \hat{v} \frac{\partial^2 \hat{v}}{\partial \hat{x} \partial \hat{y}} + \hat{v} \frac{\partial^2 \hat{u}}{\partial \hat{y}^2} - \frac{\partial \hat{v}}{\partial \hat{x}} \frac{\partial \hat{u}}{\partial \hat{x}} + \frac{\partial \hat{v}}{\partial \hat{y}} \frac{\partial \hat{v}}{\partial \hat{x}} + \frac{\partial \hat{u}}{\partial \hat{x}} \frac{\partial \hat{u}}{\partial \hat{y}} - \frac{\partial \hat{u}}{\partial \hat{y}} \frac{\partial \hat{v}}{\partial \hat{y}} \left. \right) \right] &- \frac{1}{\rho} \left(\frac{c_{FP} \rho \varphi}{\sqrt{K}} \right) u_o^2 \hat{u}^2 - \sigma B_o^2 (u_o \hat{u}). \end{aligned}$$

$$\begin{aligned} \frac{\partial \hat{u}}{\partial \hat{t}} + \hat{u} \frac{\partial \hat{u}}{\partial \hat{x}} + \hat{v} \frac{\partial \hat{u}}{\partial \hat{y}} &= -\frac{\partial P}{\partial \hat{x}} + \left(\frac{1}{Lu_o} \frac{\mu}{\rho} + \gamma \frac{\partial}{\partial \hat{t}} \right) \left[2 \frac{\partial^2 \hat{u}}{\partial \hat{x}^2} + \left(\frac{\partial^2 \hat{v}}{\partial \hat{x} \partial \hat{y}} \right. \right. \\ &+ \left. \left. \frac{\partial^2 \hat{u}}{\partial \hat{y}^2} \right) \right] - \left[\left(\frac{L}{u_o} \frac{\mu}{\rho} \frac{1}{L^2} + \gamma \frac{\partial}{\partial \hat{t}} \right) \lambda + \frac{L}{u_o} \sigma B_o^2 \right] \hat{u} + \gamma \frac{\partial}{\partial \hat{x}} \left[\left(2 \left(\hat{u} \frac{\partial^2 \hat{u}}{\partial \hat{x}^2} + \hat{v} \frac{\partial^2 \hat{u}}{\partial \hat{x} \partial \hat{y}} \right) \right. \right. \\ &+ \left. \left. \frac{\partial^2 \hat{v}}{\partial \hat{x}^2} - \frac{\partial^2 \hat{u}}{\partial \hat{y}^2} \right) \right] + \gamma \frac{\partial}{\partial \hat{y}} \left[\left(\hat{u} \frac{\partial^2 \hat{v}}{\partial \hat{x}^2} + \hat{u} \frac{\partial^2 \hat{u}}{\partial \hat{x} \partial \hat{y}} + \hat{v} \frac{\partial^2 \hat{v}}{\partial \hat{x} \partial \hat{y}} + \hat{v} \frac{\partial^2 \hat{u}}{\partial \hat{y}^2} - \frac{\partial \hat{v}}{\partial \hat{x}} \frac{\partial \hat{u}}{\partial \hat{x}} + \frac{\partial \hat{v}}{\partial \hat{y}} \frac{\partial \hat{v}}{\partial \hat{x}} \right. \right. \\ &+ \left. \left. \frac{\partial \hat{u}}{\partial \hat{x}} \frac{\partial \hat{u}}{\partial \hat{y}} - \frac{\partial \hat{u}}{\partial \hat{y}} \frac{\partial \hat{v}}{\partial \hat{y}} \right) \right] - L \left(\frac{c_F \rho \varphi}{\sqrt{K}} \right) \hat{u}^2. \end{aligned}$$

$$\begin{aligned} \frac{\partial \hat{u}}{\partial \hat{t}} + \hat{u} \frac{\partial \hat{u}}{\partial \hat{x}} + \hat{v} \frac{\partial \hat{u}}{\partial \hat{y}} &= -\frac{\partial P}{\partial \hat{x}} + \left(\frac{1}{Lu_o} \frac{\mu}{\rho} + \gamma \frac{\partial}{\partial \hat{t}} \right) \left[2 \frac{\partial^2 \hat{u}}{\partial \hat{x}^2} + \left(\frac{\partial^2 \hat{v}}{\partial \hat{x} \partial \hat{y}} \right. \right. \\ &+ \left. \left. \frac{\partial^2 \hat{u}}{\partial \hat{y}^2} \right) \right] - \left[\left(\frac{1}{Lu_o} \frac{\mu}{\rho} + \gamma \frac{\partial}{\partial \hat{t}} \right) \lambda + Ha \right] \hat{u} + \gamma \frac{\partial}{\partial \hat{x}} \left[\left(2 \left(\hat{u} \frac{\partial^2 \hat{u}}{\partial \hat{x}^2} + \hat{v} \frac{\partial^2 \hat{u}}{\partial \hat{x} \partial \hat{y}} \right) \right. \right. \\ &+ \left. \left. \frac{\partial^2 \hat{v}}{\partial \hat{x}^2} - \frac{\partial^2 \hat{u}}{\partial \hat{y}^2} \right) \right] + \gamma \frac{\partial}{\partial \hat{y}} \left[\left(\hat{u} \frac{\partial^2 \hat{v}}{\partial \hat{x}^2} + \hat{u} \frac{\partial^2 \hat{u}}{\partial \hat{x} \partial \hat{y}} + \hat{v} \frac{\partial^2 \hat{v}}{\partial \hat{x} \partial \hat{y}} + \hat{v} \frac{\partial^2 \hat{u}}{\partial \hat{y}^2} - \frac{\partial \hat{v}}{\partial \hat{x}} \frac{\partial \hat{u}}{\partial \hat{x}} + \frac{\partial \hat{v}}{\partial \hat{y}} \frac{\partial \hat{v}}{\partial \hat{x}} \right. \right. \\ &+ \left. \left. \frac{\partial \hat{u}}{\partial \hat{x}} \frac{\partial \hat{u}}{\partial \hat{y}} - \frac{\partial \hat{u}}{\partial \hat{y}} \frac{\partial \hat{v}}{\partial \hat{y}} \right) \right] - F_r \hat{u}^2. \end{aligned}$$

Equation (4.17) becomes:

$$\begin{aligned} \frac{\partial v}{\partial t} + u \frac{\partial v}{\partial x} + v \frac{\partial v}{\partial y} &= \frac{1}{\rho} \\ &\left[-\frac{\partial p}{\partial y} + \left(\mu + \alpha_1 \frac{\partial}{\partial t} \right) \left\{ 2 \frac{\partial^2 v}{\partial y^2} + \left(\frac{\partial^2 u}{\partial x \partial y} + \frac{\partial^2 v}{\partial x^2} \right) - \frac{\varphi}{K} v \right\} + \alpha_1 \frac{\partial}{\partial x} \left[u \frac{\partial^2 u}{\partial x \partial y} + u \frac{\partial^2 v}{\partial x^2} \right] \right. \\ &+ v \frac{\partial^2 u}{\partial y^2} + v \frac{\partial^2 v}{\partial x \partial y} + \frac{\partial u}{\partial x} \frac{\partial u}{\partial y} - \frac{\partial u}{\partial y} \frac{\partial v}{\partial y} - \frac{\partial v}{\partial x} \frac{\partial u}{\partial x} + \frac{\partial v}{\partial y} \frac{\partial v}{\partial x} \left. \right] + \alpha_1 \frac{\partial}{\partial y} \left[2u \frac{\partial^2 v}{\partial x \partial y} + 2v \frac{\partial^2 v}{\partial y^2} \right. \\ &\quad \left. + \left(\frac{\partial u}{\partial y} \right)^2 + 4 \left(\frac{\partial v}{\partial y} \right)^2 - 4 \frac{\partial^2 v}{\partial y^2} - \left(\frac{\partial v}{\partial x} \right)^2 \right] - \left(\frac{c_F \rho \varphi}{\sqrt{K}} \right) v^2 \\ &\quad - \sigma B_o^2 v + \rho g_y (\beta_\theta) (\theta - \theta_o). \end{aligned}$$

or,

$$\begin{aligned} \frac{u_o^2}{L} \frac{\partial \hat{v}}{\partial \hat{t}} + \frac{u_o^2}{L} \hat{u} \frac{\partial \hat{v}}{\partial \hat{x}} + \frac{u_o^2}{L} \hat{v} \frac{\partial \hat{v}}{\partial \hat{y}} &= \frac{1}{\rho} \\ &\left[-\frac{\partial p}{\partial y} + \left(\mu + \alpha_1 \frac{\partial}{\partial \hat{t}} \right) \left\{ 2 \frac{u_o}{L^2} \frac{\partial^2 \hat{v}}{\partial \hat{y}^2} + \left(\frac{u_o}{L^2} \frac{\partial^2 \hat{u}}{\partial \hat{x} \partial \hat{y}} + \frac{u_o}{L^2} \frac{\partial^2 \hat{v}}{\partial \hat{x}^2} \right) - \frac{\varphi}{K} (u_o \hat{v}) \right\} + \alpha_1 \frac{\partial}{\partial \hat{x}} \frac{\partial \hat{x}}{\partial x} \right. \\ &\left[\frac{u_o^2}{L^2} \hat{u} \frac{\partial^2 \hat{u}}{\partial \hat{x} \partial \hat{y}} + \frac{u_o^2}{L^2} \hat{u} \frac{\partial^2 \hat{v}}{\partial \hat{x}^2} + \frac{u_o^2}{L^2} \hat{v} \frac{\partial^2 \hat{u}}{\partial \hat{y}^2} + \frac{u_o^2}{L^2} \hat{v} \frac{\partial^2 \hat{v}}{\partial \hat{x} \partial \hat{y}} + \frac{u_o^2}{L^2} \frac{\partial \hat{u}}{\partial \hat{x}} \frac{\partial \hat{u}}{\partial \hat{y}} - \frac{u_o^2}{L^2} \frac{\partial \hat{u}}{\partial \hat{y}} \frac{\partial \hat{v}}{\partial \hat{y}} - \frac{u_o^2}{L^2} \frac{\partial \hat{v}}{\partial \hat{x}} \frac{\partial \hat{u}}{\partial \hat{x}} + \right. \\ &\left. \frac{u_o^2}{L^2} \frac{\partial \hat{v}}{\partial \hat{y}} \frac{\partial \hat{v}}{\partial \hat{x}} \right] + \alpha_1 \frac{\partial}{\partial \hat{y}} \frac{\partial \hat{y}}{\partial y} \left[2 \frac{u_o^2}{L^2} \hat{u} \frac{\partial^2 \hat{v}}{\partial \hat{x} \partial \hat{y}} + 2 \frac{u_o^2}{L^2} \hat{v} \frac{\partial^2 \hat{v}}{\partial \hat{y}^2} + \frac{u_o^2}{L^2} \left(\frac{\partial \hat{u}}{\partial \hat{y}} \right)^2 + 4 \frac{u_o^2}{L^2} \left(\frac{\partial \hat{v}}{\partial \hat{y}} \right)^2 - 4 \frac{u_o}{L^2} \frac{\partial^2 \hat{v}}{\partial \hat{y}^2} \right. \\ &\quad \left. - \frac{u_o^2}{L^2} \left(\frac{\partial \hat{v}}{\partial \hat{x}} \right)^2 \right] - \left(\frac{c_F \rho \varphi}{\sqrt{K}} \right) (u_o \hat{v})^2 \\ &\quad - \sigma B_o^2 (u_o \hat{v}) + \rho g_y (\beta_\theta) (\theta_o + \theta_o \hat{\theta} - \theta_o). \end{aligned}$$

or,

$$\begin{aligned}
\frac{\partial \hat{v}}{\partial \hat{t}} + \hat{u} \frac{\partial \hat{v}}{\partial \hat{x}} + \hat{v} \frac{\partial \hat{v}}{\partial \hat{y}} &= -\frac{L}{u_o^2} \frac{1}{\rho} \frac{\partial}{\partial \hat{y}} \frac{\partial \hat{y}}{\partial y} (p) + \\
\frac{1}{\rho} \left(\frac{L}{u_o^2} \frac{u_o}{L^2} \mu + \frac{L}{u_o^2} \alpha_1 \frac{\partial}{\partial \hat{t}} \frac{u_o^2}{L^3} \right) &\left[2 \frac{\partial^2 \hat{v}}{\partial \hat{y}^2} + \left(\frac{\partial^2 \hat{u}}{\partial \hat{x} \partial \hat{y}} + \frac{\partial^2 \hat{v}}{\partial \hat{x}^2} \right) \right] - \frac{1}{\rho} \left(\frac{L}{u_o^2} u_o \mu + \frac{L}{u_o^2} \alpha_1 \frac{\partial}{\partial \hat{t}} \frac{u_o^2}{L} \right) \\
\frac{\varphi}{K} \hat{v} + \frac{1}{\rho} \alpha_1 \frac{\partial}{\partial \hat{x}} &\left[\frac{L}{u_o^2} \frac{u_o^2}{L^3} \left(\hat{u} \frac{\partial^2 \hat{u}}{\partial \hat{x} \partial \hat{y}} + \hat{u} \frac{\partial^2 \hat{v}}{\partial \hat{x}^2} + \hat{v} \frac{\partial^2 \hat{u}}{\partial \hat{y}^2} + \hat{v} \frac{\partial^2 \hat{v}}{\partial \hat{x} \partial \hat{y}} + \frac{\partial \hat{u}}{\partial \hat{x}} \frac{\partial \hat{u}}{\partial \hat{y}} - \frac{\partial \hat{u}}{\partial \hat{y}} \frac{\partial \hat{v}}{\partial \hat{y}} - \frac{\partial \hat{v}}{\partial \hat{x}} \frac{\partial \hat{u}}{\partial \hat{x}} \right. \right. \\
&\left. \left. + \frac{\partial \hat{v}}{\partial \hat{y}} \frac{\partial \hat{v}}{\partial \hat{x}} \right) \right] + \frac{1}{\rho} \alpha_1 \frac{\partial}{\partial \hat{y}} \left[\frac{L}{u_o^2} \frac{u_o^2}{L^3} \left(2 \hat{u} \frac{\partial^2 \hat{v}}{\partial \hat{x} \partial \hat{y}} + 2 \hat{v} \frac{\partial^2 \hat{v}}{\partial \hat{y}^2} + \left(\frac{\partial \hat{u}}{\partial \hat{y}} \right)^2 + 4 \left(\frac{\partial \hat{v}}{\partial \hat{y}} \right)^2 - 4 \frac{1}{u_o} \frac{\partial^2 \hat{v}}{\partial \hat{y}^2} \right. \right. \\
&\left. \left. - \left(\frac{\partial \hat{v}}{\partial \hat{x}} \right)^2 \right) \right] - \frac{L}{u_o^2} \frac{1}{\rho} \left(\frac{c_F \rho \varphi}{\sqrt{K}} \right) u_o^2 \hat{v}^2 - \frac{L}{u_o^2} \sigma B_o^2 u_o \hat{v} + \frac{L}{u_o^2} \rho g_y (\beta_\theta) \theta_o \hat{\theta}.
\end{aligned}$$

or,

$$\begin{aligned}
\frac{\partial \hat{v}}{\partial \hat{t}} + \hat{u} \frac{\partial \hat{v}}{\partial \hat{x}} + \hat{v} \frac{\partial \hat{v}}{\partial \hat{y}} &= -L \frac{\partial}{\partial \hat{y}} \frac{1}{L} \left(\frac{p}{\rho u_o^2} \right) + \\
\frac{1}{\rho} \left(\frac{1}{L u_o} \mu + \alpha_1 \frac{\partial}{\partial \hat{t}} \frac{1}{L^2} \right) &\left[2 \frac{\partial^2 \hat{v}}{\partial \hat{y}^2} + \left(\frac{\partial^2 \hat{u}}{\partial \hat{x} \partial \hat{y}} + \frac{\partial^2 \hat{v}}{\partial \hat{x}^2} \right) \right] - \frac{1}{\rho} \left(\frac{L}{u_o} \mu + \alpha_1 \frac{\partial}{\partial \hat{t}} \right) \frac{\varphi}{K} \hat{v} + \\
\frac{1}{\rho} \alpha_1 \frac{\partial}{\partial \hat{x}} &\left[\frac{1}{L^2} \left(\hat{u} \frac{\partial^2 \hat{u}}{\partial \hat{x} \partial \hat{y}} + \hat{u} \frac{\partial^2 \hat{v}}{\partial \hat{x}^2} + \hat{v} \frac{\partial^2 \hat{u}}{\partial \hat{y}^2} + \hat{v} \frac{\partial^2 \hat{v}}{\partial \hat{x} \partial \hat{y}} + \frac{\partial \hat{u}}{\partial \hat{x}} \frac{\partial \hat{u}}{\partial \hat{y}} - \frac{\partial \hat{u}}{\partial \hat{y}} \frac{\partial \hat{v}}{\partial \hat{y}} - \frac{\partial \hat{v}}{\partial \hat{x}} \frac{\partial \hat{u}}{\partial \hat{x}} + \frac{\partial \hat{v}}{\partial \hat{y}} \frac{\partial \hat{v}}{\partial \hat{x}} \right) \right] \\
&+ \frac{1}{\rho} \alpha_1 \frac{\partial}{\partial \hat{y}} \left[\frac{1}{L^2} \left(2 \hat{u} \frac{\partial^2 \hat{v}}{\partial \hat{x} \partial \hat{y}} + 2 \hat{v} \frac{\partial^2 \hat{v}}{\partial \hat{y}^2} + \left(\frac{\partial \hat{u}}{\partial \hat{y}} \right)^2 + 4 \left(\frac{\partial \hat{v}}{\partial \hat{y}} \right)^2 - 4 \frac{1}{u_o} \frac{\partial^2 \hat{v}}{\partial \hat{y}^2} - \left(\frac{\partial \hat{v}}{\partial \hat{x}} \right)^2 \right) \right] \\
&- L \frac{1}{\rho} \left(\frac{c_F \rho \varphi}{\sqrt{K}} \right) \hat{v}^2 - \frac{L}{u_o} \sigma B_o^2 \hat{v} + \frac{L^3 \rho g_y (\beta_\theta) \theta_o}{\frac{u_o^2 L^2}{\nu^2}} \hat{\theta}.
\end{aligned}$$

or,

$$\begin{aligned}
\frac{\partial \hat{v}}{\partial \hat{t}} + \hat{u} \frac{\partial \hat{v}}{\partial \hat{x}} + \hat{v} \frac{\partial \hat{v}}{\partial \hat{y}} &= -\frac{\partial P}{\partial y} + \\
\left(\frac{1}{L u_o} \frac{\mu}{\rho} + \frac{\alpha_1}{\rho} \frac{\partial}{\partial \hat{t}} \frac{1}{L^2} \right) &\left[2 \frac{\partial^2 \hat{v}}{\partial \hat{y}^2} + \left(\frac{\partial^2 \hat{u}}{\partial \hat{x} \partial \hat{y}} + \frac{\partial^2 \hat{v}}{\partial \hat{x}^2} \right) \right] - \left(\frac{L}{u_o} \frac{\mu}{\rho} + \frac{\alpha_1}{\rho} \frac{\partial}{\partial \hat{t}} \right) \frac{\varphi}{K} \hat{v} + \\
\frac{1}{\rho} \alpha_1 \frac{\partial}{\partial \hat{x}} &\left[\frac{1}{L^2} \left(\hat{u} \frac{\partial^2 \hat{u}}{\partial \hat{x} \partial \hat{y}} + \hat{u} \frac{\partial^2 \hat{v}}{\partial \hat{x}^2} + \hat{v} \frac{\partial^2 \hat{u}}{\partial \hat{y}^2} + \hat{v} \frac{\partial^2 \hat{v}}{\partial \hat{x} \partial \hat{y}} + \frac{\partial \hat{u}}{\partial \hat{x}} \frac{\partial \hat{u}}{\partial \hat{y}} - \frac{\partial \hat{u}}{\partial \hat{y}} \frac{\partial \hat{v}}{\partial \hat{y}} - \frac{\partial \hat{v}}{\partial \hat{x}} \frac{\partial \hat{u}}{\partial \hat{x}} + \frac{\partial \hat{v}}{\partial \hat{y}} \frac{\partial \hat{v}}{\partial \hat{x}} \right) \right] \\
&+ \frac{1}{\rho} \alpha_1 \frac{\partial}{\partial \hat{y}} \left[\frac{1}{L^2} \left(2 \hat{u} \frac{\partial^2 \hat{v}}{\partial \hat{x} \partial \hat{y}} + 2 \hat{v} \frac{\partial^2 \hat{v}}{\partial \hat{y}^2} + \left(\frac{\partial \hat{u}}{\partial \hat{y}} \right)^2 + 4 \left(\frac{\partial \hat{v}}{\partial \hat{y}} \right)^2 - 4 \frac{1}{u_o} \frac{\partial^2 \hat{v}}{\partial \hat{y}^2} - \left(\frac{\partial \hat{v}}{\partial \hat{x}} \right)^2 \right) \right] \\
&- L \left(\frac{c_F \varphi}{\sqrt{K}} \right) \hat{v}^2 - \frac{L}{u_o} \sigma B_o^2 \hat{v} + \frac{G_r}{Re^2} \hat{\theta}.
\end{aligned}$$

or,

$$\begin{aligned} \frac{\partial \hat{v}}{\partial \hat{t}} + \hat{u} \frac{\partial \hat{v}}{\partial \hat{x}} + \hat{v} \frac{\partial \hat{v}}{\partial \hat{y}} = & -\frac{\partial P}{\partial y} + \left(\frac{1}{Lu_o} \frac{\mu}{\rho} + \frac{\alpha_1}{\rho} \frac{\partial}{\partial \hat{t}} \frac{1}{L^2} \right) \left[2 \frac{\partial^2 \hat{v}}{\partial \hat{y}^2} + \left(\frac{\partial^2 \hat{u}}{\partial \hat{x} \partial \hat{y}} + \frac{\partial^2 \hat{v}}{\partial \hat{x}^2} \right) \right] - \\ & \left[\left(\frac{L}{u_o} \frac{\mu}{\rho} \frac{1}{L^2} + \frac{\alpha_1}{\rho} \frac{\partial}{\partial \hat{t}} \frac{1}{L^2} \right) L^2 \frac{\varphi}{K} + \frac{L}{u_o} \sigma B_o^2 \right] \hat{v} + \frac{1}{\rho} \alpha_1 \frac{\partial}{\partial \hat{x}} \left[\frac{1}{L^2} \left(\hat{u} \frac{\partial^2 \hat{u}}{\partial \hat{x} \partial \hat{y}} + \hat{u} \frac{\partial^2 \hat{v}}{\partial \hat{x}^2} + \hat{v} \frac{\partial^2 \hat{u}}{\partial \hat{y}^2} \right. \right. \\ & \left. \left. + \hat{v} \frac{\partial^2 \hat{v}}{\partial \hat{x} \partial \hat{y}} + \frac{\partial \hat{u}}{\partial \hat{x}} \frac{\partial \hat{u}}{\partial \hat{y}} - \frac{\partial \hat{u}}{\partial \hat{y}} \frac{\partial \hat{v}}{\partial \hat{y}} - \frac{\partial \hat{v}}{\partial \hat{x}} \frac{\partial \hat{u}}{\partial \hat{x}} + \frac{\partial \hat{v}}{\partial \hat{y}} \frac{\partial \hat{v}}{\partial \hat{x}} \right) \right] + \frac{1}{\rho} \alpha_1 \frac{\partial}{\partial \hat{y}} \left[\frac{1}{L^2} \left(2 \hat{u} \frac{\partial^2 \hat{v}}{\partial \hat{x} \partial \hat{y}} + 2 \hat{v} \frac{\partial^2 \hat{v}}{\partial \hat{y}^2} + \right. \right. \\ & \left. \left. \left(\frac{\partial \hat{u}}{\partial \hat{y}} \right)^2 + 4 \left(\frac{\partial \hat{v}}{\partial \hat{y}} \right)^2 - 4 \frac{1}{u_o} \frac{\partial^2 \hat{v}}{\partial \hat{y}^2} - \left(\frac{\partial \hat{v}}{\partial \hat{x}} \right)^2 \right) \right] - L \left(\frac{c_F \varphi}{\sqrt{K}} \right) \hat{v}^2 + \frac{G_r}{Re^2} \hat{\theta}. \end{aligned}$$

or,

$$\begin{aligned} \frac{\partial \hat{v}}{\partial \hat{t}} + \hat{u} \frac{\partial \hat{v}}{\partial \hat{x}} + \hat{v} \frac{\partial \hat{v}}{\partial \hat{y}} = & -\frac{\partial P}{\partial y} + \left(\frac{1}{Re} + \gamma \frac{\partial}{\partial \hat{t}} \right) \left[2 \frac{\partial^2 \hat{v}}{\partial \hat{y}^2} + \left(\frac{\partial^2 \hat{u}}{\partial \hat{x} \partial \hat{y}} + \frac{\partial^2 \hat{v}}{\partial \hat{x}^2} \right) \right] - \left[\left(\frac{1}{Re} + \gamma \frac{\partial}{\partial \hat{t}} \right) \lambda + \right. \\ & \left. Ha \right] \hat{v} + \gamma \frac{\partial}{\partial \hat{x}} \left[\left(\hat{u} \frac{\partial^2 \hat{u}}{\partial \hat{x} \partial \hat{y}} + \hat{u} \frac{\partial^2 \hat{v}}{\partial \hat{x}^2} + \hat{v} \frac{\partial^2 \hat{u}}{\partial \hat{y}^2} + \hat{v} \frac{\partial^2 \hat{v}}{\partial \hat{x} \partial \hat{y}} + \frac{\partial \hat{u}}{\partial \hat{x}} \frac{\partial \hat{u}}{\partial \hat{y}} - \frac{\partial \hat{u}}{\partial \hat{y}} \frac{\partial \hat{v}}{\partial \hat{y}} - \frac{\partial \hat{v}}{\partial \hat{x}} \frac{\partial \hat{u}}{\partial \hat{x}} + \frac{\partial \hat{v}}{\partial \hat{y}} \frac{\partial \hat{v}}{\partial \hat{x}} \right) \right] \\ & + \gamma \frac{\partial}{\partial \hat{y}} \left[\left(2 \hat{u} \frac{\partial^2 \hat{v}}{\partial \hat{x} \partial \hat{y}} + 2 \hat{v} \frac{\partial^2 \hat{v}}{\partial \hat{y}^2} + \left(\frac{\partial \hat{u}}{\partial \hat{y}} \right)^2 + 4 \left(\frac{\partial \hat{v}}{\partial \hat{y}} \right)^2 - 4 \frac{1}{u_o} \frac{\partial^2 \hat{v}}{\partial \hat{y}^2} - \left(\frac{\partial \hat{v}}{\partial \hat{x}} \right)^2 \right) \right] - F_r \hat{v}^2 + \frac{G_r}{Re^2} \hat{\theta}. \end{aligned}$$

Equation (4.18) becomes:

$$\frac{\partial \theta}{\partial t} + u \frac{\partial \theta}{\partial x} + v \frac{\partial \theta}{\partial y} = \frac{k}{\rho C_p} \left(\frac{\partial^2 \theta}{\partial x^2} + \frac{\partial^2 \theta}{\partial y^2} \right).$$

or,

$$\frac{u_o}{L} \theta_o \frac{\partial \hat{\theta}}{\partial \hat{t}} + u_o \hat{u} \frac{\theta_o}{L} \frac{\partial \hat{\theta}}{\partial \hat{x}} + u_o \hat{v} \frac{\theta_o}{L} \frac{\partial \hat{\theta}}{\partial \hat{y}} = \frac{k}{\rho C_p} \left(\frac{\theta_o}{L^2} \frac{\partial^2 \hat{\theta}}{\partial \hat{x}^2} + \frac{\theta_o}{L^2} \frac{\partial^2 \hat{\theta}}{\partial \hat{y}^2} \right).$$

or,

$$\frac{u_o}{L} \theta_o \left(\frac{\partial \hat{\theta}}{\partial \hat{t}} + \hat{u} \frac{\partial \hat{\theta}}{\partial \hat{x}} + \hat{v} \frac{\partial \hat{\theta}}{\partial \hat{y}} \right) = \frac{\theta_o}{L^2} \frac{k}{\rho C_p} \left(\frac{\partial^2 \hat{\theta}}{\partial \hat{x}^2} + \frac{\partial^2 \hat{\theta}}{\partial \hat{y}^2} \right).$$

or,

$$u_o \left(\frac{\partial \hat{\theta}}{\partial \hat{t}} + \hat{u} \frac{\partial \hat{\theta}}{\partial \hat{x}} + \hat{v} \frac{\partial \hat{\theta}}{\partial \hat{y}} \right) = \frac{1}{L} \frac{k}{\rho C_p} \left(\frac{\partial^2 \hat{\theta}}{\partial \hat{x}^2} + \frac{\partial^2 \hat{\theta}}{\partial \hat{y}^2} \right).$$

or,

$$\frac{\partial \hat{\theta}}{\partial \hat{t}} + \hat{u} \frac{\partial \hat{\theta}}{\partial \hat{x}} + \hat{v} \frac{\partial \hat{\theta}}{\partial \hat{y}} = \frac{\mu}{Lu_o \rho} \frac{k}{\mu C_p} \left(\frac{\partial^2 \hat{\theta}}{\partial \hat{x}^2} + \frac{\partial^2 \hat{\theta}}{\partial \hat{y}^2} \right).$$

or,

$$\frac{\partial \hat{\theta}}{\partial \hat{t}} + \hat{u} \frac{\partial \hat{\theta}}{\partial \hat{x}} + \hat{v} \frac{\partial \hat{\theta}}{\partial \hat{y}} = \frac{1}{Re Pr} \left(\frac{\partial^2 \hat{\theta}}{\partial \hat{x}^2} + \frac{\partial^2 \hat{\theta}}{\partial \hat{y}^2} \right).$$

By simple manipulations and after ignoring the hats on the variables for convenience,

$$\begin{aligned}
\frac{\partial u}{\partial t} + u \frac{\partial u}{\partial x} + v \frac{\partial u}{\partial y} &= -\frac{\partial P}{\partial x} + \left(\frac{1}{Re} + \gamma \frac{\partial}{\partial t} \right) \left[2 \frac{\partial^2 u}{\partial x^2} + \left(\frac{\partial^2 v}{\partial x \partial y} + \frac{\partial^2 u}{\partial y^2} \right) \right] \\
&- \left[\left(\frac{1}{Re} + \gamma \frac{\partial}{\partial t} \right) \lambda + Ha \right] u + \gamma \frac{\partial}{\partial x} \left[\left(2 \left(u \frac{\partial^2 u}{\partial x^2} + v \frac{\partial^2 u}{\partial x \partial y} \right) + \frac{\partial^2 v}{\partial x^2} - \frac{\partial^2 u}{\partial y^2} \right) \right] \\
&+ \gamma \frac{\partial}{\partial y} \left[\left(u \frac{\partial^2 v}{\partial x^2} + u \frac{\partial^2 u}{\partial x \partial y} + v \frac{\partial^2 v}{\partial x \partial y} + v \frac{\partial^2 u}{\partial y^2} - \frac{\partial v}{\partial x} \frac{\partial u}{\partial x} + \frac{\partial v}{\partial y} \frac{\partial v}{\partial x} + \frac{\partial u}{\partial x} \frac{\partial u}{\partial y} - \frac{\partial u}{\partial y} \frac{\partial v}{\partial y} \right) \right] - F_r u^2.
\end{aligned} \tag{4.24}$$

$$\begin{aligned}
\frac{\partial v}{\partial t} + u \frac{\partial v}{\partial x} + v \frac{\partial v}{\partial y} &= -\frac{\partial P}{\partial y} + \left(\frac{1}{Re} + \gamma \frac{\partial}{\partial t} \right) \left[2 \frac{\partial^2 v}{\partial y^2} + \left(\frac{\partial^2 u}{\partial x \partial y} + \frac{\partial^2 v}{\partial x^2} \right) \right] - \left[\left(\frac{1}{Re} + \gamma \frac{\partial}{\partial t} \right) \lambda + \right. \\
Ha \left. \right] v + \gamma \frac{\partial}{\partial x} \left[\left(u \frac{\partial^2 u}{\partial x \partial y} + u \frac{\partial^2 v}{\partial x^2} + v \frac{\partial^2 u}{\partial y^2} + v \frac{\partial^2 v}{\partial x \partial y} + \frac{\partial u}{\partial x} \frac{\partial u}{\partial y} - \frac{\partial u}{\partial y} \frac{\partial v}{\partial y} - \frac{\partial v}{\partial x} \frac{\partial u}{\partial x} + \frac{\partial v}{\partial y} \frac{\partial v}{\partial x} \right) \right] \\
&+ \gamma \frac{\partial}{\partial y} \left[\left(2u \frac{\partial^2 v}{\partial x \partial y} + 2v \frac{\partial^2 v}{\partial y^2} + \left(\frac{\partial u}{\partial y} \right)^2 + 4 \left(\frac{\partial v}{\partial y} \right)^2 - 4 \frac{1}{u_o} \frac{\partial^2 v}{\partial y^2} - \left(\frac{\partial v}{\partial x} \right)^2 \right) \right] - F_r v^2 + \frac{G_r}{Re^2} \theta.
\end{aligned} \tag{4.25}$$

$$\frac{\partial \theta}{\partial t} + u \frac{\partial \theta}{\partial x} + v \frac{\partial \theta}{\partial y} = \frac{1}{RePr} \left(\frac{\partial^2 \theta}{\partial x^2} + \frac{\partial^2 \theta}{\partial y^2} \right). \tag{4.26}$$

4.3 Dimensionless Governing Equations

In the absence of viscous elasticity, the model reduces to $\gamma = 0$. The set of transformed dimensionless equations can be written as

x-Component of Momentum Equation:

$$\frac{\partial u}{\partial t} + u \frac{\partial u}{\partial x} + v \frac{\partial u}{\partial y} = -\frac{\partial P}{\partial x} + \frac{1}{Re} \left[2 \frac{\partial^2 u}{\partial x^2} + \left(\frac{\partial^2 v}{\partial x \partial y} + \frac{\partial^2 u}{\partial y^2} \right) \right] - \left[\frac{\lambda}{Re} + Ha \right] u - F_r u^2. \tag{4.27}$$

y-Component of Momentum Equation:

$$\frac{\partial v}{\partial t} + u \frac{\partial v}{\partial x} + v \frac{\partial v}{\partial y} = -\frac{\partial P}{\partial y} + \frac{1}{Re} \left[2 \frac{\partial^2 v}{\partial y^2} + \left(\frac{\partial^2 u}{\partial x \partial y} + \frac{\partial^2 v}{\partial x^2} \right) \right] - \left[\frac{\lambda}{Re} + Ha \right] v - F_r v^2 + \frac{G_r}{Re^2} \theta. \tag{4.28}$$

Energy Equation:

$$\frac{\partial \theta}{\partial t} + u \frac{\partial \theta}{\partial x} + v \frac{\partial \theta}{\partial y} = \frac{1}{RePr} \left(\frac{\partial^2 \theta}{\partial x^2} + \frac{\partial^2 \theta}{\partial y^2} \right). \tag{4.29}$$

The associated dimensionless boundary conditions are as follows:

- On the cavity's left wall (Γ_3)

$$u = v = 0, \quad \text{and } \theta = 0. \quad (4.30)$$

- On the cavity's right wall (Γ_3)

$$u = v = 0, \quad \text{and } \theta = 0. \quad (4.31)$$

- On the cavity's bottom portions (Γ_2, Γ_3)

$$\begin{aligned} u = v = 0, \quad \text{and } \theta = 0, \\ \text{and} \\ u = v = 0, \quad \text{and } \theta = 100. \end{aligned} \quad (4.32)$$

- On the cavity's top wall (Γ_1)

$$v = \theta = 0, \quad \text{and } u = 0. \quad (4.33)$$

The dimensionless parameters are:

$$\lambda = \frac{L^2 \varphi}{K}, \quad Ha = \frac{L}{u_o} \sigma B_o^2, \quad Fr = \frac{L c_F \varphi}{\sqrt{K}}, \quad Re = \frac{u_o L}{\nu}, \quad Gr = \frac{L^3 \rho g (\beta_\theta) \theta_o}{\nu^2}, \quad Pr = \frac{\mu C_p}{k}. \quad (4.34)$$

Chapter 5

Finite Element Formulation and Numerical Procedure

5.1 Numerical Solution

The Galerkin based Finite Element Method (FEM) is utilized to numerically solve the nonlinear partial coupled (PDEs) (4.27) to (4.29) with corresponding boundary conditions (4.30) to (4.33). For weak formulation, the dimensional form is converted into dimensionless form through similarity transformations. The strong form of the equations is converted into the weak form by multiply PDEs by test functions of the same space and the equations are integrated over the entire domain. Finally, we used the set of approximated trial functions valid only over a part of the domain to get approximated solution.

The main steps for the methodology are further listed below:

5.1.1 Strong Form of Governing Equations

The set of governing PDEs from Eqs. (4.27) to (4.29) are initially known as strong form which are re-written as

$$\frac{\partial u}{\partial t} + u \frac{\partial u}{\partial x} + v \frac{\partial u}{\partial y} = -\frac{\partial P}{\partial x} + a_1 \left[2 \frac{\partial^2 u}{\partial x^2} + \left(\frac{\partial^2 v}{\partial x \partial y} + \frac{\partial^2 u}{\partial y^2} \right) \right] - a_2 u - a_3 u^2, \quad (5.1)$$

$$\frac{\partial v}{\partial t} + u \frac{\partial v}{\partial x} + v \frac{\partial v}{\partial y} = -\frac{\partial P}{\partial y} + a_4 \left[2 \frac{\partial^2 v}{\partial y^2} + \left(\frac{\partial^2 u}{\partial x \partial y} + \frac{\partial^2 v}{\partial x^2} \right) \right] - a_5 v - a_6 v^2 + a_7 \theta, \quad (5.2)$$

and

$$\frac{\partial \theta}{\partial t} + u \frac{\partial \theta}{\partial x} + v \frac{\partial \theta}{\partial y} = a_8 \left(\frac{\partial^2 \theta}{\partial x^2} + \frac{\partial^2 \theta}{\partial y^2} \right). \quad (5.3)$$

In the above set of equations, the values of a_1, a_2, \dots, a_8 are expressed as:

$$\begin{aligned} a_1 = a_4 = \frac{1}{Re}, & \quad a_2 = a_5 = \left[\frac{\lambda}{Re} + Ha \right], & \quad a_3 = a_6 = Fr, \\ a_7 = \frac{Gr}{Re^2}, & \quad \text{and} & \quad a_8 = \frac{1}{RePr}. \end{aligned}$$

5.1.2 Weak/Variational Formulation

Weak formulation is a variational method which is used to transform differential equations into integral form by multiplying the dependent variables with suitable test function and then integrated over the whole computational domain. Here u, v, θ and P are solution spaces defined on continuously varying infinite dimensional space Ω , the matter of fact is that the achievement of the solution in such a large space is not possible. The main objective is to find some suitable spaces to get functions with finite properties or parameters. To start with weak formulation we need to define some special functions, which we called test functions for the residuals to find approximate solution. Let \mathbf{W} and Q be the test space of infinite dimensions in which $\mathbf{W} = [H_1(\Omega), H_1(\Omega), H_1(\Omega)]$ and $Q = L_2(\Omega)$. Let \tilde{w} be the respective test function such that $\tilde{w} \in \mathbf{W}$. For the variational formulation the components of momentum and energy equations are multiplied by test function $\tilde{w} \in \mathbf{W}$. The weak formulation of the strong form of governing PDEs from Eqs. (5.1) to (5.3) is written below:

The weak form for x -component of momentum equation (5.1) as follows:

$$\frac{\partial u}{\partial t} + u \frac{\partial u}{\partial x} + v \frac{\partial u}{\partial y} = -\frac{\partial P}{\partial x} + a_1 \left[2 \frac{\partial^2 u}{\partial x^2} + \left(\frac{\partial^2 v}{\partial x \partial y} + \frac{\partial^2 u}{\partial y^2} \right) \right] - a_2 u - a_3 u^2.$$

Multiplying by test function \tilde{w} first and then integrate over computational domain,

$$\begin{aligned} \frac{\partial u}{\partial t} \tilde{w} + \left[\left(u \frac{\partial u}{\partial x} \right) + \left(v \frac{\partial u}{\partial y} \right) \right] \tilde{w} = & -\frac{\partial P}{\partial x} \tilde{w} + 2a_1 \frac{\partial^2 u}{\partial x^2} \tilde{w} \\ & + a_1 \frac{\partial^2 v}{\partial x \partial y} \tilde{w} + a_1 \frac{\partial^2 u}{\partial y^2} \tilde{w} - a_2 u \tilde{w} - a_3 u^2 \tilde{w}. \end{aligned} \quad (5.4)$$

$$\begin{aligned} \text{As } \quad & -\frac{\partial}{\partial x}(P\tilde{w}) + P\frac{\partial\tilde{w}}{\partial x} = -\frac{\partial P}{\partial x}\tilde{w}, \\ & \frac{\partial}{\partial x}\left(\frac{\partial v}{\partial y}\tilde{w}\right) = \frac{\partial v}{\partial y}\frac{\partial\tilde{w}}{\partial x} + \frac{\partial v}{\partial x}\frac{\partial\tilde{w}}{\partial y}. \end{aligned}$$

So, equation (5.4) becomes:

$$\begin{aligned} \frac{\partial u}{\partial t}\tilde{w} + \left[\left(u\frac{\partial u}{\partial x}\right) + \left(v\frac{\partial u}{\partial y}\right)\right]\tilde{w} &= -\frac{\partial}{\partial x}(P\tilde{w}) + P\frac{\partial\tilde{w}}{\partial x} + 2a_1\frac{\partial^2 u}{\partial x^2}\tilde{w} + a_1\left[\frac{\partial v}{\partial y}\frac{\partial\tilde{w}}{\partial x} + \frac{\partial v}{\partial x}\frac{\partial\tilde{w}}{\partial y}\right] \\ &+ a_1\frac{\partial^2 u}{\partial y^2}\tilde{w} - a_2u\tilde{w} - a_3u^2\tilde{w}. \end{aligned}$$

$$\begin{aligned} \int_{\Omega^n} \frac{\partial u}{\partial t}\tilde{w}d\Omega + \int_{\Omega^n} \left[\left(u\frac{\partial u}{\partial x}\right) + \left(v\frac{\partial u}{\partial y}\right)\right]\tilde{w}d\Omega \\ &= -\int_{\Omega^n} \frac{\partial}{\partial x}(P\tilde{w})d\Omega + P\int_{\Omega^n} \frac{\partial\tilde{w}}{\partial x}d\Omega + 2a_1\int_{\Omega^n} \frac{\partial^2 u}{\partial x^2}\tilde{w}d\Omega + a_1\int_{\Omega^n} \left[\frac{\partial v}{\partial y}\frac{\partial\tilde{w}}{\partial x} \right. \\ &\quad \left. + \frac{\partial v}{\partial x}\frac{\partial\tilde{w}}{\partial y}\right]d\Omega + a_1\int_{\Omega^n} \frac{\partial^2 u}{\partial y^2}\tilde{w}d\Omega - a_2\int_{\Omega^n} u\tilde{w}d\Omega - a_3\int_{\Omega^n} u^2\tilde{w}d\Omega. \end{aligned}$$

$$\begin{aligned} \text{As } \int_{\Omega^n} \frac{\partial u}{\partial t}\tilde{w}d\Omega + \int_{\Omega^n} \left[u\frac{\partial u}{\partial x} + v\frac{\partial u}{\partial y}\right]\tilde{w}d\Omega \\ &= \int_{\Omega^n} \frac{(u^{n+1} - u^n)}{\delta t}\tilde{w}d\Omega + \int_{\Omega^n} \left[u\frac{\partial u}{\partial x} + v\frac{\partial u}{\partial y}\right]\tilde{w}d\Omega. \\ &= \frac{1}{\delta t}\int_{\Omega^n} u^{n+1}\tilde{w}d\Omega - \frac{1}{\delta t}\int_{\Omega^n} u^n\tilde{w}d\Omega + \int_{\Omega^n} \left[u\frac{\partial u}{\partial x} + v\frac{\partial u}{\partial y}\right]\tilde{w}d\Omega. \\ &= \frac{1}{\delta t}\int_{\Omega^n} u^{n+1}\tilde{w}d\Omega - \frac{1}{\delta t}\left(u^n \circ x^n\right)\tilde{w}d\Omega. \end{aligned}$$

$$\begin{aligned} \frac{1}{\delta t}\int_{\Omega^n} u^{n+1}\tilde{w}d\Omega - \frac{1}{\delta t}\left(u^n \circ x^n\right)\tilde{w}d\Omega \\ &= -\int_{\Omega^n} \frac{\partial}{\partial x}(P\tilde{w})d\Omega + P\int_{\Omega^n} \frac{\partial\tilde{w}}{\partial x}d\Omega + 2a_1\int_{\Omega^n} \frac{\partial^2 u}{\partial x^2}\tilde{w}d\Omega + a_1\int_{\Omega^n} \left[\frac{\partial v}{\partial y}\frac{\partial\tilde{w}}{\partial x} \right. \\ &\quad \left. + \frac{\partial v}{\partial x}\frac{\partial\tilde{w}}{\partial y}\right]d\Omega + a_1\int_{\Omega^n} \frac{\partial^2 u}{\partial y^2}\tilde{w}d\Omega - a_2\int_{\Omega^n} u\tilde{w}d\Omega - a_3\int_{\Omega^n} u^2\tilde{w}d\Omega. \end{aligned}$$

$$\begin{aligned} \frac{1}{\delta t}\int_{\Omega^n} u^{n+1}\tilde{w}d\Omega - \frac{1}{\delta t}\left(u^n \circ x^n\right)\tilde{w}d\Omega \\ &= -\int_{\Omega^n} \frac{\partial}{\partial x}(P\tilde{w})d\Omega \overset{0}{\cancel{\phantom{-\int_{\Omega^n} \frac{\partial}{\partial x}(P\tilde{w})d\Omega}}} + P\int_{\Omega^n} \frac{\partial\tilde{w}}{\partial x}d\Omega + 2a_1\int_{\Omega^n} \frac{\partial^2 u}{\partial x^2}\tilde{w}d\Omega + a_1\int_{\Omega^n} \left[\frac{\partial v}{\partial y}\frac{\partial\tilde{w}}{\partial x} \right. \end{aligned}$$

$$\begin{aligned}
& + \frac{\partial v}{\partial x} \frac{\partial \tilde{w}}{\partial y} \Big] d\Omega + a_1 \int_{\Omega^n} \frac{\partial^2 u}{\partial y^2} \tilde{w} d\Omega - a_2 \int_{\Omega^n} u \tilde{w} d\Omega - a_3 \int_{\Omega^n} u^2 \tilde{w} d\Omega \\
\frac{1}{\delta t} \int_{\Omega^n} u^{n+1} \tilde{w} d\Omega - \frac{1}{\delta t} \left(u^n \circ x^n \right) \tilde{w} d\Omega \\
& = P \int_{\Omega^n} \frac{\partial \tilde{w}}{\partial x} d\Omega + 2a_1 \int_{\Omega^n} \frac{\partial^2 u}{\partial x^2} \tilde{w} d\Omega + a_1 \int_{\Omega^n} \left[\frac{\partial v}{\partial y} \frac{\partial \tilde{w}}{\partial x} + \frac{\partial v}{\partial x} \frac{\partial \tilde{w}}{\partial y} \right] d\Omega \\
& + a_1 \int_{\Omega^n} \frac{\partial^2 u}{\partial y^2} \tilde{w} d\Omega - a_2 \int_{\Omega^n} u \tilde{w} d\Omega - a_3 \int_{\Omega^n} u^2 \tilde{w} d\Omega
\end{aligned} \tag{5.5}$$

Using Green's theorem for Laplacian term as

$$\int_{\Omega} \psi \Delta \phi \, d\Omega = - \int_{\Omega} \nabla \phi \nabla \psi \, d\Omega + \int_{\Omega} \psi (\nabla \phi n) \, d\Gamma$$

$$\text{Here, } \psi = \tilde{w}, \Delta \phi = \frac{\partial^2 u}{\partial x^2}, \Delta \phi = \frac{\partial^2 u}{\partial y^2}, \nabla \phi = \frac{\partial u}{\partial x}, \nabla \phi = \frac{\partial u}{\partial y}, \nabla \psi = \frac{\partial \tilde{w}}{\partial x}, \nabla \psi = \frac{\partial \tilde{w}}{\partial y}$$

$$\text{As } \nabla \phi n = \frac{\partial \phi}{\partial n} = n_x \frac{\partial \phi}{\partial x} + n_y \frac{\partial \phi}{\partial y} \quad (\phi = u)$$

So,

$$\begin{aligned}
& \int_{\Omega^n} \left[\frac{\partial^2 u}{\partial x^2} + \frac{\partial^2 u}{\partial y^2} \right] \tilde{w} d\Omega \\
& = \left[- \int_{\Omega^n} \frac{\partial u}{\partial x} \frac{\partial \tilde{w}}{\partial x} d\Omega + \oint_{\Gamma} \tilde{w} \left(n_x \frac{\partial u}{\partial x} \right) d\Gamma \right] + \left[- \int_{\Omega^n} \frac{\partial u}{\partial y} \frac{\partial \tilde{w}}{\partial y} d\Omega + \oint_{\Gamma} \tilde{w} \left(n_y \frac{\partial u}{\partial y} \right) d\Gamma \right]
\end{aligned}$$

Now (5.5) becomes as

$$\begin{aligned}
& \frac{1}{\delta t} \int_{\Omega^n} u^{n+1} \tilde{w} d\Omega - \frac{1}{\delta t} \left(u^n \circ x^n \right) \tilde{w} d\Omega = \\
& P \int_{\Omega^n} \frac{\partial \tilde{w}}{\partial x} d\Omega + 2a_1 \left[- \int_{\Omega^n} \frac{\partial u}{\partial x} \frac{\partial \tilde{w}}{\partial x} d\Omega + \oint_{\Gamma} \tilde{w} \left(n_x \frac{\partial u}{\partial x} \right) d\Gamma \right] + a_1 \int_{\Omega^n} \left[\frac{\partial v}{\partial y} \frac{\partial \tilde{w}}{\partial x} + \frac{\partial v}{\partial x} \frac{\partial \tilde{w}}{\partial y} \right] d\Omega \\
& + a_1 \left[- \int_{\Omega^n} \frac{\partial u}{\partial y} \frac{\partial \tilde{w}}{\partial y} d\Omega + \oint_{\Gamma} \tilde{w} \left(n_y \frac{\partial u}{\partial y} \right) d\Gamma \right] - a_2 \int_{\Omega^n} u \tilde{w} d\Omega - a_3 \int_{\Omega^n} u^2 \tilde{w} d\Omega
\end{aligned}$$

Taking Domain as current time step value, we have

$$\begin{aligned} & \frac{1}{\delta t} \int_{\Omega^{n+1}} u^{n+1} \tilde{w} d\Omega - \frac{1}{\delta t} \left(u^n \circ x^n \right) \tilde{w} d\Omega = P^{n+1} \int_{\Omega^{n+1}} \frac{\partial \tilde{w}}{\partial x^{n+1}} d\Omega + \\ & 2a_1 \left[- \int_{\Omega^{n+1}} \frac{\partial u^{n+1}}{\partial x^{n+1}} \frac{\partial \tilde{w}}{\partial x^{n+1}} d\Omega + \oint_{\Gamma} \tilde{w} \left(n_x \frac{\partial u^{n+1}}{\partial x^{n+1}} \right) d\Gamma \right] + a_1 \int_{\Omega^{n+1}} \left[\frac{\partial v^{n+1}}{\partial y^{n+1}} \frac{\partial \tilde{w}}{\partial x^{n+1}} + \frac{\partial v^{n+1}}{\partial x^{n+1}} \right. \\ & \left. \frac{\partial \tilde{w}}{\partial y^{n+1}} \right] d\Omega + a_1 \left[- \int_{\Omega^{n+1}} \frac{\partial u^{n+1}}{\partial y^{n+1}} \frac{\partial \tilde{w}}{\partial y^{n+1}} d\Omega \right. \\ & \left. + \oint_{\Gamma} \tilde{w} \left(n_y \frac{\partial u^{n+1}}{\partial y^{n+1}} \right) d\Gamma \right] - a_2 \int_{\Omega^{n+1}} u^{n+1} \tilde{w} d\Omega - a_3 \int_{\Omega^{n+1}} u^n u^{n+1} \tilde{w} d\Omega \end{aligned}$$

which is weak form of x -component of momentum equation.

Similarly, we obtain the weak form for y -component of momentum equation (5.2) as follows:

$$\frac{\partial v}{\partial t} + u \frac{\partial v}{\partial x} + v \frac{\partial v}{\partial y} = - \frac{\partial P}{\partial y} + a_4 \left[2 \frac{\partial^2 v}{\partial y^2} + \left(\frac{\partial^2 u}{\partial x \partial y} + \frac{\partial^2 v}{\partial x^2} \right) \right] - a_5 v - a_6 v^2 + a_7 \theta.$$

Multiplying by test function \tilde{w} first and then integrate over computational domain,

$$\begin{aligned} \frac{\partial v}{\partial t} \tilde{w} + \left[\left(u \frac{\partial v}{\partial x} \right) + \left(v \frac{\partial v}{\partial y} \right) \right] \tilde{w} &= - \frac{\partial P}{\partial y} \tilde{w} + 2a_4 \frac{\partial^2 v}{\partial y^2} \tilde{w} \\ &+ a_4 \frac{\partial^2 u}{\partial x \partial y} \tilde{w} + a_4 \frac{\partial^2 v}{\partial x^2} \tilde{w} - a_5 v \tilde{w} - a_6 v^2 \tilde{w} + a_7 \theta \tilde{w} \end{aligned} \quad (5.6)$$

$$\begin{aligned} \text{As} \quad & - \frac{\partial}{\partial y} (P \tilde{w}) + P \frac{\partial \tilde{w}}{\partial y} = - \frac{\partial P}{\partial y} \tilde{w} \\ & \frac{\partial}{\partial x} \left(\frac{\partial u}{\partial y} \tilde{w} \right) = \frac{\partial u}{\partial y} \frac{\partial \tilde{w}}{\partial x} + \frac{\partial u}{\partial x} \frac{\partial \tilde{w}}{\partial y} \end{aligned}$$

So, equation (5.6) becomes:

$$\begin{aligned} \frac{\partial v}{\partial t} \tilde{w} + \left[\left(u \frac{\partial v}{\partial x} \right) + \left(v \frac{\partial v}{\partial y} \right) \right] \tilde{w} &= - \frac{\partial}{\partial y} (P \tilde{w}) + P \frac{\partial \tilde{w}}{\partial y} + 2a_4 \frac{\partial^2 v}{\partial y^2} \tilde{w} + a_4 \left[\frac{\partial u}{\partial y} \frac{\partial \tilde{w}}{\partial x} + \frac{\partial u}{\partial x} \frac{\partial \tilde{w}}{\partial y} \right] \\ &+ a_4 \frac{\partial^2 v}{\partial x^2} \tilde{w} - a_5 v \tilde{w} - a_6 v^2 \tilde{w} + a_7 \theta \tilde{w}. \end{aligned}$$

$$\int_{\Omega^n} \frac{\partial v}{\partial t} \tilde{w} d\Omega + \int_{\Omega^n} \left[\left(u \frac{\partial v}{\partial x} \right) + \left(v \frac{\partial v}{\partial y} \right) \right] \tilde{w} d\Omega$$

$$\begin{aligned}
&= - \int_{\Omega^n} \frac{\partial}{\partial y} (P\tilde{w}) d\Omega + P \int_{\Omega^n} \frac{\partial \tilde{w}}{\partial y} d\Omega + 2a_4 \int_{\Omega^n} \frac{\partial^2 v}{\partial y^2} \tilde{w} d\Omega + a_4 \int_{\Omega^n} \left[\frac{\partial u}{\partial y} \frac{\partial \tilde{w}}{\partial x} \right. \\
&\quad \left. + \frac{\partial u}{\partial x} \frac{\partial \tilde{w}}{\partial y} \right] d\Omega + a_4 \int_{\Omega^n} \frac{\partial^2 v}{\partial x^2} \tilde{w} d\Omega - a_5 \int_{\Omega^n} v \tilde{w} d\Omega - a_6 \int_{\Omega^n} v^2 \tilde{w} d\Omega + a_7 \int_{\Omega^n} \theta \tilde{w} d\Omega \\
As \int_{\Omega^n} \frac{\partial v}{\partial t} \tilde{w} d\Omega &+ \int_{\Omega^n} \left[u \frac{\partial v}{\partial x} + v \frac{\partial v}{\partial y} \right] \tilde{w} d\Omega \\
&= \int_{\Omega^n} \frac{(v^{n+1} - v^n)}{\delta t} \tilde{w} d\Omega + \int_{\Omega^n} \left[u \frac{\partial v}{\partial x} + v \frac{\partial v}{\partial y} \right] \tilde{w} d\Omega \\
&= \frac{1}{\delta t} \int_{\Omega^n} v^{n+1} \tilde{w} d\Omega - \frac{1}{\delta t} \int_{\Omega^n} v^n \tilde{w} d\Omega + \int_{\Omega^n} \left[u \frac{\partial v}{\partial x} + v \frac{\partial v}{\partial y} \right] \tilde{w} d\Omega \\
&= \frac{1}{\delta t} \int_{\Omega^n} v^{n+1} \tilde{w} d\Omega - \frac{1}{\delta t} \left(v^n \circ y^n \right) \tilde{w} d\Omega.
\end{aligned}$$

$$\begin{aligned}
&\frac{1}{\delta t} \int_{\Omega^n} v^{n+1} \tilde{w} d\Omega - \frac{1}{\delta t} \left(v^n \circ y^n \right) \tilde{w} d\Omega \\
&= - \int_{\Omega^n} \frac{\partial}{\partial y} (P\tilde{w}) d\Omega + P \int_{\Omega^n} \frac{\partial \tilde{w}}{\partial y} d\Omega + 2a_4 \int_{\Omega^n} \frac{\partial^2 v}{\partial y^2} \tilde{w} d\Omega + a_4 \int_{\Omega^n} \left[\frac{\partial u}{\partial y} \frac{\partial \tilde{w}}{\partial x} \right. \\
&\quad \left. + \frac{\partial u}{\partial x} \frac{\partial \tilde{w}}{\partial y} \right] d\Omega + a_4 \int_{\Omega^n} \frac{\partial^2 v}{\partial x^2} \tilde{w} d\Omega - a_5 \int_{\Omega^n} v \tilde{w} d\Omega - a_6 \int_{\Omega^n} v^2 \tilde{w} d\Omega + a_7 \int_{\Omega^n} \theta \tilde{w} d\Omega
\end{aligned}$$

$$\begin{aligned}
&\frac{1}{\delta t} \int_{\Omega^n} v^{n+1} \tilde{w} d\Omega - \frac{1}{\delta t} \left(v^n \circ y^n \right) \tilde{w} d\Omega \\
&= - \int_{\Omega^n} \frac{\partial}{\partial y} (P\tilde{w}) d\Omega \overset{0}{\rightarrow} + P \int_{\Omega^n} \frac{\partial \tilde{w}}{\partial y} d\Omega + 2a_4 \int_{\Omega^n} \frac{\partial^2 v}{\partial y^2} \tilde{w} d\Omega + a_4 \int_{\Omega^n} \left[\frac{\partial u}{\partial y} \frac{\partial \tilde{w}}{\partial x} \right. \\
&\quad \left. + \frac{\partial u}{\partial x} \frac{\partial \tilde{w}}{\partial y} \right] d\Omega + a_4 \int_{\Omega^n} \frac{\partial^2 v}{\partial x^2} \tilde{w} d\Omega - a_5 \int_{\Omega^n} v \tilde{w} d\Omega - a_6 \int_{\Omega^n} v^2 \tilde{w} d\Omega + a_7 \int_{\Omega^n} \theta \tilde{w} d\Omega
\end{aligned}$$

$$\begin{aligned}
&\frac{1}{\delta t} \int_{\Omega^n} v^{n+1} \tilde{w} d\Omega - \frac{1}{\delta t} \left(v^n \circ y^n \right) \tilde{w} d\Omega \\
&= P \int_{\Omega^n} \frac{\partial \tilde{w}}{\partial y} d\Omega + 2a_4 \int_{\Omega^n} \frac{\partial^2 v}{\partial y^2} \tilde{w} d\Omega + a_4 \int_{\Omega^n} \left[\frac{\partial u}{\partial y} \frac{\partial \tilde{w}}{\partial x} + \frac{\partial u}{\partial x} \frac{\partial \tilde{w}}{\partial y} \right] d\Omega \\
&\quad + a_4 \int_{\Omega^n} \frac{\partial^2 v}{\partial x^2} \tilde{w} d\Omega - a_5 \int_{\Omega^n} v \tilde{w} d\Omega - a_6 \int_{\Omega^n} v^2 \tilde{w} d\Omega + a_7 \int_{\Omega^n} \theta \tilde{w} d\Omega.
\end{aligned}$$

(5.7)

Using Green's theorem for Laplacian term as

$$\int_{\Omega} \psi \Delta \phi \, d\Omega = - \int_{\Omega} \nabla \phi \nabla \psi \, d\Omega + \int_{\Omega} \psi (\nabla \phi n) \, d\Gamma$$

Here, $\psi = \tilde{w}$, $\Delta \phi = \frac{\partial^2 v}{\partial x^2}$, $\Delta \phi = \frac{\partial^2 v}{\partial y^2}$, $\nabla \phi = \frac{\partial v}{\partial x}$, $\nabla \phi = \frac{\partial v}{\partial y}$, $\nabla \psi = \frac{\partial \tilde{w}}{\partial x}$, $\nabla \psi = \frac{\partial \tilde{w}}{\partial y}$

$$\begin{aligned} & \int_{\Omega^n} \left[\frac{\partial^2 v}{\partial x^2} + \frac{\partial^2 v}{\partial y^2} \right] \tilde{w} d\Omega \\ &= \left[- \int_{\Omega^n} \frac{\partial v}{\partial x} \frac{\partial \tilde{w}}{\partial x} d\Omega + \oint_{\Gamma} \tilde{w} \left(n_x \frac{\partial v}{\partial x} \right) d\Gamma \right] + \left[- \int_{\Omega^n} \frac{\partial v}{\partial y} \frac{\partial \tilde{w}}{\partial y} d\Omega + \oint_{\Gamma} \tilde{w} \left(n_y \frac{\partial v}{\partial y} \right) d\Gamma \right]. \end{aligned}$$

Now (5.7) becomes as

$$\begin{aligned} & \frac{1}{\delta t} \int_{\Omega^n} v^{n+1} \tilde{w} d\Omega - \frac{1}{\delta t} \left(v^n \circ y^n \right) \tilde{w} d\Omega = \\ & P \int_{\Omega^n} \frac{\partial \tilde{w}}{\partial y} d\Omega + 2a_4 \left[- \int_{\Omega^n} \frac{\partial v}{\partial x} \frac{\partial \tilde{w}}{\partial x} d\Omega + \oint_{\Gamma} \tilde{w} \left(n_x \frac{\partial v}{\partial x} \right) d\Gamma \right] + a_4 \int_{\Omega^n} \left[\frac{\partial u}{\partial y} \frac{\partial \tilde{w}}{\partial x} + \frac{\partial u}{\partial x} \frac{\partial \tilde{w}}{\partial y} \right] d\Omega \\ & + a_4 \left[- \int_{\Omega^n} \frac{\partial v}{\partial y} \frac{\partial \tilde{w}}{\partial y} d\Omega + \oint_{\Gamma} \tilde{w} \left(n_y \frac{\partial v}{\partial y} \right) d\Gamma \right] - a_5 \int_{\Omega^n} v \tilde{w} d\Omega - a_6 \int_{\Omega^n} v^2 \tilde{w} d\Omega + a_7 \int_{\Omega^n} \theta \tilde{w} d\Omega \end{aligned}$$

Taking Domain as current time step value, we have

$$\begin{aligned} & \frac{1}{\delta t} \int_{\Omega^{n+1}} v^{n+1} \tilde{w} d\Omega - \frac{1}{\delta t} \left(v^n \circ y^n \right) \tilde{w} d\Omega = P^{n+1} \int_{\Omega^{n+1}} \frac{\partial \tilde{w}}{\partial y^{n+1}} d\Omega + \\ & 2a_4 \left[- \int_{\Omega^{n+1}} \frac{\partial v^{n+1}}{\partial x^{n+1}} \frac{\partial \tilde{w}}{\partial x^{n+1}} d\Omega + \oint_{\Gamma} \tilde{w} \left(n_x \frac{\partial v^{n+1}}{\partial x^{n+1}} \right) d\Gamma \right] + a_4 \int_{\Omega^{n+1}} \left[\frac{\partial u^{n+1}}{\partial y^{n+1}} \frac{\partial \tilde{w}}{\partial x^{n+1}} + \frac{\partial u^{n+1}}{\partial x^{n+1}} \right. \\ & \left. \frac{\partial \tilde{w}}{\partial y^{n+1}} \right] d\Omega + a_4 \left[- \int_{\Omega^{n+1}} \frac{\partial v^{n+1}}{\partial y^{n+1}} \frac{\partial \tilde{w}}{\partial y^{n+1}} d\Omega \right. \\ & \left. + \oint_{\Gamma} \tilde{w} \left(n_y \frac{\partial v^{n+1}}{\partial y^{n+1}} \right) d\Gamma \right] - a_5 \int_{\Omega^{n+1}} v^{n+1} \tilde{w} d\Omega - a_6 \int_{\Omega^{n+1}} v^n v^{n+1} \tilde{w} d\Omega + a_7 \int_{\Omega^{n+1}} \theta^{n+1} \tilde{w} d\Omega \end{aligned}$$

which is weak form of y -component of momentum equation.

The energy equation in the same way becomes:

$$\frac{\partial \theta}{\partial t} + u \frac{\partial \theta}{\partial x} + v \frac{\partial \theta}{\partial y} = a_8 \left(\frac{\partial^2 \theta}{\partial x^2} + \frac{\partial^2 \theta}{\partial y^2} \right)$$

Multiplying by test function \tilde{w} first and then integrate over computational domain,

$$\frac{\partial \theta}{\partial t} \tilde{w} + \left[\left(u \frac{\partial \theta}{\partial x} \right) + \left(v \frac{\partial \theta}{\partial y} \right) \right] \tilde{w} = a_8 \left(\frac{\partial^2 \theta}{\partial x^2} + \frac{\partial^2 \theta}{\partial y^2} \right) \tilde{w}$$

$$\int_{\Omega^n} \frac{\partial \theta}{\partial t} \tilde{w} d\Omega + \int_{\Omega^n} \left[\left(u \frac{\partial \theta}{\partial x} \right) + \left(v \frac{\partial \theta}{\partial y} \right) \right] \tilde{w} d\Omega = a_8 \int_{\Omega^n} \left(\frac{\partial^2 \theta}{\partial x^2} + \frac{\partial^2 \theta}{\partial y^2} \right) \tilde{w} d\Omega$$

$$\begin{aligned} \text{As } \int_{\Omega^n} \frac{\partial \theta}{\partial t} \tilde{w} d\Omega + \int_{\Omega^n} \left[u \frac{\partial \theta}{\partial x} + v \frac{\partial \theta}{\partial y} \right] \tilde{w} d\Omega & \\ &= \int_{\Omega^n} \frac{(\theta^{n+1} - \theta^n)}{\delta t} \tilde{w} d\Omega + \int_{\Omega^n} \left[u \frac{\partial \theta}{\partial x} + v \frac{\partial \theta}{\partial y} \right] \tilde{w} d\Omega \\ &= \frac{1}{\delta t} \int_{\Omega^n} \theta^{n+1} \tilde{w} d\Omega - \frac{1}{\delta t} \int_{\Omega^n} \theta^n \tilde{w} d\Omega + \int_{\Omega^n} \left[u \frac{\partial \theta}{\partial x} + v \frac{\partial \theta}{\partial y} \right] \tilde{w} d\Omega \\ &= \frac{1}{\delta t} \int_{\Omega^n} \theta^{n+1} \tilde{w} d\Omega - \frac{1}{\delta t} \left(\theta^n \circ x^n \right) \tilde{w} d\Omega \\ \frac{1}{\delta t} \int_{\Omega^n} \theta^{n+1} \tilde{w} d\Omega - \frac{1}{\delta t} \left(\theta^n \circ x^n \right) \tilde{w} d\Omega &= a_8 \int_{\Omega^n} \left(\frac{\partial^2 \theta}{\partial x^2} + \frac{\partial^2 \theta}{\partial y^2} \right) \tilde{w} d\Omega \end{aligned} \quad (5.8)$$

Using Green's theorem for Laplacian term as

$$\int_{\Omega} \psi \Delta \phi \, d\Omega = - \int_{\Omega} \nabla \phi \nabla \psi \, d\Omega + \int_{\Omega} \psi (\nabla \phi \cdot n) \, d\Gamma$$

So,

$$\begin{aligned} \int_{\Omega^n} \left[\frac{\partial^2 \theta}{\partial x^2} + \frac{\partial^2 \theta}{\partial y^2} \right] \tilde{w} d\Omega & \\ &= \left[- \int_{\Omega^n} \frac{\partial \theta}{\partial x} \frac{\partial \tilde{w}}{\partial x} d\Omega + \oint_{\Gamma} \tilde{w} \left(n_x \frac{\partial \theta}{\partial x} \right) d\Gamma - \int_{\Omega^n} \frac{\partial \theta}{\partial y} \frac{\partial \tilde{w}}{\partial y} d\Omega + \oint_{\Gamma} \tilde{w} \left(n_y \frac{\partial \theta}{\partial y} \right) d\Gamma \right] \end{aligned}$$

Now (5.8), becomes:

$$\begin{aligned} \frac{1}{\delta t} \int_{\Omega^n} \theta^{n+1} \tilde{w} d\Omega - \frac{1}{\delta t} \left(\theta^n \circ x^n \right) \tilde{w} d\Omega &= \\ a_8 \left[- \int_{\Omega^n} \frac{\partial \theta}{\partial x} \frac{\partial \tilde{w}}{\partial x} d\Omega + \oint_{\Gamma} \tilde{w} \left(n_x \frac{\partial \theta}{\partial x} \right) d\Gamma - \int_{\Omega^n} \frac{\partial \theta}{\partial y} \frac{\partial \tilde{w}}{\partial y} d\Omega + \oint_{\Gamma} \tilde{w} \left(n_y \frac{\partial \theta}{\partial y} \right) d\Gamma \right] \end{aligned}$$

Taking Domain as current time step value, we have

$$\begin{aligned} \frac{1}{\delta t} \int_{\Omega^{n+1}} \theta^{n+1} \tilde{w} d\Omega - \frac{1}{\delta t} \left(\theta^n \circ x^n \right) \tilde{w} d\Omega = a_8 \left[- \int_{\Omega^{n+1}} \frac{\partial \theta^{n+1}}{\partial x^{n+1}} \frac{\partial \tilde{w}}{\partial x^{n+1}} d\Omega \right. \\ \left. + \oint_{\Gamma} \tilde{w} \left(n_x \frac{\partial \theta^{n+1}}{\partial x^{n+1}} \right) d\Gamma - \int_{\Omega^{n+1}} \frac{\partial \theta^{n+1}}{\partial y^{n+1}} \frac{\partial \tilde{w}}{\partial y^{n+1}} d\Omega + \oint_{\Gamma} \tilde{w} \left(n_y \frac{\partial \theta^{n+1}}{\partial y^{n+1}} \right) d\Gamma \right] \end{aligned}$$

Find $(u, v, \theta) \in W$ and $P \in Q$ such that

$$\begin{aligned} \frac{1}{\delta t} \int_{\Omega^{n+1}} u^{n+1} \tilde{w} d\Omega - \frac{1}{\delta t} \left(u^n \circ x^n \right) \tilde{w} d\Omega - P^{n+1} \int_{\Omega^{n+1}} \frac{\partial \tilde{w}}{\partial x^{n+1}} d\Omega - \\ 2a_1 \left[- \int_{\Omega^{n+1}} \frac{\partial u^{n+1}}{\partial x^{n+1}} \frac{\partial \tilde{w}}{\partial x^{n+1}} d\Omega + \oint_{\Gamma} \tilde{w} \left(n_x \frac{\partial u^{n+1}}{\partial x^{n+1}} \right) d\Gamma \right] - a_1 \int_{\Omega^{n+1}} \left[\frac{\partial v^{n+1}}{\partial y^{n+1}} \frac{\partial \tilde{w}}{\partial x^{n+1}} + \frac{\partial v^{n+1}}{\partial x^{n+1}} \right. \\ \left. \frac{\partial \tilde{w}}{\partial y^{n+1}} \right] d\Omega - a_1 \left[- \int_{\Omega^{n+1}} \frac{\partial u^{n+1}}{\partial y^{n+1}} \frac{\partial \tilde{w}}{\partial y^{n+1}} d\Omega + \right. \\ \left. \oint_{\Gamma} \tilde{w} \left(n_y \frac{\partial u^{n+1}}{\partial y^{n+1}} \right) d\Gamma \right] + a_2 \int_{\Omega^{n+1}} u^{n+1} \tilde{w} d\Omega + a_3 \int_{\Omega^{n+1}} u^n u^{n+1} \tilde{w} d\Omega = 0, \end{aligned} \quad (5.9)$$

$$\begin{aligned} \frac{1}{\delta t} \int_{\Omega^{n+1}} v^{n+1} \tilde{w} d\Omega - \frac{1}{\delta t} \left(v^n \circ y^n \right) \tilde{w} d\Omega - P^{n+1} \int_{\Omega^{n+1}} \frac{\partial \tilde{w}}{\partial y^{n+1}} d\Omega - \\ 2a_4 \left[- \int_{\Omega^{n+1}} \frac{\partial v^{n+1}}{\partial x^{n+1}} \frac{\partial \tilde{w}}{\partial x^{n+1}} d\Omega + \oint_{\Gamma} \tilde{w} \left(n_x \frac{\partial v^{n+1}}{\partial x^{n+1}} \right) d\Gamma \right] - a_4 \int_{\Omega^{n+1}} \left[\frac{\partial u^{n+1}}{\partial y^{n+1}} \frac{\partial \tilde{w}}{\partial x^{n+1}} + \frac{\partial u^{n+1}}{\partial x^{n+1}} \right. \\ \left. \frac{\partial \tilde{w}}{\partial y^{n+1}} \right] d\Omega - a_4 \left[- \int_{\Omega^{n+1}} \frac{\partial v^{n+1}}{\partial y^{n+1}} \frac{\partial \tilde{w}}{\partial y^{n+1}} d\Omega + \right. \\ \left. \oint_{\Gamma} \tilde{w} \left(n_y \frac{\partial v^{n+1}}{\partial y^{n+1}} \right) d\Gamma \right] + a_5 \int_{\Omega^{n+1}} v^{n+1} \tilde{w} d\Omega + a_6 \int_{\Omega^{n+1}} v^n v^{n+1} \tilde{w} d\Omega - a_7 \int_{\Omega^{n+1}} \theta^{n+1} \tilde{w} d\Omega = 0, \end{aligned} \quad (5.10)$$

$$\begin{aligned} \frac{1}{\delta t} \int_{\Omega^{n+1}} \theta^{n+1} \tilde{w} d\Omega - \frac{1}{\delta t} \left(\theta^n \circ x^n \right) \tilde{w} d\Omega - a_8 \left[- \int_{\Omega^{n+1}} \frac{\partial \theta^{n+1}}{\partial x^{n+1}} \frac{\partial \tilde{w}}{\partial x^{n+1}} d\Omega \right. \\ \left. + \oint_{\Gamma} \tilde{w} \left(n_x \frac{\partial \theta^{n+1}}{\partial x^{n+1}} \right) d\Gamma - \int_{\Omega^{n+1}} \frac{\partial \theta^{n+1}}{\partial y^{n+1}} \frac{\partial \tilde{w}}{\partial y^{n+1}} d\Omega + \oint_{\Gamma} \tilde{w} \left(n_y \frac{\partial \theta^{n+1}}{\partial y^{n+1}} \right) d\Gamma \right] = 0. \end{aligned} \quad (5.11)$$

for all $\tilde{w} \in W$ and $P \in Q$.

For the Galerkin discretization, the infinite dimensional test and trial spaces are approximated by finite dimensional spaces. In particular, following are the trial and test spaces

Trial Spaces:

$$u \approx u_h, \quad v \approx v_h, \quad \theta \approx \theta_h \quad \text{and} \quad P \approx P_h.$$

Test Spaces:

$$W \approx W_h \quad \text{and} \quad Q \approx Q_h.$$

Find $(u_h, v_h, \theta_h) \in W_h$ and $P_h \in Q_h$ such that

$$\begin{aligned} & \frac{1}{\delta t} \int_{\Omega^{n+1}} u_h^{n+1} \tilde{w}_h d\Omega - \frac{1}{\delta t} \left(u_h^n \circ x^n \right) \tilde{w}_h d\Omega - P_h^{n+1} \int_{\Omega^{n+1}} \frac{\partial \tilde{w}_h}{\partial x^{n+1}} d\Omega \\ & - 2a_1 \left[- \int_{\Omega^{n+1}} \frac{\partial u_h^{n+1}}{\partial x^{n+1}} \frac{\partial \tilde{w}_h}{\partial x^{n+1}} d\Omega + \oint_{\Gamma} \tilde{w}_h \left(n_x \frac{\partial u_h^{n+1}}{\partial x^{n+1}} \right) d\Gamma \right] - a_1 \int_{\Omega^{n+1}} \left[\frac{\partial v_h^{n+1}}{\partial y^{n+1}} \frac{\partial \tilde{w}_h}{\partial x^{n+1}} \right. \\ & \left. + \frac{\partial v_h^{n+1}}{\partial x^{n+1}} \frac{\partial \tilde{w}_h}{\partial y^{n+1}} \right] d\Omega - a_1 \left[- \int_{\Omega^{n+1}} \frac{\partial u_h^{n+1}}{\partial y^{n+1}} \frac{\partial \tilde{w}_h}{\partial y^{n+1}} d\Omega + \oint_{\Gamma} \tilde{w}_h \left(n_y \frac{\partial u_h^{n+1}}{\partial y^{n+1}} \right) d\Gamma \right] \\ & + a_2 \int_{\Omega^{n+1}} u_h^{n+1} \tilde{w}_h d\Omega + a_3 \int_{\Omega^{n+1}} u_h^n u_h^{n+1} \tilde{w}_h d\Omega = 0, \end{aligned} \tag{5.12}$$

$$\begin{aligned} & \frac{1}{\delta t} \int_{\Omega^{n+1}} v_h^{n+1} \tilde{w}_h d\Omega - \frac{1}{\delta t} \left(v_h^n \circ y^n \right) \tilde{w}_h d\Omega - P_h^{n+1} \int_{\Omega^{n+1}} \frac{\partial \tilde{w}_h}{\partial y^{n+1}} d\Omega \\ & - 2a_4 \left[- \int_{\Omega^{n+1}} \frac{\partial v_h^{n+1}}{\partial x^{n+1}} \frac{\partial \tilde{w}_h}{\partial x^{n+1}} d\Omega + \oint_{\Gamma} \tilde{w}_h \left(n_x \frac{\partial v_h^{n+1}}{\partial x^{n+1}} \right) d\Gamma \right] - a_4 \int_{\Omega^{n+1}} \left[\frac{\partial u_h^{n+1}}{\partial y^{n+1}} \frac{\partial \tilde{w}_h}{\partial x^{n+1}} \right. \\ & \left. + \frac{\partial u_h^{n+1}}{\partial x^{n+1}} \frac{\partial \tilde{w}_h}{\partial y^{n+1}} \right] d\Omega - a_4 \left[- \int_{\Omega^{n+1}} \frac{\partial v_h^{n+1}}{\partial y^{n+1}} \frac{\partial \tilde{w}_h}{\partial y^{n+1}} d\Omega + \oint_{\Gamma} \tilde{w}_h \left(n_y \frac{\partial v_h^{n+1}}{\partial y^{n+1}} \right) d\Gamma \right] \\ & + a_5 \int_{\Omega^{n+1}} v_h^{n+1} \tilde{w}_h d\Omega + a_6 \int_{\Omega^{n+1}} v_h^n v_h^{n+1} \tilde{w}_h d\Omega - a_7 \int_{\Omega^{n+1}} \theta_h^{n+1} \tilde{w}_h d\Omega = 0, \end{aligned} \tag{5.13}$$

$$\begin{aligned} & \frac{1}{\delta t} \int_{\Omega^{n+1}} \theta_h^{n+1} \tilde{w}_h d\Omega - \frac{1}{\delta t} \left(\theta_h^n \circ x^n \right) \tilde{w}_h d\Omega - a_8 \left[- \int_{\Omega^{n+1}} \frac{\partial \theta_h^{n+1}}{\partial x^{n+1}} \frac{\partial \tilde{w}_h}{\partial x^{n+1}} d\Omega \right. \\ & \left. + \oint_{\Gamma} \tilde{w}_h \left(n_x \frac{\partial \theta_h^{n+1}}{\partial x^{n+1}} \right) d\Gamma - \int_{\Omega^{n+1}} \frac{\partial \theta_h^{n+1}}{\partial y^{n+1}} \frac{\partial \tilde{w}_h}{\partial y^{n+1}} d\Omega + \oint_{\Gamma} \tilde{w}_h \left(n_y \frac{\partial \theta_h^{n+1}}{\partial y^{n+1}} \right) d\Gamma \right] = 0. \end{aligned} \tag{5.14}$$

for all $\tilde{w}_h \in W_h$ and $P_h \in Q_h$.

FEM approximation is achieved by using the approximate trial solution functions and trial test functions. These functions are the linear combination of nodal unknowns and shape functions which are linearly independent. Given below are the trial solution functions:

$$u_h = \sum_{j=1}^m u_j \xi_j, \quad v_h = \sum_{j=1}^m v_j \xi_j, \quad \theta_h = \sum_{j=1}^m \theta_j \xi_j, \quad P_h = \sum_{j=1}^l P_j \eta_j.$$

Similarly following trial approximated functions are defined for test spaces:

$$\tilde{w}_h = \sum_{i=1}^m \tilde{w}_i \xi_i.$$

In all above relations ξ_j and η_j are the shape functions. By using these approximations in Eqs. (5.12) to (5.14), weak formulation can be expressed as

(5.12) \Rightarrow

$$\begin{aligned} & \frac{1}{\delta t} \int_{\Omega^{n+1}} \left[\left(\sum_{j=1}^m u_j \xi_j \right)^{n+1} - \left(\left(\sum_{j=1}^m u_j \xi_j \right)^n \circ x^n \right) \right] \xi_i d\Omega - \left(\sum_{j=1}^l P_j \eta_j \right) \int_{\Omega^{n+1}} \frac{\partial \xi_i}{\partial x} d\Omega - \\ & 2a_1 \left[- \int_{\Omega^{n+1}} \frac{\partial}{\partial x} \left(\sum_{j=1}^m u_j \xi_j \right) \frac{\partial \xi_i}{\partial x} d\Omega + \oint_{\Gamma} \xi_i \left(n_x \frac{\partial}{\partial x} \left(\sum_{j=1}^m u_j \xi_j \right) \right) d\Gamma \right] - \\ & a_1 \int_{\Omega^{n+1}} \left[\frac{\partial}{\partial y} \left(\sum_{j=1}^m v_j \xi_j \right) \frac{\partial \xi_i}{\partial x} + \frac{\partial}{\partial x} \left(\sum_{j=1}^m v_j \xi_j \right) \frac{\partial \xi_i}{\partial y} \right] d\Omega - a_1 \left[- \int_{\Omega^{n+1}} \frac{\partial}{\partial y} \left(\sum_{j=1}^m u_j \xi_j \right) \frac{\partial \xi_i}{\partial y} d\Omega \right. \\ & \left. + \oint_{\Gamma} \xi_i \left(n_y \frac{\partial}{\partial y} \left(\sum_{j=1}^m u_j \xi_j \right) \right) d\Gamma \right] + a_2 \int_{\Omega^{n+1}} \left(\sum_{j=1}^m u_j \xi_j \right) \xi_i d\Omega \\ & + a_3 \int_{\Omega^{n+1}} \left(\sum_{j=1}^m u_j \xi_j \right)^n \left(\sum_{j=1}^m u_j \xi_j \right)^{n+1} \xi_i d\Omega = 0. \end{aligned}$$

$$\begin{aligned} & \frac{1}{\delta t} \int_{\Omega^{n+1}} \left[\left(\sum_{j=1}^m u_j \xi_j \right)^{n+1} - \left(\left(\sum_{j=1}^m u_j \xi_j \right)^n \circ x^n \right) \right] \xi_i d\Omega - \sum_{j=1}^l \int_{\Omega^{n+1}} \frac{\partial \xi_i}{\partial x^{n+1}} \eta_j^{n+1} d\Omega \{P_j^{n+1}\} + 2 \\ & a_1 \sum_{j=1}^m \int_{\Omega^{n+1}} \frac{\partial \xi_j^{n+1}}{\partial x^{n+1}} \frac{\partial \xi_i}{\partial x^{n+1}} d\Omega \{u_j^{n+1}\} - a_1 \sum_{j=1}^m \int_{\Omega^{n+1}} \left[\frac{\partial \xi_j^{n+1}}{\partial y^{n+1}} \frac{\partial \xi_i}{\partial x^{n+1}} + \frac{\partial \xi_j^{n+1}}{\partial x^{n+1}} \frac{\partial \xi_i}{\partial y^{n+1}} \right] d\Omega \{v_j^{n+1}\} \\ & + a_1 \sum_{j=1}^m \int_{\Omega^{n+1}} \frac{\partial \xi_j^{n+1}}{\partial y^{n+1}} \frac{\partial \xi_i}{\partial y^{n+1}} d\Omega \{u_j^{n+1}\} + a_2 \sum_{j=1}^m \int_{\Omega^{n+1}} \xi_j^{n+1} \xi_i d\Omega \{u_j^{n+1}\} \end{aligned}$$

$$\begin{aligned}
& + a_3 \int_{\Omega^{n+1}} \left(\sum_{j=1}^m u_j \xi_j \right)^n \left(\sum_{j=1}^m u_j \xi_j \right)^{n+1} \xi_i d\Omega = \\
& \sum_{j=1}^m \oint_{\Gamma} \xi_i \left[\left(n_x \frac{\partial \xi_j^{n+1}}{\partial x^{n+1}} \right) + \left(n_y \frac{\partial \xi_j^{n+1}}{\partial y^{n+1}} \right) \right] d\Gamma \{u_j^{n+1}\}.
\end{aligned} \tag{5.15}$$

(5.13) \Rightarrow

$$\begin{aligned}
& \frac{1}{\delta t} \int_{\Omega^{n+1}} \left[\left(\sum_{j=1}^m v_j \xi_j \right)^{n+1} - \left(\left(\sum_{j=1}^m v_j \xi_j \right)^n \circ y^n \right) \right] \xi_i d\Omega - \left(\sum_{j=1}^l P_j \eta_j \right) \int_{\Omega^{n+1}} \frac{\partial \xi_i}{\partial y} d\Omega - \\
& 2a_4 \left[- \int_{\Omega^{n+1}} \frac{\partial}{\partial x} \left(\sum_{j=1}^m v_j \xi_j \right) \frac{\partial \xi_i}{\partial x} d\Omega + \oint_{\Gamma} \xi_i \left(n_x \frac{\partial}{\partial x} \left(\sum_{j=1}^m v_j \xi_j \right) \right) d\Gamma \right] - \\
& a_4 \int_{\Omega^{n+1}} \left[\frac{\partial}{\partial y} \left(\sum_{j=1}^m u_j \xi_j \right) \frac{\partial \xi_i}{\partial x} + \frac{\partial}{\partial x} \left(\sum_{j=1}^m u_j \xi_j \right) \frac{\partial \xi_i}{\partial y} \right] d\Omega - a_4 \left[- \int_{\Omega^{n+1}} \frac{\partial}{\partial y} \left(\sum_{j=1}^m v_j \xi_j \right) \frac{\partial \xi_i}{\partial y} d\Omega \right. \\
& \left. + \oint_{\Gamma} \xi_i \left(n_y \frac{\partial}{\partial y} \left(\sum_{j=1}^m v_j \xi_j \right) \right) d\Gamma \right] + a_5 \int_{\Omega^{n+1}} \left(\sum_{j=1}^m v_j \xi_j \right) \xi_i d\Omega \\
& + a_6 \int_{\Omega^{n+1}} \left(\sum_{j=1}^m v_j \xi_j \right)^n \left(\sum_{j=1}^m v_j \xi_j \right)^{n+1} \xi_i d\Omega - a_7 \int_{\Omega^{n+1}} \left(\sum_{j=1}^m \theta_j \xi_j \right)^{n+1} \xi_i d\Omega = 0, \\
& \frac{1}{\delta t} \int_{\Omega^{n+1}} \left[\left(\sum_{j=1}^m v_j \xi_j \right)^{n+1} - \left(\left(\sum_{j=1}^m v_j \xi_j \right)^n \circ y^n \right) \right] \xi_i d\Omega - \sum_{j=1}^l \int_{\Omega^{n+1}} \frac{\partial \xi_i}{\partial y^{n+1}} \eta_j^{n+1} d\Omega \{P_j^{n+1}\} + 2 \\
& a_4 \sum_{j=1}^m \int_{\Omega^{n+1}} \frac{\partial \xi_j^{n+1}}{\partial x^{n+1}} \frac{\partial \xi_i}{\partial x^{n+1}} d\Omega \{v_j^{n+1}\} - a_4 \sum_{j=1}^m \int_{\Omega^{n+1}} \left[\frac{\partial \xi_j^{n+1}}{\partial y^{n+1}} \frac{\partial \xi_i}{\partial x^{n+1}} + \frac{\partial \xi_j^{n+1}}{\partial x^{n+1}} \frac{\partial \xi_i}{\partial y^{n+1}} \right] d\Omega \{u_j^{n+1}\} \\
& + a_4 \sum_{j=1}^m \int_{\Omega^{n+1}} \frac{\partial \xi_j^{n+1}}{\partial y^{n+1}} \frac{\partial \xi_i}{\partial y^{n+1}} d\Omega \{v_j^{n+1}\} + a_5 \sum_{j=1}^m \int_{\Omega^{n+1}} \xi_j^{n+1} \xi_i d\Omega \{v_j^{n+1}\} \\
& + a_6 \int_{\Omega^{n+1}} \left(\sum_{j=1}^m v_j \xi_j \right)^n \left(\sum_{j=1}^m v_j \xi_j \right)^{n+1} \xi_i d\Omega - a_7 \sum_{j=1}^m \int_{\Omega^{n+1}} \xi_j^{n+1} \xi_i d\Omega \{\theta_j^{n+1}\} = \\
& \sum_{j=1}^m \oint_{\Gamma} \xi_i \left[\left(n_x \frac{\partial \xi_j^{n+1}}{\partial x^{n+1}} \right) + \left(n_y \frac{\partial \xi_j^{n+1}}{\partial y^{n+1}} \right) \right] d\Gamma \{v_j^{n+1}\}
\end{aligned} \tag{5.16}$$

(5.14) \Rightarrow

$$\frac{1}{\delta t} \int_{\Omega^{n+1}} \left[\left(\sum_{j=1}^m \theta_j \xi_j \right)^{n+1} - \left(\left(\sum_{j=1}^m \theta_j \xi_j \right)^n \circ x^n \right) \right] \xi_i d\Omega - a_8 \left[- \int_{\Omega^{n+1}} \frac{\partial}{\partial x} \left(\sum_{j=1}^m \theta_j \xi_j \right) \frac{\partial \xi_i}{\partial x} d\Omega \right.$$

$$\begin{aligned}
& + \oint_{\Gamma} \xi_i \left(n_x \frac{\partial}{\partial x} \left(\sum_{j=1}^m \theta_j \xi_j \right) \right) d\Gamma - \int_{\Omega^{n+1}} \frac{\partial}{\partial y} \left(\sum_{j=1}^m \theta_j \xi_j \right) \frac{\partial \xi_i}{\partial y} d\Omega \\
& \quad + \left[\oint_{\Gamma} \xi_i \left(n_y \frac{\partial}{\partial y} \left(\sum_{j=1}^m \theta_j \xi_j \right) \right) d\Gamma \right] = 0. \\
& \frac{1}{\delta t} \int_{\Omega^{n+1}} \left[\left(\sum_{j=1}^m \theta_j \xi_j \right)^{n+1} - \left(\left(\sum_{j=1}^m \theta_j \xi_j \right)^n \circ x^n \right) \right] \xi_i d\Omega + a_8 \sum_{j=1}^m \int_{\Omega^{n+1}} \frac{\partial \xi_j^{n+1}}{\partial x^{n+1}} \frac{\partial \xi_i}{\partial x^{n+1}} d\Omega \{\theta_j^{n+1}\} \\
& + \sum_{j=1}^m \int_{\Omega^{n+1}} \frac{\partial \xi_j^{n+1}}{\partial y^{n+1}} \frac{\partial \xi_i}{\partial y^{n+1}} d\Omega \{\theta_j^{n+1}\} = \sum_{j=1}^m \oint_{\Gamma} \xi_i \left[\left(n_x \frac{\partial \xi_j^{n+1}}{\partial x^{n+1}} \right) + \left(n_y \frac{\partial \xi_j^{n+1}}{\partial y^{n+1}} \right) \right] d\Gamma \{\theta_j^{n+1}\}.
\end{aligned} \tag{5.17}$$

From Eqs. (5.15) to (5.17), we get the discretized system of nonlinear algebraic equations as

$$[A^*(u, v)]\{X^*\} = \{F^*\} + \{Q^*\}.$$

The matrix notation of $A^*(u, v)$, X^* , F^* and Q^* can be written as

$$\underbrace{\begin{bmatrix} K^{11} & K^{12} & B_1 & K^{14} \\ K^{21} & K^{22} & B_2 & K^{24} \\ B_1^T & B_2^T & K^{33} & K^{34} \\ K^{41} & K^{42} & K^{43} & K^{44} \end{bmatrix}}_{A^*} \underbrace{\begin{bmatrix} u \\ v \\ P \\ \theta \end{bmatrix}}_{X^*} = \underbrace{\begin{bmatrix} F_1 \\ F_2 \\ F_3 \\ F_4 \end{bmatrix}}_{F^*} + \underbrace{\begin{bmatrix} Q_1 \\ Q_2 \\ Q_3 \\ Q_4 \end{bmatrix}}_{Q^*}. \tag{5.18}$$

Here A^* , X^* , F^* and Q^* are called block stiffness matrix, block solution vector, block load vector and block boundary vector respectively. The local elemental entries of block stiffness matrix are given as

$$\begin{aligned}
K^{11} &= \frac{1}{\delta t} \int_{\Omega^{n+1}} \left[\left(\sum_{j=1}^m u_j \xi_j \right)^{n+1} - \left(\left(\sum_{j=1}^m u_j \xi_j \right)^n \circ x^n \right) \right] \xi_i d\Omega + 2a_1 \sum_{j=1}^m \int_{\Omega^{n+1}} \frac{\partial \xi_j^{n+1}}{\partial x^{n+1}} \frac{\partial \xi_i}{\partial x^{n+1}} \\
& \quad d\Omega \{u_j^{n+1}\} + a_1 \sum_{j=1}^m \int_{\Omega^{n+1}} \frac{\partial \xi_j^{n+1}}{\partial y^{n+1}} \frac{\partial \xi_i}{\partial y^{n+1}} d\Omega \{u_j^{n+1}\} + a_2 \sum_{j=1}^m \int_{\Omega^{n+1}} \xi_j^{n+1} \xi_i d\Omega \{u_j^{n+1}\} \\
& \quad + a_3 \int_{\Omega^{n+1}} \left(\sum_{j=1}^m u_j \xi_j \right)^n \left(\sum_{j=1}^m u_j \xi_j \right)^{n+1} \xi_i d\Omega,
\end{aligned}$$

$$K^{12} = -a_1 \sum_{j=1}^m \int_{\Omega^{n+1}} \left[\frac{\partial \xi_j^{n+1}}{\partial y^{n+1}} \frac{\partial \xi_i}{\partial x^{n+1}} + \frac{\partial \xi_j^{n+1}}{\partial x^{n+1}} \frac{\partial \xi_i}{\partial y^{n+1}} \right] d\Omega \{v_j^{n+1}\},$$

$$K^{14} = 0,$$

$$K^{21} = -a_4 \sum_{j=1}^m \int_{\Omega^{n+1}} \left[\frac{\partial \xi_j^{n+1}}{\partial y^{n+1}} \frac{\partial \xi_i}{\partial x^{n+1}} + \frac{\partial \xi_j^{n+1}}{\partial x^{n+1}} \frac{\partial \xi_i}{\partial y^{n+1}} \right] d\Omega \{u_j^{n+1}\},$$

$$\begin{aligned} K^{22} &= \frac{1}{\delta t} \int_{\Omega^{n+1}} \left[\left(\sum_{j=1}^m v_j \xi_j \right)^{n+1} - \left(\left(\sum_{j=1}^m v_j \xi_j \right)^n \circ y^n \right) \right] \xi_i d\Omega + 2a_4 \sum_{j=1}^m \int_{\Omega^{n+1}} \frac{\partial \xi_j^{n+1}}{\partial x^{n+1}} \frac{\partial \xi_i}{\partial x^{n+1}} \\ &\quad d\Omega \{v_j^{n+1}\} + a_4 \sum_{j=1}^m \int_{\Omega^{n+1}} \frac{\partial \xi_j^{n+1}}{\partial y^{n+1}} \frac{\partial \xi_i}{\partial y^{n+1}} d\Omega \{v_j^{n+1}\} \\ &\quad + a_4 \sum_{j=1}^m \int_{\Omega^{n+1}} \xi_j^{n+1} \xi_i d\Omega \{v_j^{n+1}\} + a_5 \int_{\Omega^{n+1}} \left(\sum_{j=1}^m v_j \xi_j \right)^n \left(\sum_{j=1}^m v_j \xi_j \right)^{n+1} \xi_i d\Omega, \end{aligned}$$

$$K^{24} = -a_7 \sum_{j=1}^m \int_{\Omega^{n+1}} \xi_j^{n+1} \xi_i d\Omega \{\theta_j^{n+1}\},$$

$$\begin{aligned} K^{44} &= \frac{1}{\delta t} \int_{\Omega^{n+1}} \left[\left(\sum_{j=1}^m \theta_j \xi_j \right)^{n+1} - \left(\left(\sum_{j=1}^m \theta_j \xi_j \right)^n \circ x^n \right) \right] \xi_i d\Omega + a_8 \sum_{j=1}^m \int_{\Omega^{n+1}} \frac{\partial \xi_j^{n+1}}{\partial x^{n+1}} \frac{\partial \xi_i}{\partial x^{n+1}} \\ &\quad d\Omega \{\theta_j^{n+1}\} + \sum_{j=1}^m \int_{\Omega^{n+1}} \frac{\partial \xi_j^{n+1}}{\partial y^{n+1}} \frac{\partial \xi_i}{\partial y^{n+1}} d\Omega \{\theta_j^{n+1}\} \end{aligned}$$

$$K^{33} = 0,$$

$$K^{34} = 0,$$

$$K^{41} = 0,$$

$$K^{42} = 0,$$

$$K^{43} = 0.$$

The entries K^{13} , K^{23} and K^{31} , K^{32} are the pressure matrices with their respective transposes can be written as

$$B_1^{ij} = \sum_{j=1}^l \int_{\Omega^{n+1}} \frac{\partial \xi_i}{\partial x^{n+1}} \eta_j^{n+1} d\Omega \{P_j^{n+1}\},$$

$$B_2^{ij} = \sum_{j=1}^l \int_{\Omega^{n+1}} \frac{\partial \xi_i}{\partial y^{n+1}} \eta_j^{n+1} d\Omega \{P_j^{n+1}\},$$

$$(B_1^{ij})^t = \sum_{j=1}^l \int_{\Omega^{n+1}} \frac{\partial \eta_j^{n+1}}{\partial x^{n+1}} \xi_i d\Omega \{P_j^{n+1}\},$$

$$(B_2^{ij})^t = \sum_{j=1}^l \int_{\Omega^{n+1}} \frac{\partial \eta_j^{n+1}}{\partial y^{n+1}} \xi_i d\Omega \{P_j^{n+1}\},$$

$$F_1 = 0,$$

$$F_2 = 0,$$

$$F_3 = 0,$$

$$F_4 = 0,$$

$$Q_1 = \sum_{j=1}^m \oint_{\Gamma} \xi_i \left[\left(n_x \frac{\partial \xi_j^{n+1}}{\partial x^{n+1}} \right) + \left(n_y \frac{\partial \xi_j^{n+1}}{\partial y^{n+1}} \right) \right] d\Gamma \{u_j^{n+1}\},$$

$$Q_2 = \sum_{j=1}^m \oint_{\Gamma} \xi_i \left[\left(n_x \frac{\partial \xi_j^{n+1}}{\partial x^{n+1}} \right) + \left(n_y \frac{\partial \xi_j^{n+1}}{\partial y^{n+1}} \right) \right] d\Gamma \{v_j^{n+1}\},$$

$$Q_3 = 0,$$

$$Q_4 = \sum_{j=1}^m \oint_{\Gamma} \xi_i \left[\left(n_x \frac{\partial \xi_j^{n+1}}{\partial x^{n+1}} \right) + \left(n_y \frac{\partial \xi_j^{n+1}}{\partial y^{n+1}} \right) \right] d\Gamma \{\theta_j^{n+1}\}.$$

The discrete system of non-linear algebraic equations in matrix form can be written as:

$$\begin{bmatrix} K^{11} & K^{12} & B_1 & 0 \\ K^{21} & K^{22} & B_2 & K^{24} \\ B_1^T & B_2^T & 0 & 0 \\ 0 & 0 & 0 & K^{44} \end{bmatrix} \begin{bmatrix} u \\ v \\ P \\ \theta \end{bmatrix} = \begin{bmatrix} 0 \\ 0 \\ 0 \\ 0 \end{bmatrix} + \begin{bmatrix} Q_1 \\ Q_2 \\ 0 \\ Q_4 \end{bmatrix} \quad (5.19)$$

An examination of the weak form Eqs. (5.12) to (5.14) and the finite element matrices in (5.18) shows that ξ_i should be atleast linear functions of x and y . Discretization of the domain is performed using selected two-dimensional finite elements. One of the simplest two-dimensional elements is the three-noded triangular element. This is also known as linear triangular element. The element is shown in Figure 5.2. It has three nodes at the vertices of the triangle and the variable interpolation within the element is linear in x and y as given below.

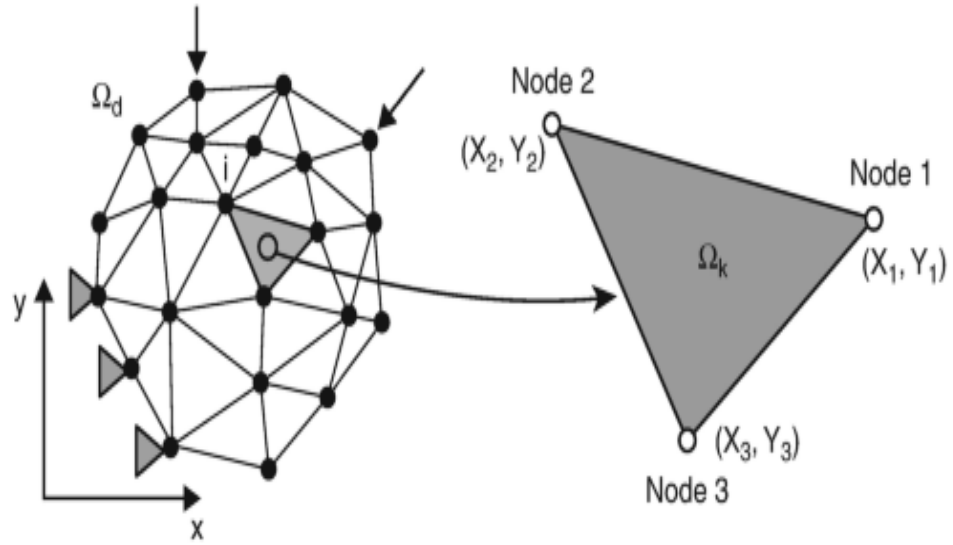


FIGURE 5.1: Systematic Computational Domain

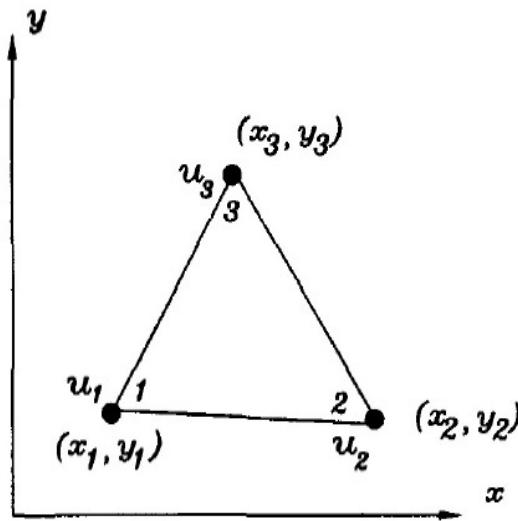


FIGURE 5.2: Linear Triangular Element

$$u = a_1 + a_2x + a_3y \quad (5.20)$$

OR

$$u = [1 \quad x \quad y] \begin{Bmatrix} a_1 \\ a_2 \\ a_3 \end{Bmatrix} \quad (5.21)$$

where a_i is the constant to be determined. The interpolation function, Eq. (5.20) should represent the nodal variables at the three nodal points. Therefore, substituting the x and y values at each nodal point gives

$$\begin{Bmatrix} u_1 \\ u_2 \\ u_3 \end{Bmatrix} = \begin{bmatrix} 1 & x_1 & y_1 \\ 1 & x_2 & y_2 \\ 1 & x_3 & y_3 \end{bmatrix} \begin{Bmatrix} a_1 \\ a_2 \\ a_3 \end{Bmatrix} \quad (5.22)$$

Here, x_i and y_i are the coordinate values at the i^{th} node and u_i is the nodal variable as seen in Figure 5.2. Inverting the matrix and rewriting Eq. (5.22) give

$$\begin{Bmatrix} a_1 \\ a_2 \\ a_3 \end{Bmatrix} = [A]^{-1} \begin{Bmatrix} u_1 \\ u_2 \\ u_3 \end{Bmatrix}$$

$$\begin{Bmatrix} a_1 \\ a_2 \\ a_3 \end{Bmatrix} = \frac{1}{|A|} \begin{bmatrix} x_2y_3 - x_3y_2 & x_3y_1 - x_1y_3 & x_1y_2 - x_2y_1 \\ y_2 - y_3 & y_3 - y_1 & y_1 - y_2 \\ x_3 - x_2 & x_1 - x_3 & x_2 - x_1 \end{bmatrix} \begin{Bmatrix} u_1 \\ u_2 \\ u_3 \end{Bmatrix} \quad (5.23)$$

For the finite element computation, the element nodal sequence must be in the same direction for every element in the domain. Substituting the Eq. (5.23) into Eq. (5.21), we obtain

$$u = \begin{bmatrix} 1 & x & y \end{bmatrix} \frac{1}{|A|} \begin{bmatrix} x_2y_3 - x_3y_2 & x_3y_1 - x_1y_3 & x_1y_2 - x_2y_1 \\ y_2 - y_3 & y_3 - y_1 & y_1 - y_2 \\ x_3 - x_2 & x_1 - x_3 & x_2 - x_1 \end{bmatrix} \begin{Bmatrix} u_1 \\ u_2 \\ u_3 \end{Bmatrix}$$

$$u = \frac{1}{|A|} \begin{bmatrix} \xi_1 & \xi_2 & \xi_3 \end{bmatrix} \begin{Bmatrix} u_1 \\ u_2 \\ u_3 \end{Bmatrix}$$

$$= \sum_{i=1}^3 \xi_i u_i$$

where,

$$\xi_1 = \frac{1}{|A|} [(x_2y_3 - x_3y_2) + x(y_2 - y_3) + y(x_3 - x_2)],$$

$$\xi_2 = \frac{1}{|A|}[(x_3y_1 - x_1y_3) + x(y_3 - y_1) + y(x_1 - x_3)],$$

$$\xi_3 = \frac{1}{|A|}[(x_1y_2 - x_2y_1) + x(y_1 - y_2) + y(x_2 - x_1)].$$

For a linear triangular element, Eq. (5.9) to (5.11), becomes

$$u = \sum_{i=1}^3 u_i \xi_i, \quad v = \sum_{i=1}^3 v_i \xi_i, \quad \theta = \sum_{i=1}^3 \theta_i \xi_i, \quad P = \sum_{i=1}^3 P_i \eta_i, \quad \tilde{w} = \sum_{j=1}^3 \tilde{w}_j \eta_j.$$

(5.9) \Rightarrow

$$\begin{aligned} & \frac{1}{\delta t} \sum_{i=1}^3 \int_{\Omega^{n+1}} \left[(u_i \xi_i)^{n+1} - \left((u_i \xi_i)^n \circ x^n \right) \right] \sum_{j=1}^3 \tilde{w}_j \eta_j^{n+1} d\Omega - \sum_{i=1}^3 \sum_{j=1}^3 (P_i \eta_i)^{n+1} \int_{\Omega^{n+1}} \frac{\partial \tilde{w}_j \eta_j^{n+1}}{\partial x^{n+1}} d\Omega \\ & - 2a_1 \sum_{i=1}^3 \sum_{j=1}^3 \left[- \int_{\Omega^{n+1}} \frac{\partial (u_i \xi_i)^{n+1}}{\partial x^{n+1}} \frac{\partial \tilde{w}_j \eta_j^{n+1}}{\partial x^{n+1}} d\Omega + \oint_{\Gamma} \tilde{w}_j \eta_j^{n+1} \left(n_x \frac{\partial (u_i \xi_i)^{n+1}}{\partial x^{n+1}} \right) d\Gamma \right] \\ & - a_1 \sum_{i=1}^3 \sum_{j=1}^3 \int_{\Omega^{n+1}} \left[\frac{\partial (v_i \xi_i)^{n+1}}{\partial y^{n+1}} \frac{\partial \tilde{w}_j \eta_j^{n+1}}{\partial x^{n+1}} + \frac{\partial (v_i \xi_i)^{n+1}}{\partial x^{n+1}} \frac{\partial \tilde{w}_j \eta_j^{n+1}}{\partial y^{n+1}} \right] d\Omega \\ & - a_1 \sum_{i=1}^3 \sum_{j=1}^3 \left[- \int_{\Omega^{n+1}} \frac{\partial (u_i \xi_i)^{n+1}}{\partial y^{n+1}} \frac{\partial \tilde{w}_j \eta_j^{n+1}}{\partial y^{n+1}} d\Omega + \oint_{\Gamma} \tilde{w}_j \eta_j^{n+1} \left(n_y \frac{\partial (u_i \xi_i)^{n+1}}{\partial y^{n+1}} \right) d\Gamma \right] \\ & + a_2 \sum_{i=1}^3 \sum_{j=1}^3 \int_{\Omega^{n+1}} (u_i \xi_i)^{n+1} \tilde{w}_j \eta_j^{n+1} d\Omega + a_3 \left(\sum_{j=1}^3 \right)^2 \sum_{j=1}^3 \int_{\Omega^{n+1}} (u_i \xi_i)^n (u_i \xi_i)^{n+1} \tilde{w}_j \eta_j^{n+1} d\Omega = 0, \end{aligned} \tag{5.24}$$

(5.10) \Rightarrow

$$\begin{aligned} & \frac{1}{\delta t} \sum_{i=1}^3 \int_{\Omega^{n+1}} \left[(v_i \xi_i)^{n+1} - \left((v_i \xi_i)^n \circ y^n \right) \right] \sum_{j=1}^3 \tilde{w}_j \eta_j^{n+1} d\Omega - \sum_{i=1}^3 \sum_{j=1}^3 (P_i \eta_i)^{n+1} \int_{\Omega^{n+1}} \frac{\partial \tilde{w}_j \eta_j^{n+1}}{\partial y^{n+1}} d\Omega \\ & - 2a_4 \sum_{i=1}^3 \sum_{j=1}^3 \left[- \int_{\Omega^{n+1}} \frac{\partial (v_i \xi_i)^{n+1}}{\partial x^{n+1}} \frac{\partial \tilde{w}_j \eta_j^{n+1}}{\partial x^{n+1}} d\Omega + \oint_{\Gamma} \tilde{w}_j \eta_j^{n+1} \left(n_x \frac{\partial (v_i \xi_i)^{n+1}}{\partial x^{n+1}} \right) d\Gamma \right] \\ & - a_4 \sum_{i=1}^3 \sum_{j=1}^3 \int_{\Omega^{n+1}} \left[\frac{\partial (u_i \xi_i)^{n+1}}{\partial y^{n+1}} \frac{\partial \tilde{w}_j \eta_j^{n+1}}{\partial x^{n+1}} + \frac{\partial (u_i \xi_i)^{n+1}}{\partial x^{n+1}} \frac{\partial \tilde{w}_j \eta_j^{n+1}}{\partial y^{n+1}} \right] d\Omega \\ & - a_4 \sum_{i=1}^3 \sum_{j=1}^3 \left[- \int_{\Omega^{n+1}} \frac{\partial (v_i \xi_i)^{n+1}}{\partial y^{n+1}} \frac{\partial \tilde{w}_j \eta_j^{n+1}}{\partial y^{n+1}} d\Omega + \oint_{\Gamma} \tilde{w}_j \eta_j^{n+1} \left(n_y \frac{\partial (v_i \xi_i)^{n+1}}{\partial y^{n+1}} \right) d\Gamma \right] \end{aligned}$$

$$\begin{aligned}
& + a_5 \sum_{i=1}^3 \sum_{j=1}^3 \int_{\Omega^{n+1}} (v_i \xi_i)^{n+1} \tilde{w}_j \eta_j^{n+1} d\Omega + a_6 \left(\sum_{i=1}^3 \right)^2 \sum_{j=1}^3 \int_{\Omega^{n+1}} (v_i \xi_i)^n (v_i \xi_i)^{n+1} \tilde{w}_j \eta_j^{n+1} d\Omega \\
& - a_7 \sum_{i=1}^3 \sum_{j=1}^3 \int_{\Omega^{n+1}} (\theta_i \xi_i)^{n+1} \tilde{w}_j \eta_j^{n+1} d\Omega = 0,
\end{aligned} \tag{5.25}$$

(5.11) \Rightarrow

$$\begin{aligned}
& \frac{1}{\delta t} \sum_{i=1}^3 \int_{\Omega^{n+1}} \left[(\theta_i \xi_i)^{n+1} - \left((\theta_i \xi_i)^n \circ x^n \right) \right] \sum_{j=1}^3 \tilde{w}_j \eta_j^{n+1} d\Omega - a_8 \sum_{i=1}^3 \sum_{j=1}^3 \left[- \int_{\Omega^{n+1}} \frac{\partial(\theta_i \xi_i)^{n+1}}{\partial x^{n+1}} \right. \\
& \left. \frac{\partial \tilde{w}_j \eta_j^{n+1}}{\partial x^{n+1}} d\Omega + \oint_{\Gamma} \tilde{w}_j \eta_j^{n+1} \left(n_x \frac{\partial(\theta_i \xi_i)^{n+1}}{\partial x^{n+1}} \right) d\Gamma - \int_{\Omega^{n+1}} \frac{\partial(\theta_i \xi_i)^{n+1}}{\partial y^{n+1}} \frac{\partial \tilde{w}_j \eta_j^{n+1}}{\partial y^{n+1}} d\Omega + \oint_{\Gamma} \tilde{w}_j \eta_j^{n+1} \right. \\
& \left. \left(n_y \frac{\partial(\theta_i \xi_i)^{n+1}}{\partial y^{n+1}} \right) d\Gamma \right] = 0.
\end{aligned} \tag{5.26}$$

Eq. (5.24) to (5.26) are solved through FEM code Free Fem++. These equations are along with B.Cs are implemented in Free Fem++, the code is used to compute the solution for variant parameter on the computational domain.

Chapter 6

Numerical Results and Discussion

6.1 Validation

To validate the numerical results obtained by the presented model and its implemented code the model is first reduced to the following

$$\begin{aligned}\frac{\partial P}{\partial x} - \frac{1}{Re} \left\{ 2 \frac{\partial^2 u}{\partial x^2} + \frac{\partial^2 v}{\partial x \partial y} + \frac{\partial^2 u}{\partial y^2} \right\} &= f_1 \\ \frac{\partial P}{\partial y} - \frac{1}{Re} \left\{ 2 \frac{\partial^2 v}{\partial y^2} + \frac{\partial^2 u}{\partial x \partial y} + \frac{\partial^2 v}{\partial x^2} \right\} &= f_2\end{aligned}\tag{6.1}$$

The assumptions used in here are the steady state case without convection. Moreover, the parameters $Fr = \lambda = Ha = 0$. Consider a unit domain Ω with the velocity fields U and V vanishing at the boundary $\partial\Omega$. The exact solution to problem with PDEs in (6.1) is given as

$$\begin{aligned}U &= Re (x^4 - 2x^3 + x^2) (4y^3 - 6y^2 + 2y), \\ V &= -Re (y^4 - 2y^3 + y^2) (4x^3 - 6x^2 + xy), \\ P &= y^5 + x^5 - 1/3,\end{aligned}\tag{6.2}$$

with

$$\begin{aligned}f_1 &= 5x^4 - (x^4 - 2x^3 + x^2) (24y - 12) - (12x^2 - 12x + 2) (4y^3 - 6y^2 + 2y), \\ f_2 &= 5y^4 + (12y^2 - 12y + 2) (4x^3 - 6x^2 + 2x) + (y^4 - 2y^3 + y^2) (24x - 12).\end{aligned}\tag{6.3}$$

The numerical results obtained through the implemented code are compared with the exact solution in Table 6.1. In Table 6.1, error norms are computed between the numerical solution of the problem with $Re = 20$ and the exact solution. It is observed that the difference between the numerical and exact solution is remarkably reduced at the mesh refinement level is increased and a good accuracy of the numerical solution is achieved. This clearly shows the efficient implementation of the code in FreeFEM++.

TABLE 6.1: L_2 - error norms of pressure and velocity values for $Re = 20$ at different mesh refinement levels.

Mesh level	No. of Triangles	No. of Vertices	P - error	U - error
1	3746	1954	0.00181821	0.000235475
2	15160	7741	0.000737664	5.45433e-05
3	61010	30826	0.000340759	1.40162e-05
4	94512	47657	0.000251415	8.49309e-06
5	137518	69240	0.000222057	6.26907e-06
6	137518	69240	0.000222057	6.26907e-06

6.2 Results and Discussion

In this section, the computed numerical results are presented in the form of tables and plots. The weak formulation of the developed model in earlier chapter is first used to derive the finite element equations in the form of matrix vector equation which is then implemented in the open source code FreeFEM++. FreeFEM++ is open source finite element code which can be modified to implement user's own mathematical model. The geometry of the problem is also implemented in the FreeFEM++ code. The results are computed for the velocities and temperature based on the finite elements model are presented. The plots of stream function Ψ are generated from the computed velocities by solving following mathematical equation.

$$\int_{\Omega} \left(\frac{\partial \Psi}{\partial x} \frac{\partial \tilde{\Psi}}{\partial x} + \frac{\partial \Psi}{\partial y} \frac{\partial \tilde{\Psi}}{\partial y} \right) d\Omega = \int_{\Omega} \tilde{\Psi} \left(\frac{\partial u}{\partial y} - \frac{\partial v}{\partial x} \right) d\Omega, \quad (6.4)$$

where $\tilde{\Psi}$ is the test function for the stream function Ψ . The stream function plots are computed for varying values of the physical parameters. The physical parameters considered in this analysis are the Reynolds number, Prandtl number, porosity parameter, Hartmann number, Forchheimer number and Grashof number. In Table 6.2 and Table 6.3 mesh independence of the numerically computed solutions are shown. Seven different mesh levels are chosen and domain of computation is discretized into finite element domains with seven different refinement levels. The number of triangular in the coarser mesh are chosen to be $ne = 62$ having vertices $nv = 45$, whereas the finer most mesh is having $ne = 21386$ number of triangular elements having vertices $nv = 10941$. In Table 6.2, the minimum and maximum values of the computed stream function values are shown. It is observed that both the minimum and maximum stream function values are not varying after the sixth mesh refinement level, i.e. when the number of the finite elements are selected to be $ne = 17684$. Moreover, in Table 6.3 the minimum and maximum values of the vertical component of the velocities are shown at varying meshes. It can be seen that both the minimum and maximum values of the velocities are invariant after the sixth mesh refinement level. Therefore, it is concluded that the for mesh independent solutions of the present problem a mesh with 17684 number of triangular elements is sufficient. Therefore, in computations of the results presented in this thesis a mesh with 17684 number of finite element is chosen.

TABLE 6.2: Streamline values at different mesh levels

Mesh level	No. of Triangles	No. of Vertices	Ψ_{min}	Ψ_{max}
1	62	45	-0.037548	0.036073
2	182	114	-0.0477243	0.0494242
3	702	397	-0.0477243	0.0494242
4	2828	1505	-0.0477243	0.0494242
5	6332	3302	-0.0480131	0.0522319
6	17684	9068	-0.0480869	0.0523016
7	21386	10941	-0.0480869	0.0523016

TABLE 6.3: Velocity values at different mesh levels

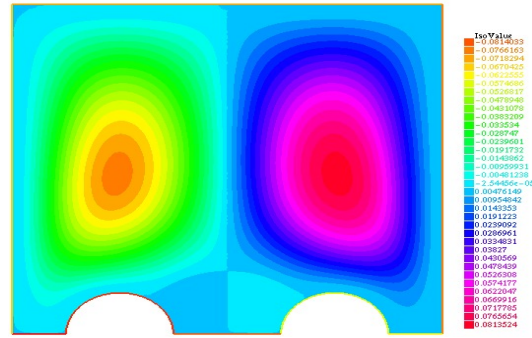
Mesh level	No. of Triangles	No. of Vertices	v_{min}	v_{max}
1	62	45	-0.406404	0.370682
2	182	114	-0.487147	0.28919
3	702	397	-0.487147	0.28919
4	2828	1505	-0.487147	0.28919
5	6332	3302	-0.472527	0.277248
6	17684	9068	-0.473467	0.277314
7	21386	10941	-0.473467	0.277314

In Figure 6.1 the streamline plots of the velocities are shown for varying Forchheimer number. The other parameters chosen are $Re = 200$, $\lambda = 5.5$, $Gr = 20.5$, $Pr = 0.3$, and $Ha = 1$. The plots are shown at the simulation time $t = 2.5$ where a time step size of $\delta t = 0.01$ is chosen in the computations. Four different values of the Forchheimer number are selected to show the behavior of the streamline velocities. It is observed by increasing the Darcy-Forchheimer number both the minima and maxima of the stream function increases. Moreover, the zero of the stream function shifts towards the negative x -axis while increasing the Darcy-Forchheimer number. In Figure 6.3 the streamline plots of the velocities are shown for varying values of the Grashof number. These streamline plots are computed with zero velocity boundary conditions while a temperature at the semi-circular boundaries is taken to be a value of 100. The physical parameters chosen in the computation of these subfigures are $Re = 200$, $\lambda = 0$, $Fr = 0$, $Pr = 0.3$, and $Ha = 1$. The velocities are generated due to the coupling of the thermal convection in the momentum equation of the model. It is seen that when $Gr = 0$ is taken in the non-dimensional model for computation then this thermal convection becomes absent in simulation model and therefore the velocities are not generated as seen in Figure 6.3 (a). However, when value of Gr is taken other than zero in the simulation the thermal convection is activated and the coupling term in the momentum equation thus leads to the generation of the non-zero velocities and therefore the streamline plots are possible to observe in this case, see for instance Figure 6.3(b). Moreover, it is observed that both the maximum and minimum values of the stream function are increased with increased in the Grashof number. In Figure 6.3, the streamline plots are shown in the test cases where the simulations are

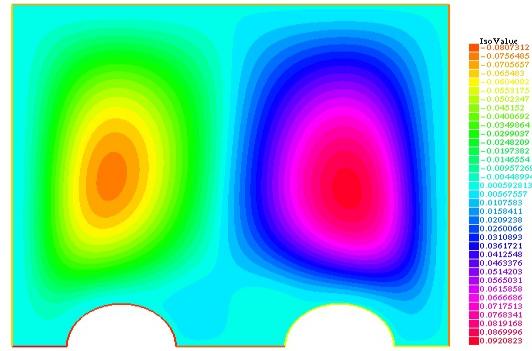
run with Forchheimer number $Fr = 100$. The streamline plots are depicted for two different Grashof number while the other parameters are chosen to be $Re = 200$, $\lambda = 5.5$, $Pr = 0.3$, and $Ha = 1$. It is observed that in this case when Darcy-Forchheimer medium is considered the stream contours of the stream function's positive plateau are expanded towards the left region of the geometry while the contours of the stream function negative plateau are contracting over the domain with higher Grashof number.

In Figure 6.4 time evolution of the stream function plots are shown. The parameters chosen in these computations are $Re = 200$, $Gr = 30$, $\lambda = 5.5$, $Fr = 100$, $Pr = 0.3$, and $Ha = 1$. The dimensionless time t is varied from $t = 0$ to $t = 0.5$ with a time step size of $\delta t = 0.01$. It is seen that initially the stream values are originated near the semi-circular boundaries of the domain. These stream contours are dominant initially in the mid-section (around $y = 0$ line) of the computational domain while with the passage of time passing the stream contours at the right and left end boundaries of the domain grows and dominate over the contours at the mid-section of the domain. In Figure 6.5, isotherms for varying values of the Prandtl number are shown. The Prandtl number is varied from $Pr = 1.3$ to $Pr = 7.3$, while the other parameters are fixed as $Re = 200$, $\lambda = 5.5$, $Fr = 100$, $Gr = 30$, and $Ha = 1$. It is seen that with increasing the Prandtl number the temperature distribution in the medium becomes slower.

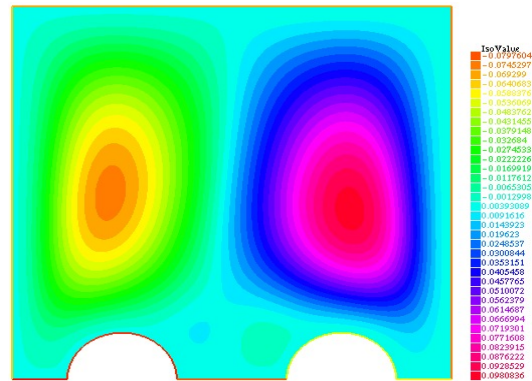
It means increasing the Prandtl number increases the thermal resistance in the medium. In Figure 6.6, isotherm plots are computed for varying values of the Hartmann number. The other parameters are chosen to be $Re = 2$, $\lambda = 5.5$, $Fr = 100$, $Gr = 80$, and $Pr = 7.3$. It is seen that with increasing the Hartmann number the temperature in the medium is distributed over a wider region. The increase in the Hartmann number leads to a decrease in the thermal resistance therefore temperature is distributed from the semi-circular boundaries to a wider area within the medium. In Figure 6.7, the porosity effect on the isotherms is depicted. The temperature distribution over a wider region is observed with changing the medium characteristic i.e. the porosity. The parameter λ is accounting here the medium porosity factor which is varied from $\lambda = 1.5$ to $\lambda = 50.5$. The computation are performed over a simulation time $t = 2.5$. The other parameters chosen in these simulations are $Re = 2$, $Ha = 7.5$, $Fr = 100$, $Gr = 80$, and $Pr = 7.3$. It is seen that the distribution of the temperature in the medium is highly effected by the medium's porosity. In a highly porous medium the temperature is more likely distributed over a wider region of the domain.



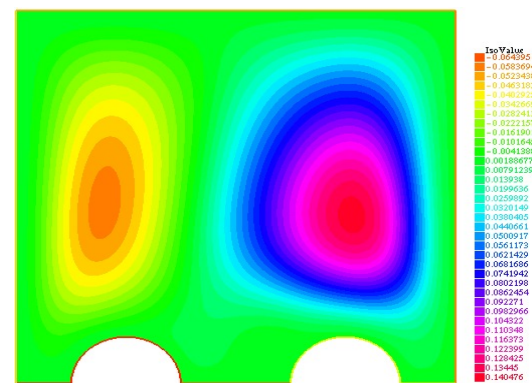
(a) Stream velocities for $Fr = 0$



(b) Stream velocities for $Fr = 100$

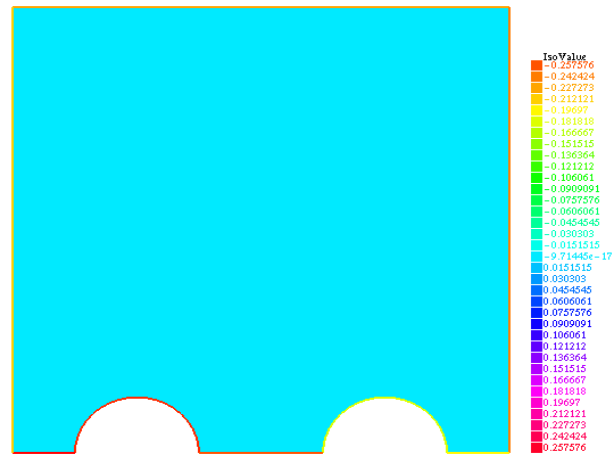


(c) Stream velocities for $Fr = 120$

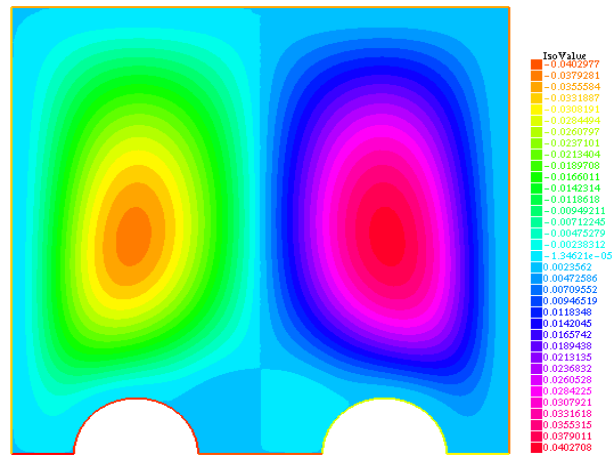


(d) Stream velocities for $Fr = 150$

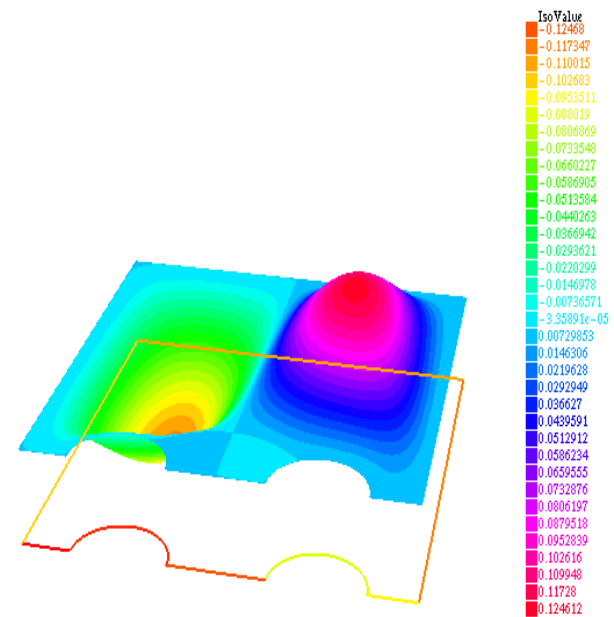
FIGURE 6.1: Streamline plots for varying values of Forchheimer number Fr .



(a)

Streamline plot for $Gr = 0$ 

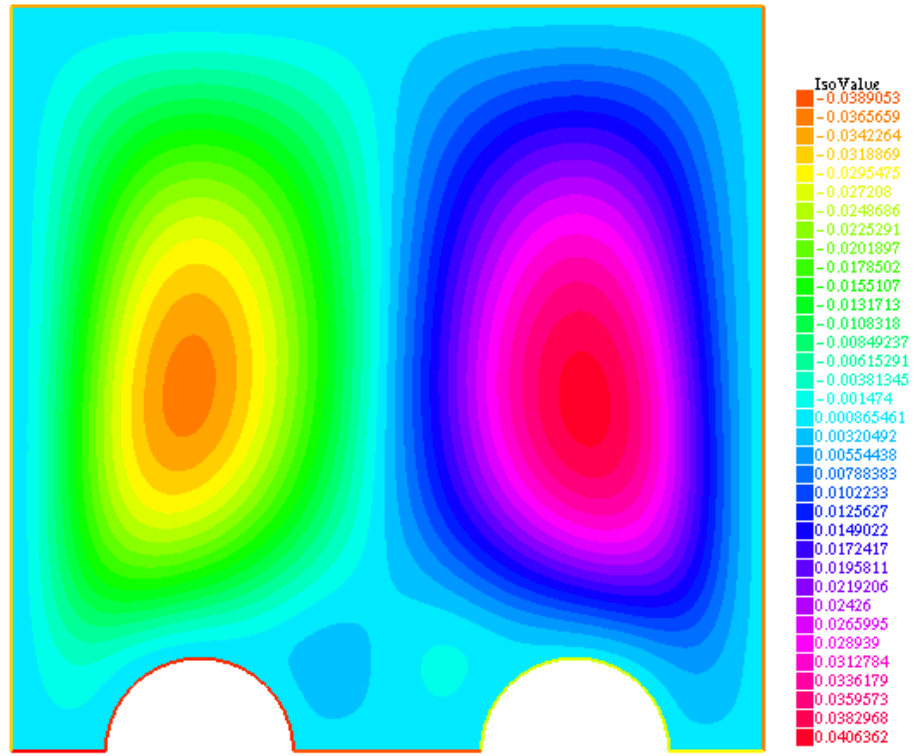
(b)

Streamline plot for $Gr = 10$ 

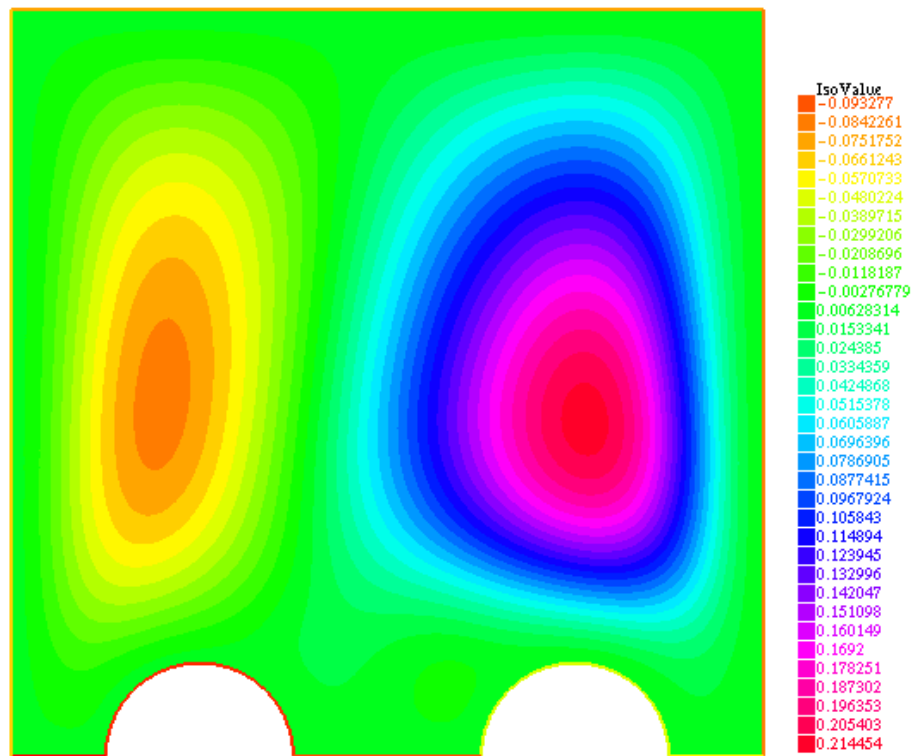
(c)

Streamline plot for $Gr = 30$

FIGURE 6.2: Streamline plots for varying values of Grashof number Gr in the non-Forchheimer medium.

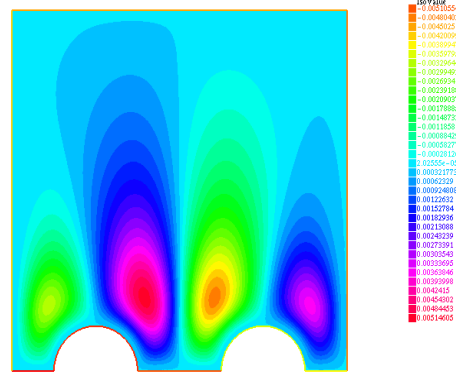


(a)

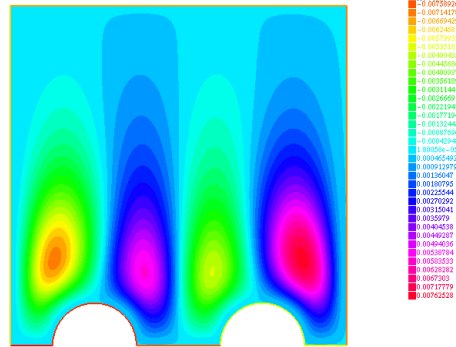
Streamline plot for $Gr = 10$ 

(b)

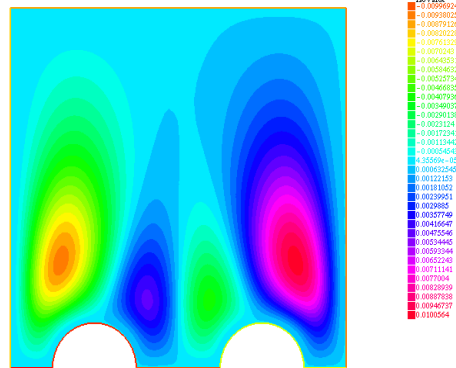
Streamline plot for $Gr = 30$ FIGURE 6.3: Streamline plots for varying values of Grashof number Gr in the Forchheimer medium.



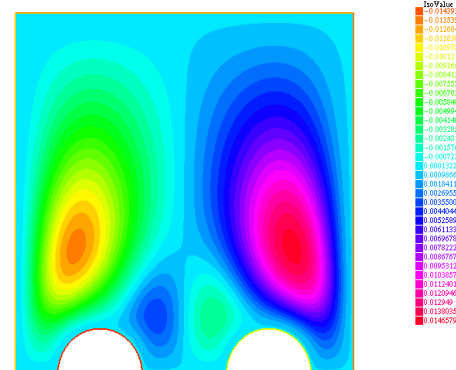
(a)

At time $t = 0.05$ 

(b)

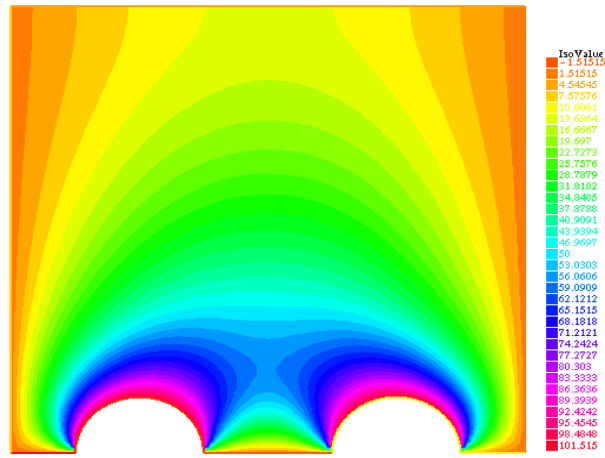
At time $t = 0.25$ 

(c)

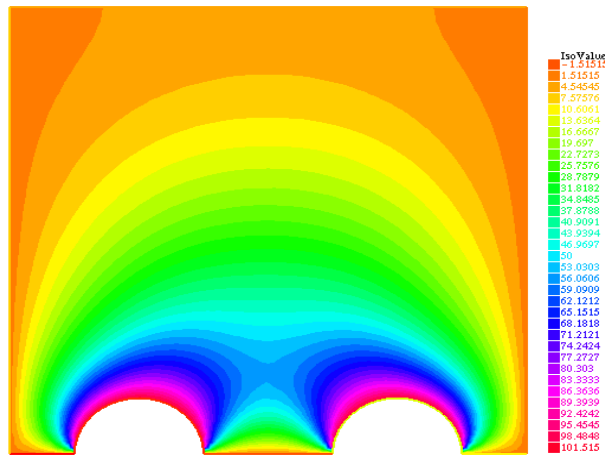
At time $t = 0.35$ 

(d)

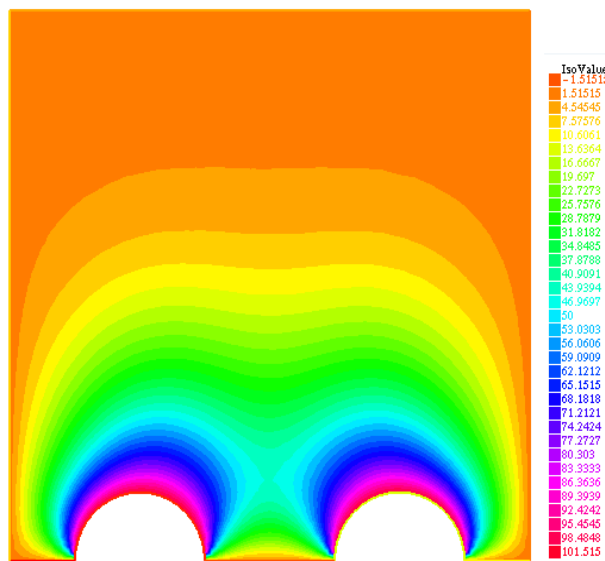
At time $t = 0.5$ FIGURE 6.4: Time evolution of the Streamline function Ψ .



(a)

For $Pr = 1.3$ 

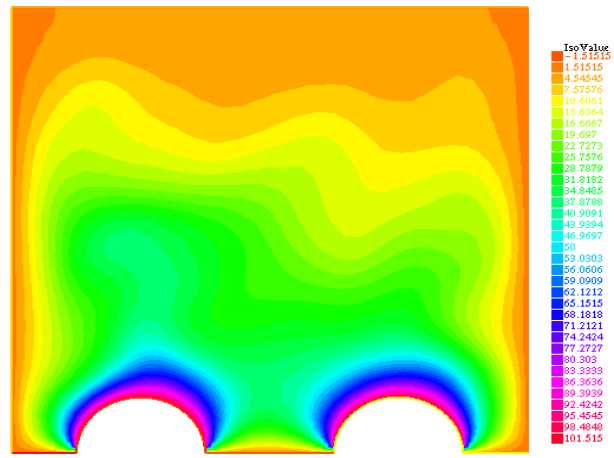
(b)

For $Pr = 3.3$ 

(c)

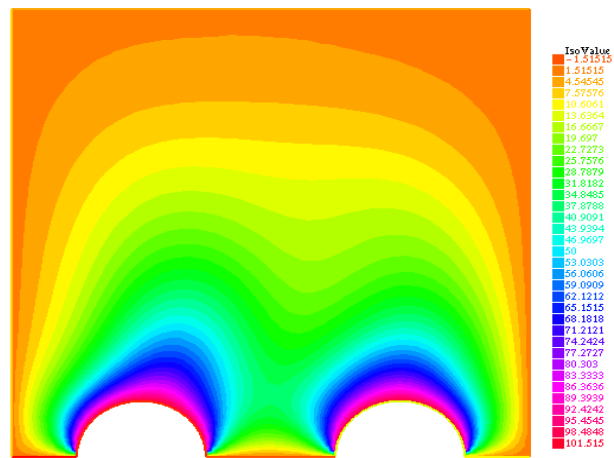
For $Pr = 7.3$

FIGURE 6.5: Isotherm plots for varying values of Prandtl number Pr in the Forchheimer medium.



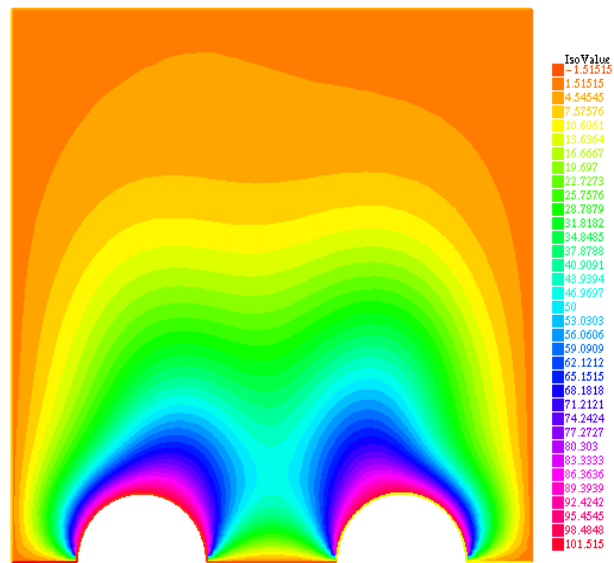
(a)

For $Ha = 1$.



(b)

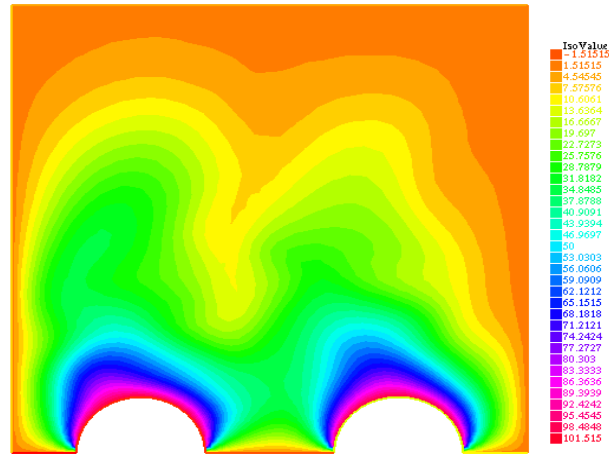
For $Ha = 5$.



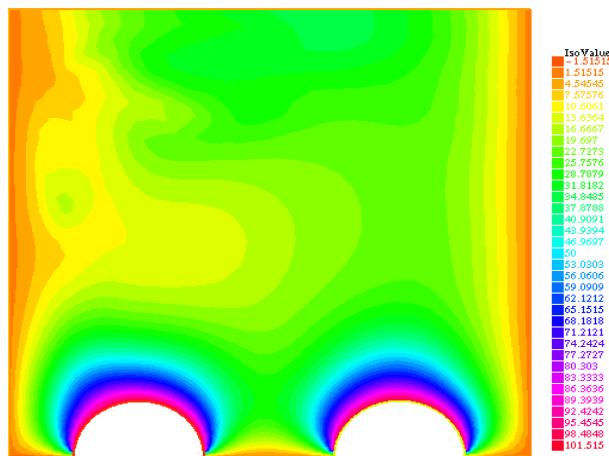
(c)

For $Ha = 10$.

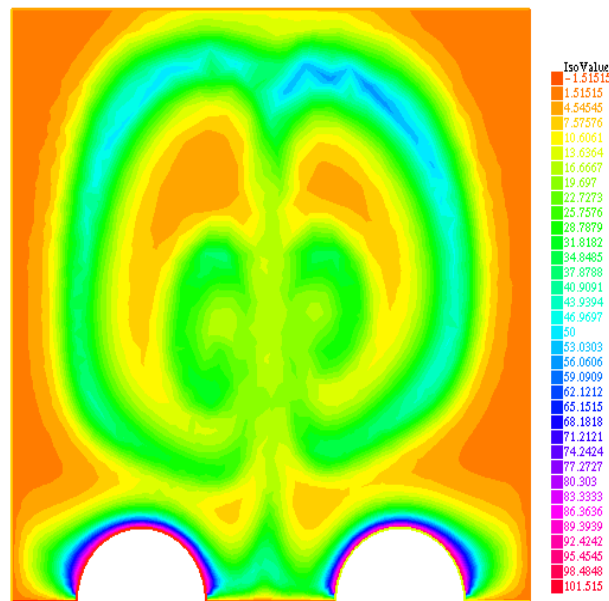
FIGURE 6.6: Isotherm plots for varying values of Hartmann number Ha in the Forchheimer medium.



(a)

For $\lambda = 1.5$ 

(b)

For $\lambda = 30.5$ 

(c)

For $\lambda = 50.5$ FIGURE 6.7: Isotherm plots for varying values of porosity parameter λ .

Chapter 7

Conclusions and Future Work

This thesis presents an analysis of a higher-grade Darcy Forchheimer porous model using the finite element method. The higher grade Darcy-Forchheimer model's flow dynamics are described using partial differential equations (PDEs) in vector tensor notation. The model's component forms are computed using tensor calculus concepts. The governing set of PDEs is produced and then non-dimensionalized by appropriate variable transformation. The domain of computation is selected and boundary conditions are described. The developed model problem is then solved using a finite element numerical approach. Weak formulation of the presented model problem is calculated. The finite element model problem is developed. The developed model problem is then implemented using open source code FreeFEM++. Different test cases are simulated for varying physical parameters. Mesh Independence analysis is also been performed where seven different mesh refinement levels are chosen. It is found that the solution gets mesh independent after sixth mesh refinement level. The results are shown for stream function plots and isotherms for these varying parameters. Some of the main findings of this investigation are summarized as:

- As the Darcy-Forchheimer number grows, the stream function's minima and maxima also increase.
- When considering the Darcy-Forchheimer medium, the positive plateau contours of the stream function expand towards the left region of the geometry, while the negative plateau contours contract over the domain with higher Grashoff numbers.

- The maximum and minimum values of the stream function rise with the Grashoff number.
- Initially, stream values begin at the domain's semi-circular boundaries. Initially, stream contours dominate the mid-section of the computational domain. However, as time passes, stream contours at the right and left end boundaries of the domain increase and take over the mid-section contours.
- Increasing the Prandtl number leads to slower temperature dispersion in the medium. Increasing the Prandtl number increases thermal resistivity in the material.
- It is observed that when the Hartmann number increases, the temperature in the medium is diffused across a larger range. As the Hartmann number increases, the thermal resistance decreases, causing temperature to spread from the semi-circular borders over a larger region of the medium.
- The porosity of the medium significantly affects its temperature distribution. In a porous media, temperature is more evenly distributed across the domain.

In future, this analysis can be extended to three dimensions. Three dimensional analysis of the model can be dealt using finite element approach. Three dimensional analysis of the model will be natural choice to observe some more realistic phenomenon which are of practical interest of the industry.

Bibliography

- [1] Zhiqiang Zhai. Application of computational fluid dynamics in building design: aspects and trends. *Indoor and built environment*, 15(4):305–313, 2006.
- [2] R Banerjee, X Bai, D Pugh, KM Isaac, D Klein, J Edson, W Breig, and L Oliver. CFD simulations of critical components in fuel filling systems. *SAE Transactions*, pages 324–340, 2002.
- [3] Chao Zhang, Mohsen Saadat, Perry Y Li, and Terrence W Simon. Heat transfer in a long, thin tube section of an air compressor: An empirical correlation from CFD and a thermodynamic modeling. In *ASME International Mechanical Engineering Congress and Exposition*, volume 45233, pages 1601–1607. American Society of Mechanical Engineers, 2012.
- [4] Bin Xia and Da-Wen Sun. Applications of computational fluid dynamics (CFD) in the food industry: a review. *Computers and electronics in agriculture*, 34(1-3):5–24, 2002.
- [5] Sumera Dero, Hisamuddin Shaikh, Ghulam Hyder Talpur, Ilyas Khan, Sayer O Alharbim, and Mulugeta Andualem. Influence of a Darcy-Forchheimer porous medium on the flow of a radiative magnetized rotating hybrid nanofluid over a shrinking surface. *Scientific Reports*, 11(1):24257, 2021.
- [6] N Vishnu Ganesh, AK Abdul Hakeem, and B Ganga. Darcy-Forchheimer flow of hydromagnetic nanofluid over a stretching/shrinking sheet in a thermally stratified porous medium with second order slip, viscous and ohmic dissipations effects. *Ain Shams Engineering Journal*, 9(4):939–951, 2018.

-
- [7] EMA Elbashbeshy and MAA Bazid. Heat transfer in a porous medium over a stretching surface with internal heat generation and suction or injection. *Applied mathematics and computation*, 158(3):799–807, 2004.
- [8] Amir Abbas, Mdi Begum Jeelani, Abeer S Alnahdi, and Asifa Ilyas. MHD williamson nanofluid fluid flow and heat transfer past a non-linear stretching sheet implanted in a porous medium: effects of heat generation and viscous dissipation. *Processes*, 10(6):1221, 2022.
- [9] K Mahmud, S Rana, A Al-Zubaidi, R Mehmood, and S Saleem. Interaction of lorentz force with cross swimming microbes in couple stress nano fluid past a porous riga plate. *International Communications in Heat and Mass Transfer*, 138:106347, 2022.
- [10] S Nadeem, Muhammad Israr-ur Rehman, S Saleem, and Ebenezer Bonyah. Dual solutions in MHD stagnation point flow of nanofluid induced by porous stretching/shrinking sheet with anisotropic slip. *AIP Advances*, 10(6), 2020.
- [11] M Abdeen and H Attia. Unsteady flow in a porous medium between parallel plates in the presence of uniform suction and injection with heat transfer. *International Journal of Civil Engineering*, 12(3):277–281, 2014.
- [12] Kohilavani Naganthran, Md Faisal Md Basir, Thirupathi Thumma, Ebenezer Olubunmi Ige, Roslinda Nazar, and Iskander Tlili. Scaling group analysis of bioconvective micropolar fluid flow and heat transfer in a porous medium. *Journal of Thermal Analysis and Calorimetry*, 143:1943–1955, 2021.
- [13] Sabeel M Khan and H Kaneez. Numerical computation of heat transfer enhancement through cosserat hybrid nanofluids using continuous Galerkin-Petrov method. *The European Physical Journal Plus*, 135(2):1–19, 2020.
- [14] A Riaz, A Zeeshan, MM Bhatti, and R Ellahi. Peristaltic propulsion of Jeffrey nanofluid and heat transfer through a symmetrical duct with moving walls in a porous medium. *Physica A: Statistical Mechanics and its Applications*, 545:123788, 2020.
- [15] K Loganathan, Nazek Alessa, K Tamilvanan, and Fehaid Salem Alshammari. Significances of Darcy-Forchheimer porous medium in third-grade nanofluid flow with

- entropy features. *The European Physical Journal Special Topics*, 230:1293–1305, 2021.
- [16] Ghulam Rasool, Anum Shafiq, and Hülya Durur. Darcy-Forchheimer relation in magnetohydrodynamic jeffrey nanofluid flow over stretching surface. *Discrete & Continuous Dynamical Systems-Series S*, 14(7), 2021.
- [17] M Habibishandiz and MZ Saghir. A critical review of heat transfer enhancement methods in the presence of porous media, nanofluids, and microorganisms. *Thermal Science and Engineering Progress*, 30:101267, 2022.
- [18] JC Umavathi. Flow characteristics in a parallel-plate porous channel under convective boundary conditions and triple diffusion for the non-darcy porous matrix. *Propulsion and Power Research*, 10(4):396–411, 2021.
- [19] Karuppusamy Loganathan, Nazek Alessa, and Safak Kayikci. Heat transfer analysis of 3-D viscoelastic nanofluid flow over a convectively heated porous riga plate with cattaneo-christov double flux. *Frontiers in Physics*, 9:641645, 2021.
- [20] Hari R Kataria and Akhil S Mittal. Velocity, mass and temperature analysis of gravity-driven convection nanofluid flow past an oscillating vertical plate in the presence of magnetic field in a porous medium. *Applied Thermal Engineering*, 110: 864–874, 2017.
- [21] M Sheikholeslami, Hari R Kataria, and Akhil S Mittal. Effect of thermal diffusion and heat-generation on mhd nanofluid flow past an oscillating vertical plate through porous medium. *Journal of Molecular Liquids*, 257:12–25, 2018.
- [22] Harshad R Patel, Akhil S Mittal, and Rakesh R Darji. MHD flow of micropolar nanofluid over a stretching/shrinking sheet considering radiation. *International Communications in Heat and Mass Transfer*, 108:104322, 2019.
- [23] Akhil S Mittal, Harshad R Patel, and Rakesh R Darji. Mixed convection micropolar ferrofluid flow with viscous dissipation, joule heating and convective boundary conditions. *International Communications in Heat and Mass Transfer*, 108:104320, 2019.

- [24] Hari R Kataria, Mital Mistry, and Akhil Mittal. Influence of nonlinear radiation on MHD micropolar fluid flow with viscous dissipation. *Heat Transfer*, 51(2):1449–1467, 2022.
- [25] Akhil S Mittal and Harshad R Patel. Influence of thermophoresis and brownian motion on mixed convection two dimensional MHD casson fluid flow with non-linear radiation and heat generation. *Physica A: Statistical Mechanics and its Applications*, 537:122710, 2020.
- [26] M Sheikholeslami, Hari R Kataria, and Akhil S Mittal. Radiation effects on heat transfer of three dimensional nanofluid flow considering thermal interfacial resistance and micro mixing in suspensions. *Chinese journal of physics*, 55(6):2254–2272, 2017.
- [27] F Mabood, S Shateyi, MM Rashidi, E Momoniat, and NJAPT Freidoonimehr. MHD stagnation point flow heat and mass transfer of nanofluids in porous medium with radiation, viscous dissipation and chemical reaction. *Advanced Powder Technology*, 27(2):742–749, 2016.
- [28] T Grosan, C Revnic, I Pop, and DB Ingham. Magnetic field and internal heat generation effects on the free convection in a rectangular cavity filled with a porous medium. *International Journal of Heat and Mass Transfer*, 52(5-6):1525–1533, 2009.
- [29] Khalil M Khanafer and Ali J Chamkha. Mixed convection flow in a lid-driven enclosure filled with a fluid-saturated porous medium. *International Journal of Heat and Mass Transfer*, 42(13):2465–2481, 1999.
- [30] Md Mustafizur Rahman, Hakan F Öztop, Rahman Saidur, Saad Mekhilef, and Khaled Al-Salem. Unsteady mixed convection in a porous media filled lid-driven cavity heated by a semi-circular heaters. *Thermal science*, 19(5):1761–1768, 2015.
- [31] Elaprolu Vishnuvardhanarao and Manab Kumar Das. Laminar mixed convection in a parallel two-sided lid-driven differentially heated square cavity filled with a fluid-saturated porous medium. *Numerical Heat Transfer, Part A: Applications*, 53(1): 88–110, 2007.

- [32] Ahlam A Hassan and Muneer A Ismael. Mixed convection in superposed nanofluid and porous layers inside lid-driven square cavity. *Int. J. of Thermal & Environmental Engineering*, 10(2):93–104, 2015.
- [33] A Hadim and G Chen. Non-Darcy mixed convection in a vertical porous channel with discrete heat sources at the walls. *International communications in heat and mass transfer*, 21(3):377–387, 1994.
- [34] S Sureshkumar and M Muthtamilselvan. A slanted porous enclosure filled with Cu-water nanofluid. *The European Physical Journal Plus*, 131:1–19, 2016.
- [35] Nithyadevi Nagarajan and Shamadhanibegum Akbar. Heat transfer enhancement of Cu-water nanofluid in a porous square enclosure driven by an incessantly moving flat plate. *Procedia Engineering*, 127:279–286, 2015.
- [36] D Santhosh Kumar, Anoop K Dass, and Anupam Dewan. Analysis of non-Darcy models for mixed convection in a porous cavity using a multigrid approach. *Numerical Heat Transfer, Part A: Applications*, 56(8):685–708, 2009.
- [37] Tzer-Ming Jeng and Sheng-Chung Tzeng. Heat transfer in a lid-driven enclosure filled with water-saturated aluminum foams. *Numerical Heat Transfer, Part A: Applications*, 54(2):178–196, 2008.
- [38] BV Rathish Kumar et al. Free convection in a non-Darcian wavy porous enclosure. *International Journal of Engineering Science*, 41(16):1827–1848, 2003.
- [39] BV Rathish Kumar et al. Free convection in a thermally stratified non-Darcian wavy porous enclosure. *Journal of Porous Media*, 7(4), 2004.
- [40] R Nasrin and MA Alim. A slanted porous enclosure filled with Cu-water nanofluid. *Heat Transfer-Asian Research*, 4:42, 2013.